Contents

Plenary Abstracts

Donald, Scott	Influence of Sub-Surface Chemical Variation on the Reduction Kinetics of PuO_2 to Pu_2O_3
Hixon, Amy	Closing the Gap: Advanced Thermodynamic Descriptions of Multivalent Plutonium Complexation and Solubility Under Repository-Relevant Conditions
Kerlin, Maryline	Informing Plutonium Anion Exchange Through Targeted Small Scale Resin Experiments
Picart, Sébastien	Production of a new certified plutonium metal reference material : the MP4 from CETAMA
Reilly, Dallas	Plutonium Characterization at the Nano-Scale
Söderlind, Per	First principles free energy model with dynamic magnetism for δ-plutonium
Taylor, Robin	Evolution of separation processes for plutonium and minor actinides
Virot, Matthieu	PuO_2 Nanoparticles in Water: Unraveling Structure, Reactivity, and Formation Pathways

Oral Abstracts

Abdul-Jabbar, Najeb	Radiogenic Effects on the Thermal Response of Plutonium
Anderson, Nickolas	Outer- Coordination Sphere Effects in Aqueous Solutions
Archer, Emma	A Crystallographic and Spectroscopic Study of Mixed Actinide Oxalates
Atta-Fynn, Raymond	Large-Scale Ab Initio Modeling of ε-Pu/δ-Pu and α-Pu/δ-Pu Interfaces
Balas, Johannes	Exploring Bonding Trends and Fundamental Properties in Pyridine-2-thiolato Complexes of Tetravalent Actinides (Th - Pu)
Batista, Enrique	Charge States, Oxygen Transport, and Helium Accumulation in PuO_2 and α-Pu_2O_3
Bauer, Eric	Nuclear magnetic resonance studies of Pu-B compounds
Beaux, Miles	Electronic and Surface Features of $PuCoGa_5$
Blakemore, James	Comparing the Reduction- and Acid-Promoted Reactivity of a Homologous Series of Plutonium, Neptunium, and Uranium Complexes
Boehm, Alex	Temperature Dependent Changes in the Photoemission Lineshape of δPlutonium
Bottin, François	Ab initio study of the Ce and Pu oxide surface reactivity with respect to O_2 and H_2O

Bouchet, Johann	Elastic properties of actinides systems at high temperature with machine learning
Bourasseau, Emeric	Thermodynamic Properties of $(U,Pu)O_2$: Impact of Defects and Fission Products on the Bredig Transition
Bourgès, Gilles	Future Aqueous Nitrate Process Line for Plutonium Recycling
Brown, Alexandra	Combustion Ion Chromatography (CIC) Method Development and Validation for Characterization of Fluoride and Chloride in Actinide Materials
Brown, Donald	Evolution of Helium Bubble Characteristics During Heating of Aged PuGa Alloys: An In-Situ Small Angle X-ray Scattering Study
Carver, D. Travis	In-Situ High Energy X-Ray Imaging and Diffraction to Monitor Corrosion of PuGa Alloy
Cette, Daphné	Enabling Americium-Powered Space Missions. High Temperature Stability of $(Ce,U)O_2$ Surrogates for the $(Am,U)O_2$ Fuel Source
Chamberlain, Jarom	Plutonium Metallurgy and Exposure onto a Tungsten Coated Substrate
Chen, Lena	Evaluating Disposal of Plutonium Wasteforms
Childs, Bradley	The Effects of Pu Particle Formation during Precipitation and Calcination on Aqueous Processing
Chung, Brandon	Mapping Morphological and Chemical Signatures of Plutonium and Uranium Materials for Nuclear Forensics
Davie, William	A Machine Learned Interatomic Potential for Helium in Plutonium Dioxide
Di Pietro, Silvina	Learning Tracks: A New Method to Develop the Next Generation
Dunn, Stuart	Nuclear Forensic Signatures of Plutonium Hydroxide Precipitation and Calcination products
El Monjid, Alison	ADOA Route for $(U,Pu)O_2$ Mixed Oxides: Multiparametric Synthesis Optimization and Preliminary Sintering Performance
Estevenon, Paul	Pu(IV) Silicate, Synthesis and Advanced Characterisation of a Key Compound for Plutonium Environmental Behavior
Farnaby, Joy	Experimental Actinide Chemistry in support of UK Civil Plutonium Inventory Technical Challenges
Fellhauer, David	Pu(VI) hydrolysis in aqueous alkali and alkaline earth metal solutions: reaction pathways and thermodynamics
Friskney, Aidan	Ceramic Wasteform and Process Development for Pu Disposition
Génin, Renaud	Influence of Cooling Speed and Aluminum Content on the Microstructure of As-Cast δ-PuAl Alloys
Gofryk, Krzysztof	Advancing Actinide Quantum Materials at INL's Glenn T. Seaborg Institute: The Case of PuB_6
Golwankar, Riddhi	Electrochemical behavior of Actinides (An) in molten alkali halide salts

Gonzales, Ivana	Computational Insights into Plutonium Chemistry: From Density Functional Theory to Kinetic Modeling
Greb, Fabian	Solubility of Np_2O_5(cr) and Hydrolysis of Np(V) in Neutral to Alkaline NaCl-NaOH Solutions
Groedler, Dennis	Metallophilic Actinide-Platinum Interactions in Bimetallic Pyridyloxy Complexes
Guilbaud, Philippe	Actinide (VI), and Nitric Acid Speciation Studies in Separation Processes using N,N-Dialkylamide Extractants
Guillaumont, Dominique	The Effect of Diluent on Uranium(VI) and Plutonium(IV) Solvent Extraction with Monoamide Extractants
Hayne, Mathew	Bridging Scales: Comparative Elastic-Modulus Measurements by Resonant Ultrasound Spectroscopy, Nano-Indentation, and Bulk Mechanical Tests
Heiner, Benjamin	Oxygen Vacancies Drive f-orbital Density into the Band Gap of Np/Pu Oxides
Hernandez, Sarah	ToF-SIMS Analysis of Heat-Treated Aged 2 at.% Ga-Stabilized δ-Pu
Higginson, Matthew	Developments in plutonium analysis at the AWE
Holmbeck, Gregory	The Influence of Transuranic Actinyl Complexation on Ligand Radiolysis
Jolly, Lionel	Study of elements distribution in the δ-Pu oxide scale
Kelly, Sheridon	Speciation of Plutonium in Molten Salt Environments
Kennedy, Rory	Plutonium Bearing Metallic Transmutation Fuels – Phase Relations and Thermal Properties
Kohlgruber, Tsuyoshi	Aqueous Recovery of Plutonium at Lawrence Livermore National Laboratory
Kravchuk, Dmytro	Reactions of Pu(VI) and Pu(V) in Alkali Hydroxide Solutions: New Pu Solid Phases and Insights into Pu Speciation at High pH
Kucinski, Theresa	Improved Characterization of Helium Bubble in Naturally Aged Plutonium with Scanning Transmission Electron Microscopy (STEM)
Kweon, Kyoung	Ab Initio modeling of He Bubbles in δ-Pu
Kynman, Amy	The Role of Transient Plutonium Oxidation States in the Radiation-Induced Redox Cycling of Pu(VI) in Aqueous Nitric Acid Solutions
La Pierre, Henry	Redox Chemistry and Reactivity of Homo-and Heteroleptic Neptunium and Plutonium Complexes
Landa, Alexander	An ab initio Molecular Dynamics Study of Key Thermodynamical Input Parameters for Computer Simulation of U-6Nb Solidification
Levin, Zachary	Micromechanical Characterization of α- and δ-Phase Plutonium via Advanced Nanoindentation Techniques
Lim, Rachel	Oxygen K-edge Scanning Transmission X-ray Microscopy (STXM) of Plutonium Oxide
Maloubier, Melody	Experimental and Quantum Chemical Insights into the coordination chemistry of Protactinium(V) in solution

Margate, Julien	Vibrational identification of uranyl peroxo-carbonate complexes in solution: insights from ^{18}O labeling and DFT
Mathew, Kattathu	Mass Fractionation Corrections in TIMS Isotope Ratio Measurements: Comparison of Correction Factors in Total Evaporation Analysis of Actinides
Mazza, Alessandro	X-ray Photoemission Studies of Pu_6Fe
Monreal, Marisa	The Launch of the Plutonium Science Laboratory (PluS Lab) at Los Alamos National Laboratory
Munoz, Maeva	Stability and Aging Pathways of Pu(IV) Hexanuclear Clusters in aqueous solution: Influence of Ligand Environment and Alpha Radiolysis
Olive, Daniel	Plutonium Oxidation Studied at Different Temperatures
Pace, Kristen	Probing the Effects of Iron and Uranium Impurities on the Melt Behavior of Plutonium Alloys using Differential Scanning Calorimetry
Parker, Gannon	Qualification of Plutonium and Iron Analysis Capabilities within Los Alamos National Laboratory Plutonium Facilities
Patenaude, Hannah	Diamonds are an Actinide's Best Friend: Electrochemical Discrimination of U and Pu Redox Couples Using Boron-Doped Diamond
Piccinelli, Davide	Multi-Fidelity Gaussian Process Regression for Modeling the Thermal Properties of MOX Nuclear Fuel
Plohr, Jeeyeon	Helium Bubble Evolution in Aged Plutonium
Ramirez, Bianca	Development of Water-Equivalent Solid Calibration Standards for Plutonium Gamma-Ray Nondestructive Assay
Ramos, Frank	Utilizing 244Pu for High Resolution Plutonium Concentration Determinations Via Isotope Dilution Measurements and Thermal Ionization Mass Spectrometry
Ravat, Brice	Oxidation of Pu Alloys Stabilized in δ-Phase: Characterization of the Microstructure of the Oxide Scale
Real, Florent	The Signature of the Mono-Oxo Bonding in Protactinium(V) in the M4-Edge HERFD spectrum: a theoretical and experimental study
Robles, Geronimo	Synthesizing Pu-U-Ga Ingots for the Advancement of the First Multiscale Alloy Prediction Model
Rodriguez, Daniel	Gas Dosing and Growth of Pu Oxycarbide Films: Characterization of the Surface using XPS and ToF-SIMS
Roussel, Paul	In search of the σ-Pu phase
Rowberg, Andrew	Point Defect and Impurity Incorporation in Plutonium Oxides
Roy, Gabriel	Nanoscale Effects in Plutonium Dioxide: How Size Shapes Structure and Electronic Properties
Schenk, Sven	Increased Sensitivity of Pu M5-edge CC-RIXS to Bond Covalency in PuO_2 in Comparison to Pu M4-edge RIXS

Schmidt, Moritz	Chemical bonding in actinide quinolinates from Th to Pu
Shauf, Elise	Investigation of Manufacturing and Processing Variables on the Mechanical Behavior of Tungsten During Actnide Pyroprocessing
Sockwell, Kirstin	Photochemistry of Aqueous Plutonium(VI) Oxalate
Startt, Jacob	Molecular Dynamics Modeling of Helium Bubbles in Delta- and Epsilon-Pu
Stuke, Kevin David	Aging and Oxidation Mechanisms of PuO_2 and Pu-doped UO_2 based Nanomaterials under Ambient Conditions in Maintaining the Stability of Spent Nuclear Fuel
Takao, Koichiro	Crystallization of UO_2^{2+} and Pu^{4+} Nitrato Complexes with 1,3-AdamantylBridged Diamide Molecules towards Direct Co-recovery of Nuclear Fuel Materials from HNO_3(aq)
Tamain, Christelle	Contribution of coordination chemistry studies to the speciation of neptunium and plutonium in organic phases
Tobin, J G	Pu 5f Population: The Case for n = 5.0
Tutchton, Roxanne	Temperature Dependent Electronic Structure and Optical Properties of δ-Pu
Weinmann-Smith, Robert	Implementing the DAIL NDA Instrument for LANL TRU Waste Material Control and Accounting
Wheeler, David	The role of helium bubbles in changes to the mechanical properties of aged plutonium
Wilson, Richard	Insights into the Solvation and Solvent Exchange Reactivity of Plutonium in Non-Aqueous Solutions
Yang, Ping	Probing the Limits of 5f Bonding in Actinides through Oxidation State Control and Redox-Active Ligands

Poster Abstracts

Adelman, Sara	Controlling Plutonium Oxidation State for the Development of a Reliable Solution-Phase Assay
Anghel, Veronica	Strain Rate Sensitivity in Actinide Materials Using Nano-Indentation Measurements
Batrice, Rami	Deployable Modular Electrochemical Decontamination for Nuclear D&D Applications
Bethea, Donald	Machine-Learning Assisted Plutonium Quantification Using High-Purity Germanium Gamma Detectors
Bottin, François	Invar Effect in δ-Pu Alloys
Castro, Leslie	Investigations Into the Spectroscopic Changes of Actinyl Based on Hydroxide and Nitrate Ligation
Coe, Camille	Growth kinetics of plutonium hydride corrosion sites

Colledge, Hannah	The UK's plutonium package surveillance programme: Long-term storage and aging of PuO_2 powder up to 50 years old
Cooper, Sophie	The modelling of the dissolution of actinide compounds – the use of ab initio methods to calculate thermodynamic data from first principles
Cross, Sam	Developments in Plutonium Recovery at AWE
Dale, Olivia	Investigation of Plutonium Metal for Materials Compatibility Testing
Dawson, Paris-Rose	A Density Functional Theory Study on the Point Defects in PuO_2
Debenedetti, William	Divergent Mechanisms of Hydrogen and Oxygen Consumption on Calcined PuO_2: Implications for Long-Term Storage
Faure, Sébastien	Speciation of Plutonium in Nitrate Media: Effect of Fluorides
Field, Gordy	Developments in HiZ Physics Package Fabrication
Figurskey, Sullivan	Ion Milling and Sputter Deposition for the HEDS of Oxide-free Plutonium
Glymond, Daniel	Hot Isostatic Pressing for Plutonium Immobilisation
Grismer, Magdalen	He bubble nucleation and growth rates in naturally aged δ-Plutonium
Gupta, Ayush	Preparation of Plutonium Arene Complexes Through Oxidative Dissolution of Plutonium Metal
Harding, Sean	Developing Dynamical Mean-Field Methods for Actinide Materials Simulation at AWE
Hernandez, Sarah	A Density Functional Theory Study on Induced Covalent Short Bond Maximization on U in Pu-Ga Alloys and Extrapolation to the ζ-Pu-U Phase
Hixon, Amy	Porphyrin-Based Plutonium Metal-Organic Frameworks: A Versatile Platform for Investigating Elusive Plutonium Cluster Chemistry
Jaramillo, Roger	Bulk vs. Nano-Indentation Stress-Relaxation of δ-Phase Plutonium Alloys: Methodology, Parameter Extraction, and Compliance Corrections
Knowles, John	Exploring the Influence of Variable Hydrogen Pressure on the Early Stages of the Plutonium–Hydrogen Reaction
Lee, Samuel	Synthesis of Actinide Fluorides for Advanced Nuclear Fuels and National Security
Li, Jun	5f-in-Core Pseudopotentials and Applications to Electronic Structure of [Pu38] Cluster
Matthews, Mike	Measuring the Density of Plutonium Surface Oxides
Moore, Gordon	Using Principal Component Analysis on Compositional Measurements of Multi-component Pu-alloys to identify potential minor phases
Park, Young-Shin	Handheld LIBS Analysis in Nuclear Material Processing
Perea, Daniel	Atomic-Scale Mapping of Pu Oxidation and Hydrogenation with Environmental Atom Probe Tomography
Peters, Scott	Critical Review and Thermodynamic Assessment of the Pu-Ni System

Ponder, William	Probing the δ to α’ phase transformation with X-ray Photoemission Spectroscopy
Preisser, Alex	Quantifying Manual Lapping for Precision Beryllium Target Components
Preisser, Alex	Femtosecond Green Laser Micromachining of Challenging Materials for Target Fabrication
Ridley, Christopher	Path-dependent Phase Selection in Compressed Cerium: Metastability and Microstructural Memory in an f-electron Metal
Rim, Jung	Developing Machine Learning Techniques for Plutonium Manufacturing Equipment Predictive Maintenance Program
Roussel, Paul	Investigating the amorphous oxide growth on plutonium metal
Samiere, Carmen	Helium Implantation Sample Preparation and Handling in the Small-Scale Transuranic Lab within the Materials Characterization Center
Samiere, Carmen	Facility Expansion and Capability Growth in the Small-Scale Transuranic Lab within the Materials Characterization Center
Schumer, Benjamin	Solubility of U in Ga-Stabilized δ-Pu Shown by Electron Probe Microanalysis
Shittu, Jibril	Early-Stage Uranium-Hydrogen Corrosion Kinetics and Mechanism
Simpson, Scott	In-situ, Real Time Detection of Impurity Transport in Plutonium Electrorefining
Smith, Douglas	Transmission Electron Microscopy Characterization of He-Bubble Evolution in Naturally Aged and Annealed δ-Plutonium
Sockwell, Kirstin	Effects of Temperature, Ionic Strength, and pH on Aqueous Plutonium(VI) Speciation in NaCl, $MgCl_2$, and $Na(CO_3)_2$
Summerscales, Owen	Actinide Research Quarterly
Terricabras, Adrien	Non-Destructive Rapid Turnaround Characterization to Support Plutonium Experimentation
Thorn, Hannah	Modelling Heat Transfer, Diffusion, Water Adsorption and Radiolysis in PuO_2 Powder under Repacking and Storage Conditions
Tobash, Paul	Structural and Thermophysical Properties of Pu Intermetallics
Varsani, Vijay	Plutonium Casting Modelling – Beyond the Present
Vauchy, Romain	Carbothermal reduction sintering of MOX fuel for fast-neutron reactors
Vu, Dung	The Plutonium-Hydrogen Interaction Studied via X-ray Photoemission
Walusiak, Benjamin	Pu LIII and Fe K Edge X-ray Absorption Spectroscopy of Bulk Pu_6Fe Synthesized via Arc Melting
Weulersse, Katia	Study of the hydriding behaviour of cerium containing iron-rich impurities
Wu, Christine	A Multiphase Equation of State for Ce
Yablinsky, Clarissa	Beyond Hardness: Measuring Elastic and Dissipative Properties by Nanoindentation

Plenary Abstracts

Donald, Scott	Influence of Sub-Surface Chemical Variation on the Reduction Kinetics of PuO_2 to Pu_2O_3
Hixon, Amy	Closing the Gap: Advanced Thermodynamic Descriptions of Multivalent Plutonium Complexation and Solubility Under Repository-Relevant Conditions
Kerlin, Maryline	Informing Plutonium Anion Exchange Through Targeted Small Scale Resin Experiments
Picart, Sébastien	Production of a new certified plutonium metal reference material : the MP4 from CETAMA
Reilly, Dallas	Plutonium Characterization at the Nano-Scale
Söderlind, Per	First principles free energy model with dynamic magnetism for δ-plutonium
Taylor, Robin	Evolution of separation processes for plutonium and minor actinides
Virot, Matthieu	PuO_2 Nanoparticles in Water: Unraveling Structure, Reactivity, and Formation Pathways

Influence of sub-surface chemical variation on the reduction kinetics of PuO_2 to Pu_2O_3

Scott Donald[1,*]

[1]Lawrence Livermore National Laboratory, Livermore, CA, USA; *donald3@llnl.gov

The corrosion of metals by atmospheric gases, particular water vapor and oxygen, continues to garner interest for establishing safe handling and storage procedures [1]. In the case of plutonium, the consequences to both human and environmental health are amplified by its toxic and radioactive nature, and the absence of a predictive capability to understand the characteristics and properties of the products resulting from exposure to common atmospheric conditions can lead to unintended outcomes. Metallic plutonium has been shown to readily oxidize when exposed to atmospheric conditions, forming a tetravalent dioxide (*i.e.,* PuO_2) with a trivalent sesquioxide (*i.e.,* Pu_2O_3) arising at the oxide metal interface due to thermodynamic constraints. The oxidation process has been found to follow a complex reaction pathway, and the kinetics have been determined to be dependent on multiple variables, including alloy composition, gas constituents, and temperature [2]. While clarity on the oxidation kinetics of plutonium metal and its alloys has improved with time, less clear how the incorporation of interstitial impurities influences the conversion of plutonium dioxide to sesquioxide when stored in a reducing environment.

At room temperature in an oxidizing environment, the sesquioxide layer is expected to be vanishingly thin (i.e., having a thickness on the order of one or two monolayers). Corrosion of plutonium metal has been observed to occur much more readily when the surface is covered with Pu_2O_3, which provides a network of periodic oxygen vacancies for fast transport of reactive species to the metal interface, and can be formed upon vacuum heating of a plutonium dioxide surface. Therefore, the knowledge of the PuO_2 to Pu_2O_3 transformation kinetics plays an important role in preventing unwanted reactions for safety during long-term metal storage. The diffusion coefficients for the PuO_2 to Pu_2O_3 conversion were measured via in situ spectroscopic ellipsometry of a Pu sample having a known initial PuO_2 thickness in a high vacuum environment, as well as via x-ray photoelectron spectroscopy, and comparison are made when interstitial elements have been incorporated into the sub-surface oxide region.

This work was performed under the auspices of the U.S. Department of Energy by Lawrence Livermore National Laboratory under Contract DE-AC52-07NA27344.

Closing the Gap: Thermodynamic Descriptions of Multivalent Plutonium Complexation and Solubility Under Repository-Relevant Conditions

Amy E. Hixon[1*], A. Kirstin Sockwell[1], Blessing Y. Adjornor[1]

[1]University of Notre Dame, Notre Dame, IN, USA; *ahixon@nd.edu

Actinide release is a critical performance measure for a geologic repository, and there are a number of potential pathways for actinide release that must be considered in a performance assessment. In all cases, it is important to determine the actinide source term, which is defined by aqueous-phase speciation and the identity and dissolution rate of solubility-controlling phases, and relies on variables such as actinide oxidation state, the presence and concentration of complexing or competing ions, and the geochemical boundary conditions of the repository (e.g., pH, redox potential, temperature). Most experiments targeted at understanding actinide solubility and speciation have been performed at 25 °C and relatively low ionic strength (I = 0.1 m), whereas geologic repositories will have elevated temperatures and/or ionic strengths. Because the predictive power and accuracy of geochemical and reactive transport models rely on robust thermodynamic datasets, the temperature and ionic-strength dependence of thermodynamic constants (e.g., solubility constants, formation constants, etc.) must be known in order to make accurate predictions of actinide transport.

Several methods exist to approximate the effect of temperature and ionic strength on solubility and speciation. Because ionic solutions depart from ideality due to long-range electrostatic interactions, different approaches are used to determine the ionic strength dependencies of chemical equilibria. The Bronsted-Gugenheim-Scatchard model, colloquially known as the Specific Ion Interaction Theory (SIT), is used to describe solutions at I < 4 m, whereas the Pitzer model is required for solutions at higher ionic strengths. Both models have a common theoretical basis in Debye-Hückel theory and while many SIT parameters are available in the literature, their variability with temperature is unknown. Significantly fewer Pitzer parameters are known, particularly for actinide ions. The approaches commonly used to determine the temperature dependencies of chemical equilibria include the constant enthalpy approach, the constant heat capacity approach, the DQUANT equation, the Ryzhenko-Bryzgalin model, and the Helgeson-Kirkham-Flowers equations. In order to apply these approaches, the enthalpy, entropy, and/or heat capacity of the given reaction must be known, yet these values are rarely available for actinide systems. When enthalpy is known at one temperature (usually 25 °C), the van't Hoff equation can be used to extrapolate the effect of temperature on the complexation constant for a reaction. However, while this approach assumes that the molar heat capacity of reaction at constant pressure ($C_{p,m}$) is not temperature dependent (i.e., that $\Delta_r C_{p,m}$ = 0 over the temperature range of interest), data presented by Hovey (1997) demonstrate that this is an invalid assumption in some cases (**Figure 1**). The limitations of these approximation approaches and lack of available data in thermodynamic databases highlights the need for reliable experimental data on the

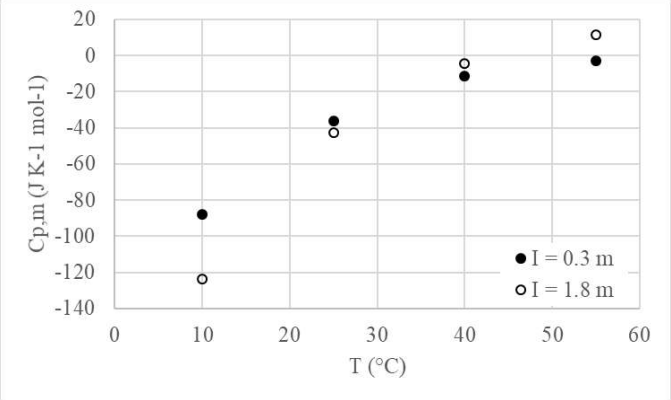


Figure 1. Molar heat capacities ($C_{p,m}$) for solutions containing $Th(ClO_4)_4$(aq) as a function of temperature (T) and ionic strength (I). Data from Hovey (1997).

complexation of actinides in solution at temperatures, ionic strengths, and pH values expected in a geologic repository.

To address this gap, we used UV-vis-NIR spectrophotometry experiments to study the effect of temperature (T = 25–95 °C), ionic strength (*I* = 0.1–10 m), and pH (pH_i = 5–12) on plutonium speciation. Solutions of Pu(III) and Pu(VI) chlorides at a given ionic strength and pH were placed in a heat-controlled stage on the spectrophotometer. Each sample was equilibrated for 15 minutes at 25 °C while being stirred, the stirring mechanism was turned off, and a spectrum was collected. This procedure was repeated at 45°C, 65 °C, 75 °C, and 95 °C. The results demonstrate that plutonium speciation is governed by complex, interdependent relationships between temperature, pH, ionic strength, and the composition of the ionic strength medium. For example, at low pH, elevated temperatures favored Pu(VI) chloride complexation, whereas at pH 5, chloride complexation competed with hydrolysis; at pH 9, increasing temperature served to primarily redistribute the relative concentrations of hydrolysis products rather than generating new ones. Increasing NaCl concentrations promoted the formation of PuO_2Cl^+ and PuO_2Cl_2, while the $MgCl_2$ system favored higher-order species such as $PuO_2Cl_3^-$.

Aqueous speciation measurements are being complemented by reaction calorimetry to determine the change in molar heat capacity of reaction ($\Delta C_{p,m}$) as a function of ionic strength at constant pH (5–12). Each experiment consisted of achieving thermal equilibrium of separate plutonium and ionic strength solutions (*I* = 0.1–10 m) at a given temperature (T_i = 25–95 °C), then allowing the two solutions to mix and monitoring the heat flow. Integration of the heat flow signal yields the molar enthalpy of reaction (ΔH_{rxn}). The temperature dependence of ΔH_{rxn} was analyzed to determine $\Delta C_{p,m}$ from the slope of ΔH_{rxn} versus temperature.

Finally, solubility experiments are being performed from undersaturation using $Pu^{III}(OH)_3(s)$ and $Pu^{IV}O_2(s)$ as the solid phases of concern. $Pu(OH)_3(s)$ was prepared as described by DiBlasi et al. (2021), whereas $PuO_2(s)$ was produced via calcination of Pu(IV) oxalate at 400 °C for 1 hour. Appropriate amounts of each solid were suspended in $NaClO_4$, NaCl, or $MgCl_2$ and adjusted to the target pH value (pH_i = 5–12) using dilute HCl, NaOH, or $Mg(OH)_2$ such that the ionic strength remained constant (*I* = 0.1–10 m). The samples were allowed to equilibrate on a temperature-controlled hotplate (T = 25–95 °C) equipped with a heating block. The pH and aqueous-phase concentration of plutonium were measured as a function of time until equilibrium was achieved after ultrafiltration through 10 kD MWCO filters. Solid phase analyses (X-ray diffraction, scanning electron microscopy, vibrational spectroscopy) were conducted prior to the start of solubility experiments and after equilibrium was achieved. Preliminary measurements suggest higher plutonium solubility in chloride media than perchlorate media; ongoing experiments will quantify these effects over the full temperature and ionic strength range.

Together, this work will provide the thermodynamic parameters needed to describe multivalent plutonium speciation and solubility over the temperature and ionic-strength conditions expected in geologic repositories.

DiBlasi, N. A.; Tasi, A. G.; Gaona, X.; Fellhauer, D.; Dardenne, K.; Rothe, J.; Reed, D. T.; Hixon, A. E.; Altmaier, M. Impact of Ca(II) on the aqueous speciation, redox behavior, and environmental mobility of Pu(IV) in the presence of EDTA. *Sci. Total Environ.* **2021**, *783*, 146993. https://www.doi.org/10.1016/j.scitotenv.2021.146993.

Hovey, J. K. Thermodynamics of Hydration of a 4+ Aqueous Ion: Partial Molar Heat Capacities and Volumes of Aqueous Thorium(IV) from 10 to 55 °C. *J. Phys. Chem. B* **1997**, *101* (21), 4321-4334. https://www.doi.org/10.1021/jp970125z.

Informing Plutonium Anion Exchange Through Targeted Small Scale Resin Experiments

Maryline G. Ferrier (Kerlin)[1*], Bradley C. Childs[1], Tsuyoshi A. Kohlgruber[1], Silvi A. Di Pietro[1], Emma R. Tardiff[1], Hiroshi H. Saito[1], Saurabh Narain[1], Jeremy A. Scher[1], Jared C. Stimac[1], and Lawrence E. Banks[1]

[1]Lawrence Livermore National Laboratory, Livermore, California, United States
* email: kerlin4@llnl.gov



Effective plutonium recovery and purification in aqueous processing depends critically on the performance of anion exchange columns. At Lawrence Livermore National Laboratory, anion exchange resin is used for plutonium purification, where overall recovery efficiency is governed by a combination of resin properties, feed composition, plutonium oxidation state distribution, and process operating conditions. To support predictive modeling of this unit operation, we have developed a program of targeted small-scale experiments that quantitatively probe plutonium behavior during loading, washing, and elution.

Batch and semi-dynamic liquid–solid contact studies are conducted to isolate the effects of key parameters such as nitric acid concentration, plutonium loading, and contact time. In contrast, column studies employ a fully dynamic approach, allowing systematic variation of parameters including solution volume, concentration, properties, and residence time within the column. This flexibility enables us to assess the significance of individual variables and investigate specific scenarios, including non-ideal conditions, to support model validation. The modular design of these experiments allows rapid adjustment of conditions to test targeted mechanistic hypotheses and process behaviors. UV vis NIR spectroscopy is used to monitor plutonium concentration and speciation throughout each experiment, providing time resolved datasets that capture both kinetic and near equilibrium behavior.

The resulting datasets are used to construct dynamic models that predict column effluent concentration profiles and to provide physically grounded inputs for computational efforts, including machine learning and quantum chemical simulations. By fitting experimental data to adsorption isotherms and transport models, we begin to delineate the range and relative abundance of plutonium molecular species that govern resin loading and elution across the recovery flowsheet. This talk will summarize the experimental framework, highlight representative results for each process stage, and discuss how small-scale experiments can be translated to larger scale behavior.

This work was performed under the auspices of the U.S. Department of Energy by Lawrence Livermore National Laboratory under Contract DE-AC52-07NA27344. LLNL-ABS-2016767

Production of a new plutonium metal Certified Reference Material: the MP4 from CETAMA

S. Picart[1], M. Crozet[1], G. Canciani[1], A. Clement[2], G. Bailly[2], D. Cardona[2], C. Rivier[1]

[1] CEA, ISEC, DMRC, CETAMA, Univ. Montpellier, Marcoule, Bagnols-sur-Cèze, France
[2] CEA, DAM, Valduc, Is-sur-Tille, France

The production and use of high-purity plutonium (Pu) metal standards is the cornerstone of the Pu fissile material nuclear accountancy implemented both in nuclear facilities and in laboratories involved in nuclear safeguards activities. Indeed, Pu certified reference materials are needed to calibrate the analytical processes used to characterize Pu-containing materials in terms of both mass fraction and isotopy.

However, the production of such standards is a highly complex task: firstly, for stability reasons, it is recommended that a Pu metal standard be composed of enriched Pu-239 (the access to which is strictly controlled); secondly, the facilities capable of purifying and producing high-purity Pu in metal form are very rare; finally, the characterization step of the material (which allows to establish the reference values) requires a large workforce and potentially a significant network of expert laboratories.

In this context, more than ten years ago, the CEA Valduc and the CETAMA (Commission for the Establishment of Analytical Methods) joined forces to launch the “MP4” program and enhance the range of Pu metal certified reference materials (CRMs) in the CETAMA's catalog. The aim of the project was to offer the CRM in the form of a metal piece with a reduced mass compared with the current MP2 CRM.

Manufacturing of the material and packaging in ampoules took place over the 2017-2019 period. Following this, material characterization was carried out through an interlaboratory comparison (ILC) involving expert laboratories within the CETAMA’s network between 2021 and 2023. In 2024, the MP4 certificate was released and the CRM was listed in the CETAMA’s catalog, becoming available for potential buyers.

The current presentation will focus on the fabrication and characterization steps which led to the creation of the MP4 CRM. The following data processing, which enabled us to determine reference values for various quantities such as the Pu isotopy and the Pu mass fraction, will also be detailed.

Furthermore, a comparison will be presented of the properties and certified values of the MP4 CRM with those of the MP2 CRM, highlighting the unique strengths of this new Pu metal standard. Finally, the applicability of the MP4 material as a radio-chronometer will be discussed.

Plutonium Characterization at the Nanoscale

Dallin Barton[1], Matthew Olszta[1], Danny Perea[1], Kayla Yano, [1], Dallas Reilly[1*]

[1]Pacific Northwest National Laboratory, Richland, WA, USA

Plutonium is among the most challenging elements to study on the periodic table. Its inherent radioactivity complicates handling, while multiple oxidation states and crystallographic phases, chemical reactivity, and self-irradiation drive complex behavior that complicates analysis and interpretation. Bulk-scale analysis methods are available, cost-effective, and well proven, but do little to help researchers understand nanoscale behavior, which ultimately defines how a material performs. These methods can obscure local segregation, interfacial chemistry, and defect-associated compositional variations. Across the world of plutonium science, but especially at PNNL, advances in technology, capability investments, and evolution of actinide-handling workflows have expanded the possibilities for nanoscale analysis. In this work, we present plutonium characterization at the nanoscale using a correlative approach centered on atom probe tomography (APT) and transmission electron microscopy (TEM) to obtain complementary chemical and structural information. APT enables three-dimensional nanoscale elemental mapping and quantification of local composition, while TEM provides high-resolution structural analysis of phases, defects, and interfaces. By integrating these datasets, we resolve nanoscale variations in composition and microstructure that are not accessible through bulk-scale measurements alone. The combined observations demonstrate that nanoscale chemical and structural heterogeneities can strongly influence—and in some cases control—apparent bulk-scale properties and performance metrics. These results highlight the importance of linking nanoscale observations to macroscopic behavior to improve mechanistic understanding and predictive models of plutonium-bearing materials.

First principles free energy model with dynamic magnetism for δ-plutonium

Per Söderlind[1*], A. Landa[1], L.X. Benedict[1], N. Goldman[1], R.Q. Hood[1], K.E. Kweon[1], E.E. Moore[1], A. Perron[1], B. Sadigh[1], C.J. Wu[1], L.H. Yang[1]

[1]Lawrence Livermore National Laboratory, Livermore, California, USA
*soderlind@llnl.gov

We present an *ab initio* free energy model derived from a fully relativistic density functional theory (DFT) electronic structure with dynamic magnetism for δ-plutonium (face-centered cubic, fcc). The DFT model is extended with orbital-orbital interaction in a parameter free orbital polarization (OP) mechanism consistent with previous modeling of plutonium. Gibbs free energy is built from components associated with the temperature dependence of the electronic structure and the corresponding electronic entropy, lattice vibrations within an anharmonic lattice dynamics model, and dynamical fluctuations of the magnetization density, i.e. magnetic fluctuations. The fluctuation model consists of transverse and longitudinal modes driven by temperature induced excitations of the DFT + OP electronic structure. The *ab initio* model thus incorporates fluctuating states beyond the electronic ground state. Thanks to the dynamic magnetism, the theory predicts excellent thermodynamic properties and Gibbs free energy in accord with CALPHAD and semi-empirical modeling developed from the thermodynamic observables. The magnetic fluctuations further explain anomalous behaviors of the thermal expansion in plutonium. Specifically, a thermal expansion for the δ-plutonium system turning from positive to negative at temperatures above room temperature, a tendency for gallium to reduce and remove the negative thermal expansion depending on composition, and a positive thermal expansion for the high temperature ε phase.

We acknowledge support from the US Department of Energy National Nuclear Security Administration's Advanced Simulation & Computing Program at the Lawrence Livermore National Laboratory. This work was performed under the auspices of the US Department of Energy by Lawrence Livermore National Laboratory under Contract No. DE-AC52-07NA27344.

.

Evolution of separation processes for plutonium and minor actinides

Robin Taylor[1,2], Michael Carrott[1], Rebecca Sanderson[1] and Dan Whittaker[1]

[1]United Kingdom National Nuclear Laboratory, Central Laboratory, Sellafield, Seascale, CA20 1PG, United Kingdom

[2]Dalton Nuclear Institute, The University of Manchester, M13 9PL, United Kingdom

Processes for the separation and recovery of plutonium and/or the minor actinides are needed for a variety of applications including the reprocessing of spent nuclear fuels, recovery of actinides from nuclear materials, wastes or residues, separation of radioisotopes for space power or other applications and analytical chemistry. Aqueous separation processes based on solvent extraction and/or ion exchange are the typical methods for these purposes. This paper will summarise some of the developments over the last two decades in our laboratories, with a particular focus on the design and testing of process flowsheets. Firstly, in the development of the PUREX process, which is based on extraction into tributyl phosphate, from established industrial processes to an 'Advanced PUREX' process for the future reprocessing of spent fuels in advanced fuel cycles. Secondly, in the development of novel processes for the recovery of minor actinides, where two scenarios – homogeneous and heterogeneous recycling – are envisaged. 'Spin-off' examples of how this knowledge has been applied to the recovery of americium-241 and plutonium-238 for space power will also be discussed.

PuO_2 Nanoparticles in Water: Unraveling Structure, Reactivity, and Formation Pathways

Matthieu Virot*

ICSM, Univ Montpellier, CEA, CNRS, ENSCM, Marcoule, France ; *matthieu.virot@cea.fr

The characterization of the structural and physicochemical properties of PuO_2 nanoparticles in aqueous solution is essential for elucidating the behavior of long-lived radionuclides in environmental context and nuclear fuel cycle conditions.[1-3] In parallel, controlling and predicting their formation remains a key challenge, with implications for spent nuclear fuel reprocessing, advanced separation processes, and the design of improved nuclear materials. From a fundamental standpoint, recent studies have significantly advanced our understanding of colloidal phases arising from the hydrolysis of Pu(IV).[4-7] These species can now be described as quasi-spherical, crystalline nanoparticles of typically 2–3 nm in diameter, exhibiting a local PuO_2-like structure with pronounced surface-induced disorder. Their formation is driven by the strong hydrolysis and condensation propensity of Pu(IV), and further complicated by coupled redox processes and complexation equilibria, making mechanistic descriptions particularly challenging.[8]

More recently, the involvement of a hexameric Pu(IV) cluster in the formation pathway of PuO_2 nanoparticles was suggested.[9] A corresponding spectroscopic signature has been directly observed under selected ligand environments and controlled experimental conditions.[9-10] The identification of such discrete polynuclear intermediates strongly suggests a non-classical nucleation mechanism, in which PuO_2 nanoparticles emerge not from monomer-by-monomer growth, but from the assembly of metastable polynuclear building units. These findings provide new insights into the molecular processes governing the formation of plutonium oxide nanomaterials. State-of-the-art X-ray absorption spectroscopy and X-ray scattering methods, available at facilities such as the ESRF and SOLEIL synchrotrons, now enable access to multi-scale structural information on such highly radioactive structures at very low concentrations while preserving their native aqueous environment.

This presentation will highlight recent advances from our team, combining laboratory-based studies and synchrotron radiation, in the characterization of colloidal PuO_2 nanoparticles, with a particular focus on their structure, reactivity, and formation mechanisms.

[1] C. Walther and M. A. Denecke, Actinide colloids and particles of environmental concern. *Chem. Rev.* 113 (**2013**) 995-1015. DOI: 10.1021/cr300343c.

[2] M. Virot et al. Synthesis and multi-scale properties of PuO2 nanoparticles: recent advances and open questions. *Nanoscale Adv.* 4 (**2022**) 4938-4971. DOI: 10.1039/D2NA00306F.

[3] L. Amidani et al. Actinide Nanoparticles: Revising Early Developments and Recent Insights from High-Energy-Resolution Fluorescence-Detected X-Ray Absorption Near Edge Structure and Synchrotron Techniques. *Small Sci.* 1 (**2026**) e202500312. DOI: 10.1002/smsc.202500312

[4] E. Gerber et al. The missing pieces of the PuO_2 nanoparticle puzzle. *Nanoscale* 12 (**2020**) 18039-18048. DOI: 10.1039/D0NR03767B.

[5] L. Bonato et al. Probing the local structure of nanoscale actinide oxides: a comparison between PuO_2 and ThO_2 nanoparticles rules out PuO_{2+x} hypothesis. *Nanoscale Adv.* 2 (**2020**) 214-224. DOI: 10.1039/C9NA00662A.

[6] E. Dalodiere et al. Insights into the sonochemical synthesis and properties of salt-free intrinsic plutonium colloids. *Sci. Rep.* 7 (**2017**) 43514. DOI: 10.1038/srep43514.

[7] C. Micheau et al. Relevance of formation conditions to the size, morphology and local structure of intrinsic plutonium colloids. *Environ. Sci.: Nano* 7 (**2020**) 2252-2266. DOI: 10.1039/D0EN00457J

[8] D. Clark, S. Hecker, G. Jarvinen and M. Neu, in The Chemistry of the Actinide and Transactinide Elements, eds. L. Morss, N. Edelstein and J. Fuger, Springer Neth., **2011**, DOI: 10.1007/978-94-007-0211-0_7, 813-1264.

[9] M. Cot-Auriol et al. First observation of $[Pu_6(OH)_4O_4]^{12+}$ cluster during the hydrolytic formation of PuO_2 nanoparticles using H/D kinetic isotope effect. *Chem. Commun.* 58 (**2022**) 13147-13150. DOI: 10.1039/D2CC04990B.

[10] Capturing the Elusive: A Snapshot of the Pu(IV) Hexanuclear Cluster Intermediate in the Birth of PuO_2 Colloidal Nanoparticles. *Inorg. Chem.* 64 (**2025**) 17178–17188. DOI: 10.1021/acs.inorgchem.5c01938.

Oral Abstracts

Abdul-Jabbar, Najeb	Radiogenic Effects on the Thermal Response of Plutonium
Anderson, Nickolas	Outer- Coordination Sphere Effects in Aqueous Solutions
Archer, Emma	A Crystallographic and Spectroscopic Study of Mixed Actinide Oxalates
Atta-Fynn, Raymond	Large-Scale Ab Initio Modeling of ε-Pu/δ-Pu and α-Pu/δ-Pu Interfaces
Balas, Johannes	Exploring Bonding Trends and Fundamental Properties in Pyridine-2-thiolato Complexes of Tetravalent Actinides (Th - Pu)
Batista, Enrique	Charge States, Oxygen Transport, and Helium Accumulation in PuO_2 and α-Pu_2O_3
Bauer, Eric	Nuclear magnetic resonance studies of Pu-B compounds
Beaux, Miles	Electronic and Surface Features of $PuCoGa_5$
Blakemore, James	Comparing the Reduction- and Acid-Promoted Reactivity of a Homologous Series of Plutonium, Neptunium, and Uranium Complexes
Boehm, Alex	Temperature Dependent Changes in the Photoemission Lineshape of δPlutonium
Bottin, François	Ab initio study of the Ce and Pu oxide surface reactivity with respect to O_2 and H_2O
Bouchet, Johann	Elastic properties of actinides systems at high temperature with machine learning
Bourasseau, Emeric	Thermodynamic Properties of $(U,Pu)O_2$: Impact of Defects and Fission Products on the Bredig Transition
Bourgès, Gilles	Future Aqueous Nitrate Process Line for Plutonium Recycling
Brown, Alexandra	Combustion Ion Chromatography (CIC) Method Development and Validation for Characterization of Fluoride and Chloride in Actinide Materials
Brown, Donald	Evolution of Helium Bubble Characteristics During Heating of Aged PuGa Alloys: An In-Situ Small Angle X-ray Scattering Study
Carver, D. Travis	In-Situ High Energy X-Ray Imaging and Diffraction to Monitor Corrosion of PuGa Alloy
Cette, Daphné	Enabling Americium-Powered Space Missions. High Temperature Stability of $(Ce,U)O_2$ Surrogates for the $(Am,U)O_2$ Fuel Source
Chamberlain, Jarom	Plutonium Metallurgy and Exposure onto a Tungsten Coated Substrate
Chen, Lena	Evaluating Disposal of Plutonium Wasteforms
Childs, Bradley	The Effects of Pu Particle Formation during Precipitation and Calcination on Aqueous Processing
Chung, Brandon	Mapping Morphological and Chemical Signatures of Plutonium and Uranium Materials for Nuclear Forensics

Davie, William	A Machine Learned Interatomic Potential for Helium in Plutonium Dioxide
Di Pietro, Silvina	Learning Tracks: A New Method to Develop the Next Generation
Dunn, Stuart	Nuclear Forensic Signatures of Plutonium Hydroxide Precipitation and Calcination products
El Monjid, Alison	ADOA Route for $(U,Pu)O_2$ Mixed Oxides: Multiparametric Synthesis Optimization and Preliminary Sintering Performance
Estevenon, Paul	Pu(IV) Silicate, Synthesis and Advanced Characterisation of a Key Compound for Plutonium Environmental Behavior
Farnaby, Joy	Experimental Actinide Chemistry in support of UK Civil Plutonium Inventory Technical Challenges
Fellhauer, David	Pu(VI) hydrolysis in aqueous alkali and alkaline earth metal solutions: reaction pathways and thermodynamics
Friskney, Aidan	Ceramic Wasteform and Process Development for Pu Disposition
Génin, Renaud	Influence of Cooling Speed and Aluminum Content on the Microstructure of As-Cast δ-PuAl Alloys
Gofryk, Krzysztof	Advancing Actinide Quantum Materials at INL's Glenn T. Seaborg Institute: The Case of PuB_6
Golwankar, Riddhi	Electrochemical behavior of Actinides (An) in molten alkali halide salts
Gonzales, Ivana	Computational Insights into Plutonium Chemistry: From Density Functional Theory to Kinetic Modeling
Greb, Fabian	Solubility of Np_2O_5(cr) and Hydrolysis of Np(V) in Neutral to Alkaline NaCl-NaOH Solutions
Groedler, Dennis	Metallophilic Actinide-Platinum Interactions in Bimetallic Pyridyloxy Complexes
Guilbaud, Philippe	Actinide (VI), and Nitric Acid Speciation Studies in Separation Processes using N,N-Dialkylamide Extractants
Guillaumont, Dominique	The Effect of Diluent on Uranium(VI) and Plutonium(IV) Solvent Extraction with Monoamide Extractants
Hayne, Mathew	Bridging Scales: Comparative Elastic-Modulus Measurements by Resonant Ultrasound Spectroscopy, Nano-Indentation, and Bulk Mechanical Tests
Heiner, Benjamin	Oxygen Vacancies Drive f-orbital Density into the Band Gap of Np/Pu Oxides
Hernandez, Sarah	ToF-SIMS Analysis of Heat-Treated Aged 2 at.% Ga-Stabilized δ-Pu
Higginson, Matthew	Developments in plutonium analysis at the AWE
Holmbeck, Gregory	The Influence of Transuranic Actinyl Complexation on Ligand Radiolysis
Jolly, Lionel	Study of elements distribution in the δ-Pu oxide scale
Kelly, Sheridon	Speciation of Plutonium in Molten Salt Environments
Kennedy, Rory	Plutonium Bearing Metallic Transmutation Fuels – Phase Relations and Thermal Properties

Kohlgruber, Tsuyoshi	Aqueous Recovery of Plutonium at Lawrence Livermore National Laboratory
Kravchuk, Dmytro	Reactions of Pu(VI) and Pu(V) in Alkali Hydroxide Solutions: New Pu Solid Phases and Insights into Pu Speciation at High pH
Kucinski, Theresa	Improved Characterization of Helium Bubble in Naturally Aged Plutonium with Scanning Transmission Electron Microscopy (STEM)
Kweon, Kyoung	Ab Initio modeling of He Bubbles in δ-Pu
Kynman, Amy	The Role of Transient Plutonium Oxidation States in the Radiation-Induced Redox Cycling of Pu(VI) in Aqueous Nitric Acid Solutions
La Pierre, Henry	Redox Chemistry and Reactivity of Homo-and Heteroleptic Neptunium and Plutonium Complexes
Landa, Alexander	An ab initio Molecular Dynamics Study of Key Thermodynamical Input Parameters for Computer Simulation of U-6Nb Solidification
Levin, Zachary	Micromechanical Characterization of α- and δ-Phase Plutonium via Advanced Nanoindentation Techniques
Lim, Rachel	Oxygen K-edge Scanning Transmission X-ray Microscopy (STXM) of Plutonium Oxide
Maloubier, Melody	Experimental and Quantum Chemical Insights into the coordination chemistry of Protactinium(V) in solution
Margate, Julien	Vibrational identification of uranyl peroxo-carbonate complexes in solution: insights from ^{18}O labeling and DFT
Mathew, Kattathu	Mass Fractionation Corrections in TIMS Isotope Ratio Measurements: Comparison of Correction Factors in Total Evaporation Analysis of Actinides
Mazza, Alessandro	X-ray Photoemission Studies of Pu_6Fe
Monreal, Marisa	The Launch of the Plutonium Science Laboratory (PluS Lab) at Los Alamos National Laboratory
Munoz, Maeva	Stability and Aging Pathways of Pu(IV) Hexanuclear Clusters in aqueous solution: Influence of Ligand Environment and Alpha Radiolysis
Olive, Daniel	Plutonium Oxidation Studied at Different Temperatures
Pace, Kristen	Probing the Effects of Iron and Uranium Impurities on the Melt Behavior of Plutonium Alloys using Differential Scanning Calorimetry
Parker, Gannon	Qualification of Plutonium and Iron Analysis Capabilities within Los Alamos National Laboratory Plutonium Facilities
Patenaude, Hannah	Diamonds are an Actinide's Best Friend: Electrochemical Discrimination of U and Pu Redox Couples Using Boron-Doped Diamond
Piccinelli, Davide	Multi-Fidelity Gaussian Process Regression for Modeling the Thermal Properties of MOX Nuclear Fuel
Plohr, Jeeyeon	Helium Bubble Evolution in Aged Plutonium

Ramirez, Bianca	Development of Water-Equivalent Solid Calibration Standards for Plutonium Gamma-Ray Nondestructive Assay
Ramos, Frank	Utilizing 244Pu for High Resolution Plutonium Concentration Determinations Via Isotope Dilution Measurements and Thermal Ionization Mass Spectrometry
Ravat, Brice	Oxidation of Pu Alloys Stabilized in δ-Phase: Characterization of the Microstructure of the Oxide Scale
Real, Florent	The Signature of the Mono-Oxo Bonding in Protactinium(V) in the M4-Edge HERFD spectrum: a theoretical and experimental study
Robles, Geronimo	Synthesizing Pu-U-Ga Ingots for the Advancement of the First Multiscale Alloy Prediction Model
Rodriguez, Daniel	Gas Dosing and Growth of Pu Oxycarbide Films: Characterization of the Surface using XPS and ToF-SIMS
Roussel, Paul	In search of the σ-Pu phase
Rowberg, Andrew	Point Defect and Impurity Incorporation in Plutonium Oxides
Roy, Gabriel	Nanoscale Effects in Plutonium Dioxide: How Size Shapes Structure and Electronic Properties
Schenk, Sven	Increased Sensitivity of Pu M5-edge CC-RIXS to Bond Covalency in PuO_2 in Comparison to Pu M4-edge RIXS
Schmidt, Moritz	Chemical bonding in actinide quinolinates from Th to Pu
Shauf, Elise	Investigation of Manufacturing and Processing Variables on the Mechanical Behavior of Tungsten During Actnide Pyroprocessing
Sockwell, Kirstin	Photochemistry of Aqueous Plutonium(VI) Oxalate
Startt, Jacob	Molecular Dynamics Modeling of Helium Bubbles in Delta- and Epsilon-Pu
Stuke, Kevin David	Aging and Oxidation Mechanisms of PuO_2 and Pu-doped UO_2 based Nanomaterials under Ambient Conditions in Maintaining the Stability of Spent Nuclear Fuel
Takao, Koichiro	Crystallization of UO_2^{2+} and Pu^{4+} Nitrato Complexes with 1,3-AdamantylBridged Diamide Molecules towards Direct Co-recovery of Nuclear Fuel Materials from HNO_3(aq)
Tamain, Christelle	Contribution of coordination chemistry studies to the speciation of neptunium and plutonium in organic phases
Tobin, J G	Pu 5f Population: The Case for n = 5.0
Tutchton, Roxanne	Temperature Dependent Electronic Structure and Optical Properties of δ-Pu
Weinmann-Smith, Robert	Implementing the DAIL NDA Instrument for LANL TRU Waste Material Control and Accounting
Wheeler, David	The role of helium bubbles in changes to the mechanical properties of aged plutonium

Wilson, Richard	Insights into the Solvation and Solvent Exchange Reactivity of Plutonium in Non-Aqueous Solutions
Yang, Ping	Probing the Limits of 5f Bonding in Actinides through Oxidation State Control and Redox-Active Ligands

Radiogenic Effects on the Thermal Response of Plutonium

Najeb Abdul-Jabbar[1*], Kristen Pace[1], Sarah Hernandez[1], Douglas Smith[1], Alberto Gomez[1], Michael Kopriva[1], Shane Mann[1], Jeremy Mitchell[1]

[1]Los Alamos National Laboratory, Los Alamos, United Sates; *najeb@lanl.gov

Crystallographic defects, chemistry variations, and helium (He) bubble ingrowth induced by radiation damage (via alpha decay) are key topics for understanding materials phenomena in aged plutonium (Pu). Past work has shown quantifiable variations in heat capacity and thermal expansion in aged Pu alloys that are not observed in newly synthesized specimens. This is driven by thermal defect recovery at sub-solidus temperature regimes in the delta phase field. Furthermore, recent calorimetry experiments up to Pu melting temperatures have revealed exothermic energy release phenomena, which may be related to the collapse of helium bubbles entrapped in bulk Pu metal. This likely stems from the mechanisms that drive He bubble coarsening in Pu, which remain a topic of debate. To probe this issue further, recent dilatometry experiments on aged Pu alloys in the epsilon phase have shown significant thermal expansion gains followed by saturation during isothermal holds exceeding 500 °C. Moreover, calorimetry measurements show this temperature-induced swelling is not accompanied by deviations in measured heat flow. Analysis via time-of-flight secondary ion mass spectrometry (ToF-SIMS) post-experiments revealed evident porosity on the sample surface, coupled with chemical heterogeneities. Bulk microstructure will be investigated using high-resolution transmission electron microscopy to probe the effects of high-temperature isothermal holds on He bubble networks and chemistry in aged Pu. The integrated results may give more direct insight into He bubble growth kinetics during the epsilon to liquid phase transformation in aged Pu alloys and will be discussed in further detail in this presentation.

Outer- Coordination Sphere Effects in Aqueous Solutions

Brittany L. Huffman, Brian T. Arko*, Julia G. Knapp, Sara L. Adelman*, Nickolas H. Anderson*, Manuel L. Besmer, Aldo M. Jordan, Stosh A. Kozimor,* Travis Marshall-Roth, Gabriella O. Morales, Monica S. Mullis, Alexandra L. Nagelski, Felipe A. Pereiro, Thomas E. Shaw, Samantha S. Stegman, Isabel J. Tang.

Los Alamos National Laboratory, Los Alamos, NM, USA.

LA-UR-26-27345

Defining the relative influence of *inter*molecular and *intra*molecular forces is a fundamental problem in chemistry that is difficult to quantify. Identifying methodologies to determine how outer-sphere ions effect reactivity in aqueous solutions is a major challenge in the actinide chemistry field. In this presentation we have discovered a system that is ripe for interrogating this critical issue in the precipitation of actinide chloride complexes ($[UCl_6^{-2}]$, $[UO_2Cl_4^{-2}]$, and $[PuCl_6^{-2}]$) with cesium cations (Cs^+). Secondary cations, like the alkali and alkali earth metals, will interact with these actinide chloride complexes and potentially inhibit the precipitation reaction with Cs^+, allowing us to interrogate the strength of the outer-sphere ion effect. Additionally, the degree by which the solvation sphere affects reactivity is impacted by the identity and speciation of the actinide in solution. Herein we reveal trends on the impact of the outer sphere cation effect that may inform the community about the importance of these tertiary ion effects and postulate how their presence may impact desired reactivity.

A Crystallographic and Spectroscopic Study of Mixed Actinide Oxalates

Emma M. Archer[1], Frances E. Zengotita[1], Brian M. Rotermund[1], S. Olivia Gunther[1], Joshua J. Woods[1], David K. Shuh[1]*, Jennifer N. Wacker[1*]

[1] Chemical Sciences Division, Lawrence Berkeley National Laboratory, Berkeley, CA USA 94720; *dkshuh@lbl.gov, *jwacker@lbl.gov

Oxalic acid is a precipitating agent commonly used for the complexation of *f*-elements in the nuclear fuel cycle (NFC), yielding metal oxalates that serve as precursors toward metal oxide materials after incineration. Owing to the high stability constants of actinides and oxalic acid, prompt precipitation of metal oxalates often yields poorly ordered or amorphous solids. This severely limits the bonding and extended structural information crucial to improving separations processes relevant to the NFC. Although many *f*-element oxalate compounds have been evaluated independently, it is of special interest to continue characterizing mixed metal oxalates that would likely be present in the NFC, expanding on existing systems that contain uranium-transition metals, uranium-plutonium, uranium-thorium, uranium-americium, and plutonium-americium. In particular, plutonium-americium oxalate compounds have been minimally explored, making it of great interest to systematically expand on the crystallographic and spectroscopic nature of these phases. These studies provide an opportunity to understand the fundamental coordination chemistry of mixed metal oxalates and yield insight into periodic bonding trends within the oxalate framework. A variety of synthetic pathways to isolate mixed metal oxalates will be discussed, highlighting structural deviations inherent to these multimetallic systems. Furthermore, employing methods – such as X-ray absorption spectroscopy (XAS) with scanning transmission X-ray microscope (STXM) – to systematically characterize composition and homogeneity of mixed actinide oxalate systems allow us to obtain signatures that assist nonproliferation efforts throughout the precipitation and incineration processes within the NFC. By selectively crystallizing discreet *f*-element oxalate phases through a variety of synthetic approaches, the oxidation states, homogeneity, and coordination behavior are identified for multiple lanthanide and actinide compounds. More broadly, crystallography and spectroscopy can bridge a gap in signature development for *f*-element oxide precursors, like oxalates, to support NFC advancement.



Figure 1. Schematic visualizing the variety of characterization techniques employed to evaluate the bimetallic *f*-element oxalate compounds. Image generated by Cborg (Supported by the Director, Office of Science, Office of Basic Energy Sciences, of the U.S. Department of Energy under Contract No. DE-AC02-05CH11231).

Large-Scale *Ab Initio* Modeling of ε-Pu/δ-Pu and α-Pu/δ-Pu Interfaces

Raymond Atta-Fynn[1*], Larissa M. Woryk[1], Sarah C. Hernandez[1], Aaron A. Kohnert[1], and Najeb Abdul-Jabbar[1]

[1]Los Alamos National Laboratory, Los Alamos, New Mexico
*attafynn@lanl.gov

Characterizing the atomic-scale structure of plutonium (Pu) interfaces is critical for the long-term management and storage of nuclear materials. To this end, we employ an efficient Density Functional Theory (DFT) framework designed to model large interfacial systems. Our methodology utilizes optimal, strictly localized basis functions--which vanish beyond a specified confinement radius--paired with norm-conserving pseudopotentials for Pu [1,2]. Compared to traditional plane-wave methods, localized bases significantly reduce the number of functions required to expand Kohn-Sham eigenstates. This computational efficiency enables structural relaxation and ab initio molecular dynamics (AIMD) over extended simulation timescales at a moderate computational cost.

In this work, we present results for large-scale ε-Pu(110)/δ-Pu(111) interfaces based on the Kurdjumov-Sachs (KS) and Nishiyama-Wassermann (NW) orientation relationships. We further investigate α-Pu(100)/δ-Pu(111) and α-Pu(001)/δ-Pu(111) interfaces, evaluating their stability through the work of adhesion and interfacial energies. Emphasis is placed on the interplay between interfacial geometry, the Pu 5*f* electronic structure, and the impact of localized defects on structural and electronic properties at these boundaries.

References:

[1] A. García, N. Papior, A. Akhtar, E. Artacho, V. Blum, E. Bosoni, P. Brandimarte, M. Brandbyge, J. I. Cerdá, F. Corsetti *et al.*, *Siesta: Recent developments and applications*, J. Chem. Phys. **152** (2020).
[2] Raymond Atta-Fynn, Sarah C. Hernandez, and Roxanne M. Tutchton, *Localized basis set for plutonium*, Phys. Rev. B **109**, 085124 (2024).

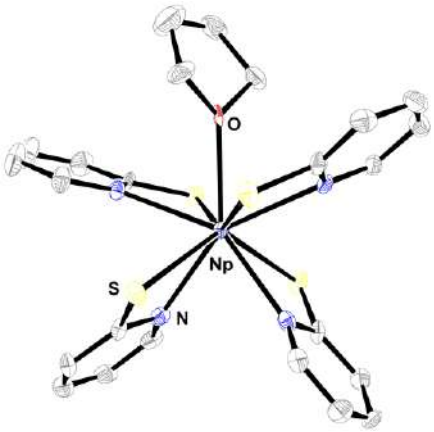
Exploring Bonding Trends and Fundamental Properties in Pyridine-2-thiolato Complexes of Tetravalent Actinides (Th – Pu)

J. Balas[1], C. Urbank[2], P. Kaden[1], M. Patzschke[1], J. März[1], K. O. Kvashnina[1,3], M. Schmidt[1,4], T. Stumpf[1], R. Gericke[1*]

[1]Helmholtz-Zentrum Dresden – Rossendorf, Dresden, Germany; [2]Institute of Inorganic and Applied Chemistry, Hamburg, Germany; [3]The Rossendorf Beamline at ESRF, Grenoble, France; [4]Institute of Materials Chemistry, Senftenberg, Germany; *r.gericke@hzdr.de

The coordination chemistry of the actinides, a key area of research for nuclear waste management and environmental assessment, remains underdeveloped compared to that of transition metals and lanthanides.[1] Previous studies have focused on thorium and uranium, typically employing hard oxygen donor ligands. To gain a deeper understanding of the unique bonding characteristics of 5*f* elements, systematic investigations with a variety of donor atoms, are essential. Early actinides, in particular, are expected to exhibit enhanced covalent bonding with soft donor ligands, such as those containing sulfur.[2,3]

To address this gap, the fundamental properties of actinide (Th – Pu) complexes featuring the soft *(N,S)*-donor ligand pyridine-2-thiolate (PyS) were systematically investigated. Inspired by the previously published $[U(PyS)_4(THF)]$ complex,[4] we synthesized $[An(PyS)_4(THF)_n]$ and $K[An(PyS)_5]$ complexes, including the first structurally characterized Np compound with mixed *(N,S)*-donor ligands $[Np(PyS)_4(THF)]$ (see figure).[2] Comprehensive characterization (single crystal X-ray diffraction, IR spectroscopy, X-ray absorption spectroscopy, NMR spectroscopy, SQUID magnetometry, and computational studies) revealed trends in electronic structure, magnetism, and bonding across the actinide series. To elucidate the nature of bonding, both qualitative and quantitative analyses were conducted. For the $[An(PyS)_4(THF)]$ complex series, quantum chemical calculations and experimental observations consistently indicate increasing covalency in the An–S bonds. Notably, the Pu–S bond exhibits substantial covalent contributions (34%), contrasting with the more ionic An–N and An–O bonds.[2] These results are relevant to the selectivity of soft donor ligands in transuranium element separations and can contribute to a better understanding of 5*f* element chemistry.



This work was funded by the German Federal Ministry of Research, Technology and Space (BMFTR, 02NUK077B, FENABIUM-II) and the German Federal Ministry for the Environment, Climate Action, Nature Conservation and Nuclear Safety (BMUKN, 1501667, Am-BALL).

[1] C. R. Groom, I. J. Bruno, M. P. Lightfoot, S. C. Ward, *Acta Crystallogr.* **2016**, *72*, 171–179.
[2] J. Balas, C. Urbank, P. Kaden, M. Patzschke, J. März, K. O. Kvashnina, M. Schmidt, T. Stumpf, R. Gericke, *Inorg. Chem.* **2025**, *64*, 21919–21931.
[3] D. Pividori, M. E. Miehlich, B. Kestel, F. W. Heinemann, A. Scheurer, M. Patzschke, K. Meyer, *Inorg. Chem.* **2021**, *60*, 16455–16465.
[4] A. J. Gaunt, B. L. Scott, M. P. Neu, *Inorg. Chem.* **2006**, *45*, 7401–7407.

Charge States, Oxygen Transport, and Helium Accumulation in PuO_2 and α-Pu_2O_3

Enrique R. Batista*, Sandip Aryal, Gaoxue Wang, Ping Yang

Theoretical Division, Los Alamos National Laboratory, Los Alamos, NM USA
*erb@lanl.gov

Plutonium metal is intrinsically protected by an oxide overlayer composed of PuO_2 and, beneath it, α-Pu_2O_3. The stability, thickness, and long-term evolution of these layers are largely governed by intrinsic oxygen point defects. In the bulk, other impurities, remnants of processing and radioactive decay byproducts, such as helium, are present. Predictive control of oxidation and aging therefore requires a quantitative understanding of defect thermodynamics and transport across both oxides and their surfaces.

Here we present a unified first-principles investigation of intrinsic defects and helium interstitials in PuO_2 and α-Pu_2O_3, focusing on formation energetics, charge-state stability, electronic structure, magnetic response, and migration barriers. Particular emphasis is placed on the oxygen-terminated PuO_2 (111) surface, which dominates the equilibrium morphology of the dioxide.

In PuO_2, oxygen and plutonium defects exhibit multiple charge states within the band gap, with stability strongly modulated by oxygen chemical potential and defect-induced redistribution of Pu 5f electrons. Defect formation generates pronounced local lattice distortions, renormalizes magnetic moments, and introduces deep electronic trap states. Oxygen vacancy diffusion proceeds via sequential nearest-neighbor hopping with well-defined activation barriers. In contrast, oxygen interstitial migration does not occur through simple direct motion; instead, we identify a lattice-mediated exchange mechanism that lowers the activation barrier substantially relative to intuitive diffusion pathways. This mechanism provides a previously unresolved description of oxygen transport in the dioxide.

At the (111) surface, oxygen vacancies are significantly more stable than in the bulk, preferentially form in the outermost layer, and are stabilized predominantly in ±2 charge states. Surface defect energetics differ qualitatively from bulk behavior, directly impacting surface termination, reactivity, and oxygen exchange with the environment. By integrating bulk and surface defect thermodynamics, we predict equilibrium relationships between PuO_2 and α-Pu_2O_3 as a function of oxygen chemical potential, establishing a direct connection between point-defect energetics and macroscopic oxide-layer thickness.

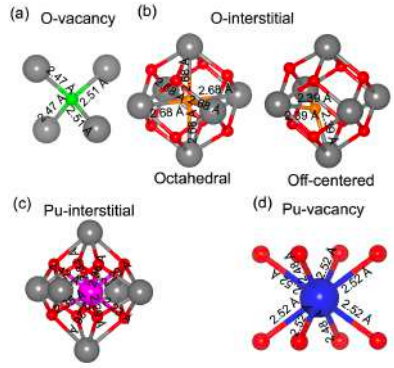


Fig. 1: Relaxed atomic configurations around the studied defect sites. Only the local atomic environment surrounding each defect is shown.

In α-Pu_2O_3, intrinsic defects likewise introduce deep in-gap states and strongly perturb local structure and magnetism. However, clear electronic distinctions emerge between the two oxides. PuO_2 exhibits charge-transfer insulating character, with defect energetics tightly coupled to oxygen chemical potential and surface stabilization. In contrast, α-Pu_2O_3 displays stronger Mott–Hubbard behavior associated with enhanced localization of Pu 5f electrons in the reduced oxidation state. This difference produces distinct defect stability trends: under O-rich/Pu-poor conditions, plutonium vacancies and oxygen interstitial

configurations are favored, whereas O-poor/Pu-rich environments stabilize oxygen vacancies. The contrasting defect chemistries underscore the central role of stoichiometry and oxidation state in governing transport and redox equilibria across plutonium oxides.

We further examine helium interstitials in both PuO_2 and α-Pu_2O_3. Helium, generated continuously by α-decay, accumulates within the oxide lattice and represents a primary driver of long-term structural evolution. Calculated formation energies identify preferred interstitial sites and quantify the energetic cost of helium incorporation. Migration pathways and activation barriers determine helium mobility and trapping propensity. Helium insertion induces local lattice swelling and modifies the surrounding electronic environment, providing atomistic insight into defect-assisted trapping and the early stages of helium accumulation. These results establish a mechanistic foundation for modeling helium retention, clustering, and their implications for long-term mechanical stability.

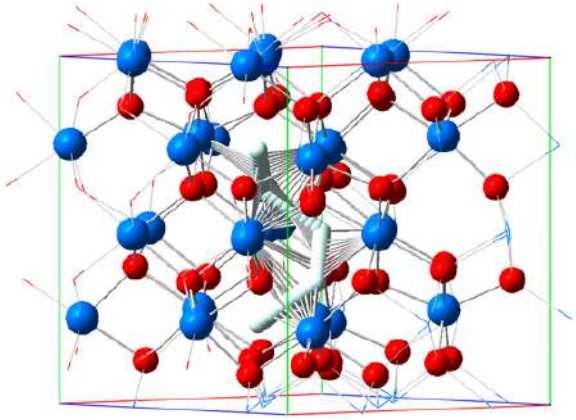


Fig. 2: Diffusion path of a single He atom through the lattice of Pu_2O_3. The activation barrier of diffusion is very low due to the wide gaps left by what would be missing oxygen atoms in PuO_2.

Together, these findings provide a coherent atomistic framework linking intrinsic defect chemistry, oxygen transport, surface stability, oxide-layer evolution, and helium accumulation in plutonium oxides. By connecting electronic structure, charge-state thermodynamics, and migration kinetics across both PuO_2 and α-Pu_2O_3, this work advances predictive modeling of oxidation and aging processes central to plutonium performance in energy and stewardship environments.

References:

- S. Aryal, G. Wang, P. Yang, and E.R. Batista, “Charged Defects and Oxygen Migration in Plutonium Dioxide: First Principles Insights into Defect Energetics and Stability,” ACS Applied Energy Materials (2026)
- S. Aryal, G. Wang, P. Yang, and E.R. Batista, “A hybrid-DFT Study of Charged Defects Formation in Pu_2O_3,” Journal Nuclear Materials (2026)

Nuclear magnetic resonance studies of Pu-B compounds

Eric D. Bauer[1*], S. Park[1], A. P. Dioguardi[1], W. A. Phelan[1], D. C. Arellano[1], D. Prada[1], J. D. Thompson[1], and M. Hirata[1]

[1]Los Alamos National Laboratory, Los Alamos, New Mexico 87545, USA; *edbauer@lanl.gov

Compounds formed of plutonium with boron and other light elements exhibit a wide range of behavior from antiferromagnetic order (PuC) [1], insulating (PuO_2, PuF_4 [2]) and mixed-valence states (PuB_6) [3], to exotic topological insulating states (PuB_4 [4,5], PuB_6 [6]). The discovery of the direct Pu-239 nuclear magnetic resonance (NMR) signal in PuO_2 [7,8] and PuB_4 [4] provides an opportunity to explore and understand the physical properties, electronic structure, and self-irradiation damage of plutonium-based materials at the atomic scale. We present a study of the physical properties and direct Pu-239 NMR resonance in a single crystal of the correlated topological insulator PuB_4, and an arc-melted, mixed-phase polycrystalline sample of PuB_6 / PuB_{12}. The temperature dependence of the Pu-239 Knight shift (K_s) and spin-lattice relaxation time (T_1) indicate that PuB_4 adopts a nonmagnetic state with gap-like behavior, consistent with the topological insulating behavior observed in electrical resistivity measurements. The damage caused by the radioactive decay of Pu-239 does not appear to affect the static properties of PuB_4 significantly, but changes in the dynamic properties (spin-lattice and spin-spin relaxation) are observed [9]. The direct Pu-239 NMR signal in PuB_6 at T=4 K is close to the resonance frequency of PuB_4 [4]. Another NMR signal at slightly higher magnetic field is also observed, consistent with the direct Pu-239 resonance of PuB_{12} in the PuB_6/PuB_{12} mixed-phase sample. B-11 NMR supports this Pu-239 signal assignment with the occurrence of two B-11 superposed spectra: high-symmetry B-11 spectral features from PuB_6, and low-symmetry B-11 features in PuB_{12}, similar to other dodecaborides. We discuss our results within the context of the structural similarities shared by the PuB_4, PuB_6, and PuB_{12} materials.

[1] J. L. Green et al. J. Nucl. Mat. **34**, 281 (1970); **[2]** D. L. Clark, S. S. Hecker, G. D. Jarvinen, M. P. Neu, in The Chemistry of the Actinides and Transactinides, 3rd Edition, L. R. Morss, N. M. Edelstein, J. Fuger, Eds. 2006, Springer, New York, 813-1264, **[3]** J. L. Smith and Z. Fisk, J. Appl. Phys. **53**, 7883 (1982); **[4]** A. P. Dioguardi et al. Phys. Rev. B **99**, 035104 (2019); **[5]** H. Choi et al. Phys. Rev. B **97**, 201114(R) (2018); **[6]** X. Deng et al. Phys. Rev. Lett. 111, 176404 (2013); **[7]** H. Yasuoka et al. Science **336**, 901 (2012); **[8]** K. Rana et al. Inorg. Chem., **64**, 21791 (2025); **[9]** S. B. Blackwell et al. Physical Review B **111**, 075152 (2025).

Electronic and Surface Features of $PuCoGa_5$

Miles F. Beaux II[1*], Benjamin R. Heiner[1], Andrew J. Yost[2], William J. I. DeBenedetti[1], David C. Arellano[1], Derek V. Prada[1], Paul H. Tobash[1]

[1]Los Alamos National Laboratory, Los Alamos, NM, USA; [2]Scienta Omicron, Inc., Denver, CO, USA; *mbeaux@lanl.gov

The first ever scanning tunneling microscopy and spectroscopy (STM/S) experiments have been performed on a plutonium intermetallic, $PuCoGa_5$, in its normal state. The first ever surface structure images of a plutonium material by STM have been taken, revealing Moiré patterns consistent with different faces of the crystal structure. STS measurements reveal $PuCoGa_5$ to be a semimetal above the critical superconducting temperature, which is corroborated by point contact spectroscopy and nuclear magnetic resonance. LA-UR-26-21931

Comparing the Reduction- and Acid-Promoted Reactivity of a Homologous Series of Plutonium, Neptunium, and Uranium Complexes

Davis Curry[1,2], Emily Mikeska[1,2], Riddhi Golwankar[1], Alexander Ervin[1,2], Natalie Lind,[1] Asmita Sen[3], Jochen Autschbach[3], Richard Wilson[2], James Blakemore[1,2*]

[1]Department of Chemistry, University of Kansas, Lawrence, Kansas, United States; [2]Chemical Sciences and Engineering Division, Argonne National Laboratory, Lemont, Illinois, United States; [3]Department of Chemistry, University at Buffalo, State University of New York, Buffalo, New York, United States; *blakemore@ku.edu

The redox chemistry of the actinyl cations (AnO_2^{n+}) heavily influences their reactivity and speciation in solution, but the redox and reactivity properties of the actinyls in non-aqueous media has received far less attention than they deserve. In this presentation, the non-aqueous electrochemistry of a homologous series of mononuclear plutonium, neptunium, and uranium complexes will be discussed, along with the reactivity that the complexes display upon reduction and treatment with acid(s) in organic solvents. On the one hand, the starting mononuclear complexes are rather stable and supported by a chelating and strongly donating pentadentate ligand that drives stabilization of the high-valent An(VI) forms of the complexes. On the other hand, reduction of the starting complexes and exposure to acid sources results in the formation of unconventional multinuclear species in all cases, indicating reactivity that can be discussed in the framework of proton-coupled electron transfer (PCET). Spectroscopic and spectrokinetic studies aimed at elucidating mechanistic details of the formation of the multinuclear species will be discussed, including findings from computational studies aimed at quantifying the properties of reduced/protonated forms of the complexes.

Temperature Dependent Changes in the Photoemission Lineshape of δ-Plutonium

Alex Boehm[1,*], William S. Ponder[1], Daniel T. Olive[1], Alessandro R. Mazza[1]

[1]Materials Science and Technology, Los Alamos National Laboratory, Los Alamos, USA;
*amboehm@lanl.gov

The actinide series exhibits a unique evolution in electronic structure as the 5f electrons transition from predominantly itinerant behavior in the early actinides to localized in the late actinides, with plutonium situated at this crossover. This dichotomy is reflected in the characteristic lineshape of the Pu 4f core-level spectrum, commonly interpreted in terms of competing screening channels of the 4f core hole and associated with the degree of 5f localization and fluctuations in the 5f occupancy. Owing to the high reactivity of Pu metal and the surface sensitivity of photoemission techniques, alternative interpretations have attributed the poorly screened spectral weight, at least in part, to surface contamination or chemical inhomogeneity.

Here we present temperature-dependent valence-band and core-level photoemission measurements of δ-Pu metal, focusing on systematic changes in the relative intensities of the well-screened and poorly screened components. By examining the evolution of both core-level lineshapes and near-Fermi-level electronic structure, we assess the extent to which the observed behavior reflects intrinsic electronic correlations versus extrinsic surface effects. These results provide new insights on 5f electron localization and core-hole screening in plutonium and establish a foundation for future temperature-dependent spectroscopic investigations of correlated actinide systems.

Ab initio study of the Ce and Pu oxide surface reactivity with respect to O_2 and H_2O

Grégory Geneste[1,2] and François Bottin[*1,2]

[1]CEA, DAM, DIF, F-91297 Arpajon, France; [2]Université Paris-Saclay, CEA, LMCE, 91680 Bruyères-le-Châtel, France;*francois.bottin@cea.fr

Understanding and interpreting experimental results of cerium and plutonium oxides under external chemical environments is crucial for nuclear fuel storage. The corresponding surfaces of these compounds are known to be ideal (AO_2) or defective (AO_{2-x}, A_2O_3...) according to the chemical environment. In this work, we consider the reaction of different gases (O_2 and H_2O) with these surfaces by means of state-of-the-art *ab initio* simulations. In this way, various chemical species and defects that can form on the surface following gas adsorption are identified. The nature of charge transfers, the potentially exothermic character of the reactions involved, and the thermodynamic stability of the terminations as a function of the external chemical environment is also studied. The associated experimental signatures -- XPS (X-ray Photoelectron Spectroscopy) and IR (Infrared) -- of these chemical species, are directly compared with experimental results.

In these simulations we consider the same calculation conditions used in previous works on the volume and clean surfaces [1, 2, 3, 4]. In particular, we carry out *ab initio* simulations using the ABINIT calculation code [5] in the PAW (Projector Augmented Wave) formalism and using the occupation matrix control method [1]. To simulate different chemical environments, we consider the adsorption of two molecules (O_2 and H_2O) on various orientations ((111), (110) and (100)) of the AO_2 surfaces, exposing understoichiometric or overstoichiometric terminations with (2x2) or (3x3) reconstructions. These surfaces are modeled using slabs with a stacking sequence of 6 AO_2 formula units (see left panel of Figure 1). The corresponding thermodynamic stability of these surfaces is deduced in the Grand canonical ensemble (see right panel of Figure 1).

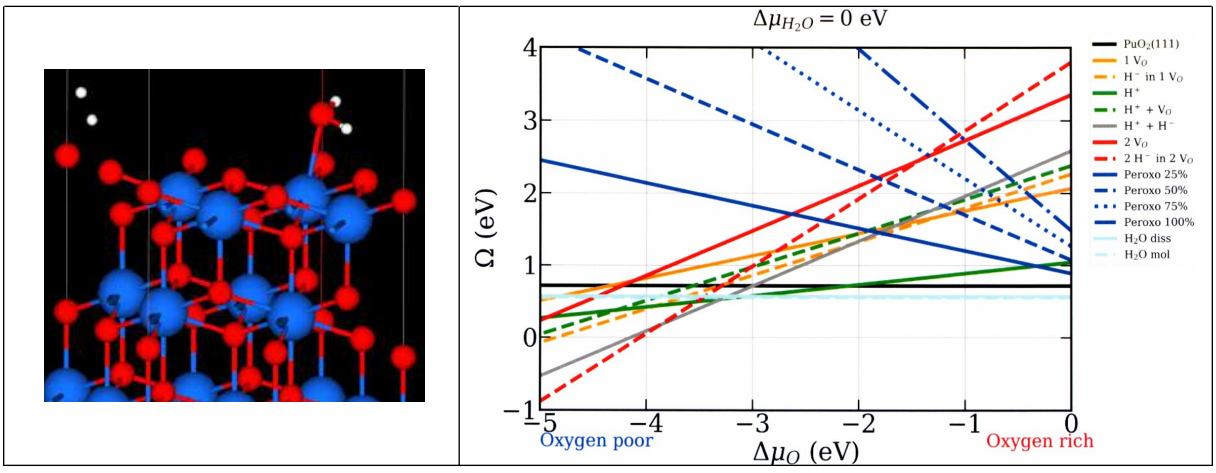


Figure 1 : Left: Adsorption of molecular H_2O on PuO_2-O(111) surfaces. Right: Surface Grand potentials of various terminations as a function of the oxygen chemical environment.

On the perfect PuO_2-O(111) surface, the H_2O molecule adsorbs either molecularly (-0.51 eV/H_2O) or dissociatively (-0.45 eV/H_2O). This process does not change the oxidation state of the surface plutonium atoms, which remain all Pu^{4+}. In contrast, the formation of OH groups results in the

reduction of a neighboring plutonium atom from Pu^{4+} to Pu^{3+}. The dissociation of the O_2 molecule on the perfect surface leads to the formation of two peroxide ions O_2^{2-} and the oxidation states of the surface Pu atoms are not modified.

On the PuO_2-O(111) oxygen-deficient surface, the oxygen vacancy is associated with the presence of two reduced plutonium atoms Pu^{3+}. Under these conditions, the H_2O molecule inserts exothermically (-1.84 eV/H_2O) into the vacancy producing a perfect surface and a re-oxidation of the Pu^{3+} to Pu^{4+}. In the same way, the dissociation of the O_2 molecule on the perfect surface is an exothermic process (-3.79 eV/O_2), with all Pu^{3+} re-oxidized to Pu^{4+}.

From a thermodynamic stability point of view, some of these species can appear under external conditions rich in water vapor (see right panel of Figure 1). In an oxygen-rich environment (no oxygen vacancies on the surface) we observe that the surface is hydrated with the presence of molecular or dissociated water. In an oxygen-poor environment (presence of vacancies), the surface contains hydride ions with the possibility of heterolytic dissociation (coexistence of hydride ions and protons) over a small window of oxygen chemical potential, and formation of two hydride ions in the vacancies for lower chemical potentials.

After evaluating the energies of the various surface chemical reactions, we are currently calculating the transition paths between these local minima to assess the energy barriers associated with the different adsorption and/or dissociation mechanisms. We will complement the thermodynamic study with a kinetic study.

[1] G. Jomard, B. Amadon, F. Bottin, and M. Torrent, Phys. Rev. B **78**, 075125 (2008).
[2] G. Jomard and F. Bottin, Phys. Rev. B **84**, 195469 (2011).
[3] G. Jomard, F. Bottin and G. Geneste, Journal of Nuclear Materials **451**, 28-34 (2014).
[4] F. Bottin, G. Geneste and G. Jomard, Phys. Rev. B **93**, 115438 (2016).
[5] M. Verstraete *et al.*, J. Chem. Phys. **163**, 164126 (2025).

Elastic properties of actinides systems at high temperature with machine learning

J. Bouchet[1*], A. Castellano[1], E. Brando[1], F. Bottin[2,3]

[1] CEA, IRESNE, DEC, Cadarache, F-13108 Saint Paul-Lez-Durance, France
[2]CEA, DAM, DIF, F-91297 Arpajon, France
[3]Université Paris-Saclay, CEA, Laboratoire Matière en Conditions Extrêmes, 91680 Bruyères-le-Châtel, France
*johann.bouhcet@cea.fr

At high temperatures, accurately describing the thermodynamic properties of materials requires considering anharmonic effects. Ab-initio molecular dynamics offers a natural approach to address this challenge by capturing atomic vibrations and obtaining phonon spectra. However, the computational expense, particularly for systems containing heavy elements, often necessitates reducing the size of the supercell to obtain timely results. To overcome this limitation, we introduce a method for accelerating the computation of finite temperature properties using Machine-Learning Assisted Canonical Sampling (MLACS)[1]. This approach involves sampling the canonical distribution using a machine learning potential adjusted through a self-consistent scheme that incorporates single-point ab-initio calculations on selected configurations generated with the potential from the previous step. With MLACS, we achieve results comparable to those obtained with ab-initio molecular dynamics but with a computational time reduced by one or two orders of magnitude. We illustrate the effectiveness of this method through examples involving complex systems containing actinide elements such UO_2, PuO_2, U_3Si_2, and pure Pu[2].

[1] A. Castellano et al., Computer Physics Communications, 316, 109730 (2025)

[2] F. Bottin, R. Béjaud, B. Amadon, A. Castellano, and J. Bouchet, Phys. Rev. B , 109(6), L060304 (2024)

"Thermodynamic Properties of $(U,Pu)O_2$: Impact of Defects and Fission Products on the Bredig Transition"

Giulia Porto, Emeric Bourasseau, Johann Bouchet

CEA, DES, IRESNE, DEC, Cadarache F 13108 St Paul Lez Durance

Accurate modeling of the thermodynamic properties of Mixed Oxide fuel (MOX - $(U,Pu)O_2$), the fuel candidate for Generation IV nuclear reactors, is essential for predicting its thermal behavior. Knowing the specific heat capacity at high temperature is particularly important. Due to the difficulty of experimental measurements, atomic-scale simulations are nowadays routinely used to gain insights into the evolution of this property with temperature [1,2]. However, previous studies often relied on simplified $(U,Pu)O_2$ models, assuming pristine conditions with fixed stoichiometry and +4 cation valence. This work bridges the gap with real-world conditions by incorporating, at the atomic scale: variable stoichiometry, cation valence fluctuations, point and extended defects, fission products.

We systematically investigated how these factors influence the Bredig transition, a critical structural phase transition affecting thermal properties. While this transition is theoretically predicted for MOX, it has been experimentally observed in UO_2. Where possible, we validated our results against experimental data, particularly from SIMFuel [3]. Key findings include:

- Attenuation of the Bredig transition effects when deviations from the ideal system are included in the atomic-scale simulations
- The necessity of precise sample characterization for meaningful comparisons between experiments and simulations

These findings have direct implications for fuel performance modeling in advanced reactors, and open perspectives on the way to couple experimental and simulation results to provide robust behavior laws for fuel performance codes.

[1] Didier Bathellier, Marc Lainet, Michel Freyss, Pär Olsson, Emeric Bourasseau "A new heat capacity law for UO2, PuO2 and (U, Pu) O2 derived from molecular dynamics simulations and useable in fuel performance codes" Journal of Nuclear Materials 549 (2021): 152877.

[2] G Porto, J Bouchet, Didier Bathellier, J Bodin, M Canducci, J Tranchida, P Fossati, P Martin, E Bourasseau "Thermodynamic and thermoelastic properties of hypostoichiometric MOX fuels with molecular dynamics simulations" Journal of Nuclear Materials 598 (2024): 155163.

[3] Rafael Caprani, Philippe Martin, Damien Prieur, et al. "Fission products speciation in nuclear fuel: Synthesis and characterisation of mixed oxide $(U,Pu)O_2$ SIMfuel." Journal of Nuclear Materials 585 (2023): 154607.

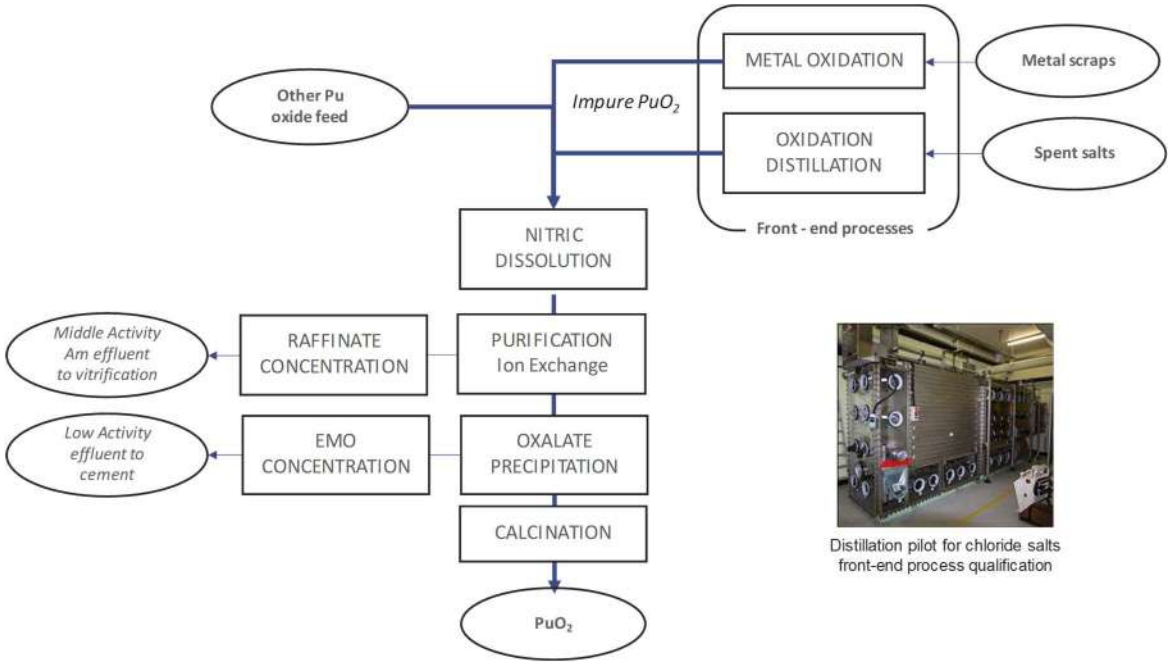
Keywords: MOX, $(U,Pu)O_2$, Bredig transition, crystal defects, fission products, thermodynamic modeling

Future Aqueous Nitrate Process Line for Plutonium Recycling

G. Bourgès*, G. Verwaerde, S. Faure

CEA VALDUC DAM, F-21120 Is sur Tille, France
*gilles.bourges@cea.fr

CEA has always considered aqueous processing as essential for closing nuclear fuel cycle. In the frame of defense programs, a closed cycle is also developed for plutonium, which includes aqueous recycling to recover plutonium from by-products and residues. Thus, CEA/DAM has been operating an aqueous recycling workshop for sixty years. Since 2012, CEA/DAM has launched a progressive replacement of its recycling facility. This project was the opportunity to design a new aqueous process line with several challenging goals such as the recycling of a larger typology of feed materials, including chlorides salts from pyroprocessing, and also to provide safety benefits by the abandon of the historic sulfamic dissolution process for metallic plutonium feeds.
The process baseline is aqueous nitrate polishing including nitric dissolution of impure plutonium oxide feed materials, purification of solutions and oxalate conversion to recover the plutonium as pure dioxide. Front-end processes have been developed, and qualified, to obtain plutonium oxide feed material, from metal scraps and from chloride salts, suitable for aqueous processing using silver (II) or nitro-fluorhydric dissolution processes.
The presentation will highlight some R&D works that supported this project.



Distillation pilot for chloride salts front-end process qualification

References:

[1] G. Bourgès & Al. - Procedia Chemistry, Ed. Elsevier: Vol. 7, pp 731-739 (2012): Vacuum distillation of plutonium pyrochemical salts

[2] M-P. Brossard & Al. - Proceeding Global 2003, "Dechlorination, Dissolution and Purification of Weapon Grade Plutonium Oxide Contaminated with Chlorides: Tests Performed in the CEA Atalante Facility for the Aqueous Polishing part of MOX Fuel Fabrication Facility"

LA-UR-26-21938

Approved for public release; distribution is unlimited.

Title:	Combustion Ion Chromatography (CIC) Method Development and Validation for Characterization of Fluoride and Chloride in Actinide Materials
Author(s):	Brown, Alexandra Nichole; Nolan, Journey Renee; Williams, Shauni Nicole; Martinez, Patrick Thomas; Matonic, John Harold; Olson, Angela Christine; Tandon, Lav
Intended for:	Plutonium Futures, 2026-09-13/2026-09-17 (Edinburgh, UNITED KINGDOM)
Issued:	2026-03-13

Los Alamos
NATIONAL LABORATORY







Los Alamos National Laboratory, an affirmative action/equal opportunity employer, is operated by Triad National Security, LLC for the National Nuclear Security Administration of U.S. Department of Energy under contract 89233218CNA000001. By approving this article, the publisher recognizes that the U.S. Government retains nonexclusive, royalty-free license to publish or reproduce the published form of this contribution, or to allow others to do so, for U.S. Government purposes. Los Alamos National Laboratory requests that the publisher identify this article as work performed under the auspices of the U.S. Department of Energy. Los Alamos National Laboratory strongly supports academic freedom and a researcher's right to publish; as an institution, however, the Laboratory does not endorse the viewpoint of a publication or guarantee its technical correctness.

Combustion Ion Chromatography (CIC) Method Development and Validation for Characterization of Fluoride and Chloride in Actinide Materials

Alexandra N. Brown[1*], Journey R. Nolan[1], Shauni N. Williams[1], Patrick T. Martinez[1], John H. Matonic[1], Angela C. Olson[1], Lav Tandon[2]

[1]Los Alamos National Laboratory, Actinide Analytical Chemistry Group, Los Alamos, New Mexico, USA; [2]Los Alamos National Laboratory, Metal Production Group, Los Alamos, New Mexico, USA; *ahowell8@lanl.gov

Fluoride (F-) and chloride (Cl-) are critical interstitial impurities in plutonium and other actinide materials. In pyrochemical processing environments – particularly electrorefining and molten salt operations – halides influence salt chemistry, redox control, corrosion of containment materials, and long-term material stability. Fluorine is highly reactive with most elements, while chloride is a strong oxidizer capable of promoting metal chlorination and corrosion phenomena. Accurate quantification of trace F- and Cl- is therefore essential for process control, quality assurance of actinide metal and oxide products, and for evaluation of long-term storage risks.

For decades, pyrohydrolysis – high-temperature combustion in a gas flow mixture of steam and argon – coupled with ion chromatography (Pyro/IC) has been considered the laboratory standard for extraction and quantification of halides in refractory actinide matrices. While robust and well-established, legacy Pyro/IC systems are typically custom-built, highly manual, and physically separated from the IC instrument. These drawbacks have limited high-throughput sample analysis, and, importantly, present operational and safety challenges in radiological facilities. This is largely due to the high temperatures needed (1000 °C) for the pyrohydrolysis reaction with the solid sample matrix resulting in risk for serious hazard during the manual insertion of sample boats into the hot furnace by the operator. This hazard has stalled continued operation of the legacy Pyro/IC method in newer radiological facilities with more stringent restrictions for high-temperature operations.

To address these limitations, a semi-automated combustion ion chromatography (CIC) systems (Mitsubishi AQF-2100H coupled to a Dionex ICS-2100) was installed and adapted for actinide applications. Unlike traditional pyrohydrolysis, CIC employs an oxygen-rich combustion environment (steam, argon and supplemental oxygen), promoting more complete and efficient oxidation with shorter extraction times. The integrated system automates sample introduction, combustion, absorption and dilution, and injection to the IC, significantly reducing analyst handling and risk for high-temperature contact by the operator.

Extensive method development was required prior to validation to adapt the AQF system, which was originally developed and manufactured for characterizing sulfates in coal-based samples, for processing actinide materials in radiological enclosures (glovebox). Combustion parameters, including oxygen introduction timing and flow, combustion duration, and accelerant usage, were optimized to ensure complete halide release without tube degradation or salt overloading. Sample size and different combustion tube characteristics were also investigated to optimize combustion tube integrity and longevity by minimizing devitrification by salt overloading. Absorption solution chemistry was modified with trace hydrogen peroxide (<0.003%) to convert excess chlorine gas (Cl_2) in the absorbed distillate to chloride, eliminating systematic low bias in chloride recoveries under oxygen-rich conditions. Distillate volume collection and dilution accuracy were also characterized to

improve concentration calculations and eliminate systematic bias in halide recoveries.

Following these method development efforts, validation of the overall instrument system (AQF and IC) was performed using traceable aqueous NIST standards, user-prepared solid reference materials, and previously characterized actinide materials and oxides. Calibration linearity ($R^2 > 0.99$), quality control recoveries (100 ± 10%), and blank performance met predefined acceptance criteria and established parameters for verifying long-term instrument control. Cross-comparison with legacy Pyro/IC data demonstrated agreement within ± 10% for both fluoride and chloride, acknowledging inherent heterogeneity in actinide sample matrices and sample handling challenges in radiological enclosure environments. The validation effort resulted in improved IC detection limits and a solid sample reporting limit that matched historical 20 ppm thresholds for both anions.

The results of this development and validation effort demonstrate that a semi-automated, oxygen-rich CIC (AQF-IC instrument system) can be successfully optimized and validated for trace halide determination under challenging radiological facility operational and safety limitations. CIC is now an established and functional method being utilized for halide characterization in a production environment. This work provides a modernization pathway for laboratories transitioning from legacy pyrohydrolysis furnace systems while maintaining rigorous radiological production facility requirements and analytical quality for actinide materials processing and characterization. Challenges, process improvements, lessons-learned and continued optimization efforts will be presented in addition to key features of the CIC method development and validation.

A figure of the AQF/IC instrument selected and adapted for the CIC method development and validation is provided below. Key improvements to the legacy Pyro/IC method are provided by each sub-unit of the overall AQF/IC system. The automatic boat controller (ABC-210) eliminates manual insertion of sample boats into a hot furnace by the operator. The horizontal tube furnace (HF-210) incorporates appropriate heat shielding and automatic operation to minimize high-temperature risks to glovebox operators. The gas absorption unit (GA-210) collects, mixes and injects the captured sample distillate – eliminating several previously highly manual analyst steps in the legacy method. Lastly, the AQF system is directly attached to a contemporary IC (Dionex ICS-2100), which utilizes improvements in suppression and detection techniques for accurately quantifying trace anions. Not shown is an additional external solution injection attachment (ES-210) – which further enhances automation to support sample throughput and operations for key Los Alamos National Laboratory missions.



Evolution of Helium Bubble Characteristics During Heating of Aged PuGa Alloys: An In-Situ Small Angle X-ray Scattering Study

[1]*D.W. Brown, [2]J. D. Almer, [1]D.T. Carver, [1]B. Clausen, [2]P. Kenesei, [1]D. Savage, [2]J.S. Park, [1]C. Yablinsky

[1]Los Alamos National Laboratory, Los Alamos, NM, 87545 USA; [2]Argonne National Laboratory, Lemont, IL,60439

*dbrown@lanl.gov

Abstract: High energy (95keV) X-rays were utilized to characterize the microstructure of eight PuGa alloy samples at room temperature and during heating to ~673 K (400 °C). The samples had different Ga content (nominally 0-3.4 at.%), age, and history. The samples span the range from nominally single-phase α (monoclinic) to δ (face-centered cubic) PuGa, as well as a two-phase α'/δ sample. Small Angle X-ray Scattering (SAXS) was used to probe helium bubble as a function of age in the as-aged samples and *in-situ* during heating from room temperature to 673 K (400 °C). In the oldest samples, greater than 40 years since fabrication, a clear feature in the SAXS signal within a *q*-range 0.02 Å^{-1} < *q* < 0.2 Å^{-1} is related to the helium bubble population. The data is not of sufficient quality to determine the complete helium bubble distribution. However, an as-aged mean bubble radius of 28.1 Å ± 1 Å and bubble number density of 8 x 10^{15}/cm^3 is determined in the oldest single-phase δ PuGa sample. The helium bubble radius slowly increases as the temperature increases above 550 K (272 °C) reaching 35.9 Å at 650 K (375 °C). Bubble growth accelerates above 650 K (372 °C) reaching 44 Å at the target hold temperature of 673 K (400 °C). While the sample temperature is constant to within ± 2 K for 35 minutes, the bubble radius increases by ~25% to 53 Å over the first 27 minutes and, subsequently, is constant to within uncertainty. These results are consistent with past studies of Jeffries et al. [1, 2] though with considerably shorter soak times at temperature. A similar feature, and subsequently similar mean radius and density, are found in a similarly aged two-phase α/δ sample. However, as there is no *a priori* reason helium diffusion should be equivalent in the distinct phases, it is likely too simplistic to interpret this data as a single radius and density within the two-phase sample. The younger samples (10-15 years) do not manifest a clear and distinct feature in the SAXS data within the available *q*-range over the background scatter from air, furnace, and triple containment. Actionable strategies to improve both the signal/background ratio and the *q*-range are presented.

1. J. R. Jeffries, J. A. Hammons, T. M. Willey, M. A. Wall, D. Ruddle, J. Ilavsky, P. G. Allen, and T. van Buuren: *Journal of Nuclear Materials* 2018, vol. 498, pp. 505-10.

2. J. R. Jeffries, M. A. Wall, K. T. Moore, and A. J. Schwartz: *Journal of Nuclear Materials* 2011, vol. 410, pp. 84-88.

In-Situ High Energy X-Ray Imaging and Diffraction to Monitor Corrosion of Pu-Ga Alloy

D.W. Brown[1], D.T. Carver[1], J.D. Almer[2], B. Clausen[1], P. Kenesei[2], D. Savage[1], J.S. Park[2], R. Pokharel[1], C. Yabilinsky[1]

[1]Los Alamos National Laboratory, Los Alamos, USA;
[2]Argonne National Laboratory, Lemont, USA;

Corrosion of metallic plutonium and Pu alloy materials, in particular oxidizing and hydriding reactions, has important implications for long term storage of components and/or waste. Because of its mixed valence state and position near the center of the actinides, Pu is extremely reactive. To the point that its reactivity, coupled with the need to keep it contained for safety reasons, makes it difficult to monitor corrosion/reactions. The advent of third generation synchrotron sources producing high energy X-rays (> 65 keV) has greatly changed the landscape of X-ray diffraction and imaging measurements, in particular, on high Z-number materials. For example, a monochromatic incident X-ray beam with energy of 100 keV, as available at 1-ID of the Advanced Photon Source [23, 24], easily penetrates a 0.5mm thick Pu sample enabling a near routine statistical measurement of microstructural features under non-ambient conditions which can complement more difficult and hazardous, though more detailed, microscopy measurements. The current work demonstrates the ability of HEXRD and μCT to characterize reacting metallic Pu samples to bulk depths. Features with sizes of order microns are identified and characterized as they form and grow under non-ambient conditions of temperature and gaseous exposure. Various structural and thermal mechanical properties of incipient phases can be extracted from the scattering data as a function of time in environment. Unforeseen contamination of one particular metallic sample during an in-situ diffraction experiment collected during elevated temperature thermal profiles enables a very strong demonstration of the utility of the same techniques to characterize the evolution of corrosion reactions in Pu alloy samples. While environmental conditions were not controlled well enough during the in-situ HEXRD experiments to determine reaction kinetics etc, the value of high energy x-ray imaging/diffraction for evolutionary studies of corrosion is unambiguous.

LA-UR-25-26207

Enabling Americium-Powered Space Missions. High Temperature Stability of $(Ce,U)O_2$ Surrogates for the $(Am,U)O_2$ Fuel Source

D.J. Cette[1,2*], J. Manaud[2], A. Syrrakou[2], C. Guéneau[3], R.J.M. Konings[1], A.L. Smith[1]

[1] Delft University of Technology, Delft, The Netherlands; [2] European Commission, Karlsruhe, Germany; [3] CEA, Gif-sur-Yvette, France

* e-mail: Daphne.CETTE@ec.europa.eu

Radioisotope Thermoelectric Generators (RTGs) and Radioisotope Heater Units (RHUs) are essential to enable the exploration of our solar system. These devices rely on the natural decay of radioisotopes, typically plutonium-238 (Pu-238), to provide spacecrafts with reliable power and heat. However, recent geopolitical events have significantly limited the availability of Pu-238 in Europe, highlighting the need for a new and more suitable radioisotope. The best candidate for that purpose is americium-241 (Am-241), a byproduct of nuclear fuel reprocessing that can be produced at acceptable costs and suitable quantities. The Rosalind Franklin rover, scheduled for launch to Mars in 2028, will carry the first Am-based RHU, marking a significant milestone in the adoption of this technology [1].

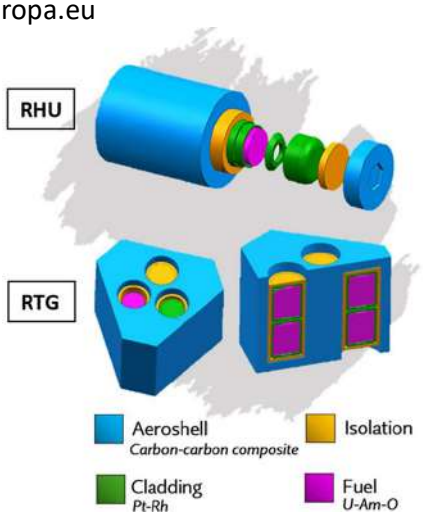


Figure 1. RHU and RTG designs developed at Leicester University. Adapted from [1].

A key challenge for Am-241 is stabilizing its oxide form, AmO_2. In RTGs and RHUs, the fuel is pelletized to limit dispersal in case of an accident. It should also have a cubic crystal structure with isotropic thermal expansion to withstand the large temperature changes during operation. Although AmO_2 is cubic, it tends to lose oxygen at higher temperatures, forming the non-cubic Am_2O_3. Recent studies at the JRC Karlsruhe have focused on developing $(Am,U)O_2$ compounds, which preserve the stable cubic structure across a wide range of temperatures. Adding uranium to the matrix mitigates radiation damage effects, reduces oxygen loss, and simplifies manufacturing processes, thereby enhancing the reliability of americium fuel for space exploration [2].

The final objective of this work is to assess the stability and performance of the Am-based fuel source under conditions relevant to RTGs and RHUs operation. This research contributes to a broader effort to develop a thermodynamic model and database for the U-Am-Np-O-Pt-Rh system using the CALPHAD method.

In this work, the high-temperature stability of the $(Am,U)O_2$ phase is assessed through a combination of experimental and computational methods. For this, the methodology is first established on $(Ce,U)O_2$ surrogate materials. Seven $U_{1-y}Ce_yO_2$ samples with compositions y = 0.2, 0.3, 0.5, 0.8, 0.85, 0.9 and 0.95 were synthesized using a powder metallurgy method and studied using HT-XRD (High-Temperature X-Ray Diffraction) and laser melting under argon. These compositions cover the full UO_2-CeO_2 range, with a focus on high cerium content, close to the americium fraction targeted for RTG and RHU fuel sources.

HT-XRD investigations indicated the formation of a second cubic phase at high cerium content, in the 150-550°C temperature range. Preliminary analyses attribute this observation to the existence of a miscibility gap between $U_{1-y}Ce_yO_2$ and the hypo-stoichiometric $U_{1-y}Ce_yO_{2-x}$ phase. A similar behavior has also been reported in the literature for $(Am,U)O_2$ compounds at high americium content, although the stability range of this miscibility gap is not well established in both the U-Am-O

and U-Ce-O systems [3,4]. Comparison with the most recent CALPHAD thermodynamic model for the U-Ce-O system reported by Guéneau [5] showed that the predicted extend of the miscibility gap is underestimated relative to the experimental results.

The effects of the reduction of the cubic $U_{1-y}Ce_yO_2$ phase were also observed on the solidus and liquidus of the $U_{1-y}Ce_yO_2$ samples (Figure 2). Similarly to AmO_2, CeO_2 tends to lose oxygen at higher temperatures which considerably lowers its melting point, from 3000 K when measured under O_2 [6] to 2670 K under argon [7]. Since the measurements in this work were performed under argon, they follow the trend reported for CeO_{2-x} melting point in argon. In contrast, the latest model from Guéneau [5] was built using the model from Zinkevich et al. [8], which predicts the $CeO_{1.86}$ = Liquid + Gas reaction at 2566 K.

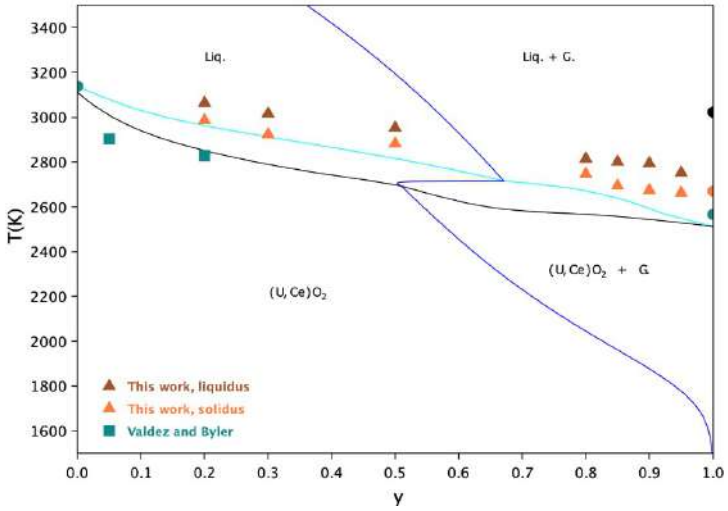


Figure 2. CALPHAD calculation of phase equilibria in the UO_2-CeO_{2-x} section [5]. $U_{1-y}Ce_yO_2$ data are from this work (liquidus ▲, solidus ▲), and Valdez and Byler [9] (■). Melting points of CeO_{2-x} are taken from Zinkevich et al. [8] for the gas-peritectic (●), Mordovin et al. [7] under Ar (●), and Tresvyatkii and Cherepanov [6] under O_2 (●).

Further analyses will quantify the degree of reduction of the $U_{1-y}Ce_yO_2$ phase using XANES. The results will then be used to improve the thermodynamic model of the U-Ce-O system using the CALPHAD method, in order to more accurately describe the impact of $U_{1-y}Ce_yO_2$ reduction on the stability of the phase. These investigations constitute a first step toward the assessment of the high-temperature stability of americium-based fuel sources intended for future RTGs and RHUs.

[1] R. Ambrosi et al., "European radioisotope thermoelectric generators (RTGs) and radioisotope heater units (RHUs) for space science and exploration," Space Science Reviews, vol. 215, p. 1-41, 2019.

[2] J.-F. Vigier et al., "Advancements in americium-based ceramics for Radioisotope Power Systems: Material selection, fabrication and thermoelectric effect demonstration," Materials Today Chemistry, vol. 50, 2025.

[3] E. Epifano, "Study of the U-Am-O ternary phase diagram," Université Paris-Saclay, 2017.

[4] T. Markin, R. Street and E. Crouch, "The uranium-cerium-oxygen ternary phase diagram," Journal of Inorganic and Nuclear Chemistry, vol. 32, no. 1, pp. 59-75, 1970.

[5] C. Guéneau, "U-Ce-O", TAF-ID, 2025.

[6] S. Tresvyatkii and A. Cherepanov, "Highly Refractory Materials and Products Made From Oxides," Metallurgizdat, p. 358, 1964.

[7] O. Mordovin, N. Timofeeva and L. Drozdova, Inorg. Mater, vol. 3, 1967.

[8] M. Zinkevich, D. Djurovic and F. Aldinger, "Thermodynamic modelling of the cerium–oxygen system.," Solid State Ionics, vol. 177, no. 11-12, p. 989–1001, 2006.

[9] J. Valdez and D. Byler, "Draft report on melting point as a function of composition for urania-based systems," Los Alamos National Laboratory (LANL), 2012.

Plutonium Metallurgy and Exposure onto a Tungsten Coated Substrate

Jarom Chamberlain[1*], Olivia Dale[1], Scott Parker[1], Tim Coons[1], Douglas Smith[1], David Arellano[1], Marisa Monreal[1], Najeb Mohammed Abdul-Jabbar [1]

[1]Los Alamos National Laboratory, Los Alamos, United States of America
*jchamberlain@lanl.gov

Molten plutonium is a challenging material to work with given its affinity to form low temperature eutectics with structural materials. Refractory metals, such as tantalum and tungsten, are generally more compatible with molten plutonium but also bring their own challenges associated with cost and fabrication for bulk materials. The application of protective refractory coatings can therefore be leveraged to address both challenges associated with refractory metal fabrication as well as ensuring compatibility with plutonium. There are limited technologies that can effectively apply refractory metals as protective coatings; one such method is molten salt electrodeposition. A molten sodium tungstate bath containing dissolved tungsten oxide is configured as an electrochemical cell to enable the deposition of tungsten metal as a coating. This electrochemical molten salt electrodeposition cell is used to apply a tungsten metal coating onto a nickel alloy substrate which is then exposed to molten plutonium to evaluate its protective performance. The plutonium exposure is done using an induction furnace to melt the plutonium onto the coated substrate.

After the plutonium exposure was complete, the coating and plutonium are partitioned with a high-speed saw and mounted in epoxy resin for polishing. The sample is then characterized by a scanning electron microscope and energy dispersive x-ray spectroscopy to evaluate the plutonium and tungsten coating interface. The characterization results are used to draw insights into the plutonium-tungsten and plutonium-nickel alloy metallurgy as well as draw conclusions on the plutonium corrosion mechanisms. Differences in coefficients of thermal expansion between the applied coating and the substrate are hypothesized to be the primary failure mechanism for the tungsten coating. A follow up exposure experiment with plutonium is also presented with a resistive type of furnace to identify if the previous induction heating method contributed to the coating failure. Further characterization of the coated sample exposed to plutonium in a resistive heated furnace is reported on for comparison. Microstructural considerations and methods for applying the coating are presented to address the difference in coefficients of thermal expansion between the coating and the substrate. Plutonium metallurgy corrosion mechanisms, interactions with tungsten and nickel-alloys are all considered and discussed to inform future materials and protective coatings decisions.

LA-UR-26-21780

Evaluating Disposal of Plutonium Wasteforms

L Chen[1*], A Mason[2], S.Pepper[2], S. Waters[1], C.L. Corkhill[1]

[1]School of Earth Science, The University of Bristol, Bristol, UK;
[2]Department of Materials Science and Engineering, University of Sheffield, Sheffield, UK
*email address for primary/corresponding author

Reprocessing of spent nuclear fuel in the UK has resulted in the production of ~140 tonnes of PuO_2, which, according to current strategy, will be immobilised in a form suitable for a Geological Disposal Facility (GDF) [1]. Understanding the long-term behaviour of this wasteform upon the eventual breach in the engineered barrier system is therefore crucial. This study investigates the leaching behaviour of two candidate ceramic wasteforms for Pu immobilisation: Disposal Mixed Oxide (DMOX) UO_2, zirconolite [(Ca,U,Gd)(Zr,U, Gd,Hf)(Ti,Fe)$_2O_7$]. A semi-dynamic leaching test based on the American Society for Testing and Materials (ASTM) C1308 method [2] was employed to assess their leaching behaviour over the course of one year. The tests were conducted at three different temperatures: 40, 60, and 90°C, and in three distinct solutions: 0.01M HNO_3, 19mM NaCl + 1mM $NaHCO_3$, and 11mM LiCl + 10mM LiOH. Dissolution rates of plutonium, using U and Th as surrogates, and neutron-absorbers, Gd and Hf, were determined. In addition, by assessing trends in other elements (Ca, Fe, Ti) under different temperatures and solutions we gain qualitative insights into the dissolution behaviour of these materials. The activation energies for dissolution were calculated by comparing the dissolution rates at different temperatures, and the experimental data was modelled to further elucidate the mechanisms governing dissolution for each wasteform. Post-leaching surface characterisation of the pellets was carried out using focused ion beam scanning electron microscopy (FIB-SEM), Transmission Kikuchi diffraction (TKD) and X-ray photoelectron spectroscopy (XPS). Overall, this investigation provides key underpinning data of the dissolution behaviour of these ceramic wasteforms under different environmental conditions, offering valuable insights into their long-term stability in a GDF.

References:

[1] Department for Energy Security and Net Zero, Plutonium Disposition Strategy, (2025)
[2] ASTM International, Standard Test Method for Accelerated Leach Test for Measuring Contaminant Releases From Solidified Waste, C1308-21, (2021)

The Effects of Pu Particle Formation during Precipitation and Calcination on Aqueous Processing

Bradley C. Childs[1*], Maryline G. Ferrier (Kerlin)[1], Tsuyoshi A. Kohlgruber[1], Donya Servanda-Williams[1], Silvi A. Di Pietro[1], Scott A. Simpson[1], Emma R. Tardiff[1], Hiroshi H. Saito[1], Saurabh Narain[1], Jeremy Scher[1], Jared Stimac[1], and Lawrence E. Banks[1]

[1]*Lawrence Livermore National Laboratory, Livermore, California, United States*

** email: childs4@llnl.gov*

Lawrence Livermore National Laboratory's plutonium facility supports the full lifecycle of plutonium (Pu) processing in which Pu is dissolved in nitric acid prior to being treated for the anion exchange process. Extensive time is spent on the dissolution process to ensure proper quantities of Pu are in solution before proceeding to the next step of the aqueous process. Particle size and formation often play key roles in dissolution and precipitation, and the steps of precipitation, filtration, and calcination all have roles in determining particle characteristics. This study focuses on enabling control of physical characteristics, which is paramount for successful processing runs.

In this work, Pu particle analysis characterization will be conducted at the steps of precipitation and calcination. Particle size and distribution studies will be conducted during Pu (III) oxalate precipitation and combined with thermokinetic studies on the calcination to PuO_2. Identical studies will be conducted from the precipitation of $Pu(OH)_4$ as well as its subsequent calcination. From there, dissolution constants will be analyzed based on multiple precipitation and calcination conditions. Data will be compared to historical values to produce a data-driven model to inform on aqueous processing conditions based on the particles produced. This work was performed under the auspices of the U.S. Department of Energy by Lawrence Livermore National Laboratory under Contract DE-AC52-07NA27344. LLNL-ABS-2016872.

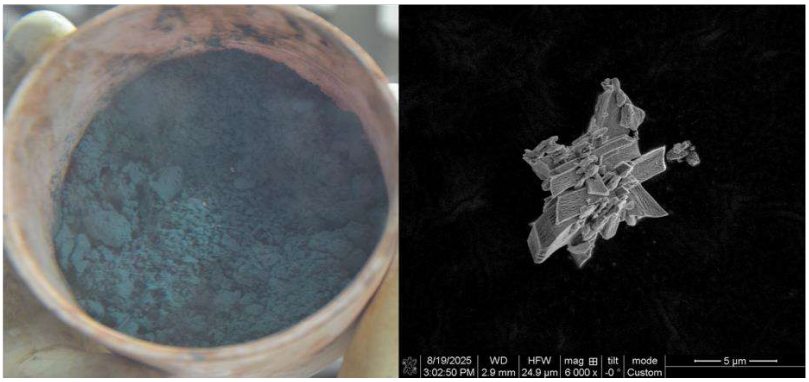


Figure 1: The above image displays Pu(III) oxalate in a crucible prior to calcination (left) and a scanning electron microscopy image post-calcination at 900 ℃.

Mapping Morphological and Chemical Signatures of Plutonium and Uranium Materials for Nuclear Forensics

Brandon W. Chung[1*], Alexander A. Baker[1], Scott B. Donald[1], Tian Li[1], Rachel Lim[1], Uday Mehta[1], Debra L. Rosas[1], Donya R. Servando-Williams[1], Alex S. Ditter[2], S. Olivia Gunther[2], David K. Shuh[2], Kari Sentz[3]

[1]Lawrence Livermore National Laboratory, Livermore, CA, USA; [2]Lawrence Berkeley National Laboratory, Berkeley, CA, USA; [3]Los Alamos National Laboratory, Los Alamos, NM, USA; *chung7@llnl.gov

In this project, we aim to develop robust characterization and multimodal data science platforms to attribute nuclear materials outside of controlled environments. There are significant interests to improve nuclear forensics analyses of plutonium (Pu) and uranium (U) metals and their byproducts from various process pathways. In addition to material signatures imparted by their source materials (e.g., spent fuel), some signatures will be propagated by their separation processes and metallurgical processing conditions. Once fabricated, both Pu and U metals are highly susceptible to environmental corrosion. Later, these metals may be calcined at high temperatures to convert them to more stable oxides for long-term storage or disposal. Relatively unexplored are the relationship between the oxide and corrosion products to their starting metal itself (e.g., trace element impurity). In this presentation, we build off the recent efforts of multiplatform characterization experiments (e.g., focused ion beam-scanning electron microscopy, transmission electron microscopy, and X-ray synchrotron spectromicroscopy) and complement them by different analytical image platforms (e.g., optical microscopy) and image-based morphological quantifications. Our recent approaches enable us to obtain key insights on the evolution of morphology and chemistry in Pu and U metals and their products. We highlight the relationship between product morphological and chemical features of both oxide and corrosion products to their starting metal characteristics and exposure environments.

A Machine Learned Interatomic Potential for Helium in Plutonium Dioxide.

William Davie[1*], Sophie Cooper[2], Daniel Bailey[3], Bartomeu Monserrat[1]

[1]Department of Material Science and Metallurgy, University of Cambridge, Cambridge, United Kingdom; [2]United Kingdom National Nuclear Laboratory; [3]Amentum ltd, Warrington, United Kingdom; [*]wd324@cam.ac.uk

Currently Sellafield holds the largest store of civil plutonium in the world. Whether in interim or long-term storage, plutonium containment systems must remain reliable for several generations, presenting numerous engineering challenges. Among these is the accumulation of helium produced through alpha decay, which can increase internal pressure and influence the mechanical properties of containment materials. As helium is produced on long time scales, experiments are inaccessible and there is urgent need to make predictions via computational modelling. Historically, the chemical complexity of plutonium has limited the accuracy of computational models. However, recent development of machine learning architectures for inter-atomic potentials (MLIPs) allows for accurate, expandable molecular dynamics (MD) simulations, given sufficient training data. We are training a machine learned interatomic potential for helium in plutonium dioxide (PuO2) informed by a quantum-scale, chemical understanding of PuO2. In doing so, we can gain MD accuracy across the plutonium disposal life cycle and parameterize macro-scale simulations for industrial applications.

Learning Tracks: A New Method to Develop the Next Generation

Silvina A. Di Pietro[1]*, Saurabh Narain[1], Bradley C. Childs[1], Maryline G. Ferrier[1], Tsuyoshi A. Kohlgruber[1], Christy Santoyo[1], Jeremy A. Scher[1], Jared Stimac[1], Scott A. Simpson[1], Emma R. Tardiff[1], John. D. Brown[1], Hiroshi H. Saito[1], and Lawrence E. Banks[1]

[1]Lawrence Livermore National Laboratory, USA, Livermore, United States
*E-mail: dipietro3@llnl.gov

Jupyter notebooks are being used to develop and onboard the future workforce supporting plutonium (Pu) recovery operations. Multiple notebooks focused on aqueous Pu processing integrate comprehensive literature searches, historical and current process data, and structured knowledge transfer from subject matter experts. Recent enhancements include embedded interactive knowledge checks, process videos, and an integrated artificial intelligence (AI) tutor deployed across current chapters to support immersive, self-paced learning. Learners can document and annotate content in their preferred style, and they can use Python syntax to explore how changes in key variables affect outcomes in representative process steps such as dissolution and anion exchange. This work presents the development and structure of these learning tracks, summarizes observed benefits for training and knowledge retention, and highlights current areas of focus to strengthen the approach, including improved interactivity, expanded process coverage, and continued refinement of AI-enabled tutoring to align with operational needs and ensure consistent technical accuracy.

This work was performed under the auspices of the U.S. Department of Energy by Lawrence Livermore National Laboratory under Contract DE-AC52-07NA27344. (LLNL-ABS-XXXXXX)

Nuclear Forensic Signatures of Plutonium Hydroxide Precipitation and Calcination Products

S Dunn[1], S Cross[1], M Higginson[1], A Nicholas[2], J Corbey[2], L Sweet[2], D Schnable[2], K Makovsky[2], C Nizinski[2], R Clark[2]

[1]AWE : Nuclear Security Technologies, Reading, UK [2]Pacific Northwest National Laboratory, Richland, USA.

Precipitation routes for recovery and conversion to plutonium oxide, such as through plutonium oxalate, have continued research for the development and interpretation of nuclear forensic signatures. This has yielded key chemical route and process condition signatures which can provide scientific support to law enforcement investigations. To date plutonium hydroxide, which is in active use as a recovery process, has received little attention from a nuclear forensics' perspective. The work presented here details the recovery of plutonium through the hydroxide route, the remaining trace actinides, and the major impurities. In addition, X-ray diffraction and Raman Spectroscopy assess the as-precipitated material. Conversion of the precipitated material was tracked using Raman Spectroscopy through a step wise temperature profile conversion to PuO_2. The work presented highlights the key material properties which would be useful in providing the processing history of PuO_2 derived through hydroxide precipitation.

UK Ministry of Defence © Crown Owned Copyright 2026/AWE

ADOA Route for $(U,Pu)O_2$ Mixed Oxides: Multiparametric Synthesis Optimization and Preliminary Sintering Performance

Alison El Monjid[1*], Paul Estevenon[1], Lucas Muller[1]

[1]CEA, DES, ISEC, DMRC, Univ Montpellier, Marcoule, France
*alison.elmonjid@cea.fr

In the framework of advanced nuclear fuel cycles and fast neutron reactor deployment, the fabrication of highly homogeneous mixed uranium–plutonium oxides $(U,Pu)O_2$ remains a key technological challenge for high-performance MOX fuels. Increasing plutonium contents and the progressive implementation of multi-recycling strategies impose stringent requirements on the homogeneity of actinide cation distribution within the fluorite lattice, which conventional fabrication routes such as mechanical blending or co-precipitation may struggle to achieve consistently [1–3].

Among emerging conversion processes, the Advanced Thermal Denitration in presence of Organic Additives (ADOA) route has recently been proposed to synthesize homogeneous actinide oxide precursors directly from nitrate solutions [4]. This process relies on the formation of a cross-linked polymeric gel that traps actinide cations at the molecular scale prior to dehydration and calcination. Such gel-based synthesis ensures an intimate mixing of the cations and leads to highly homogeneous mixed oxides after thermal treatment [4,5]. In addition, this route offers enhanced flexibility in terms of solution chemistry and avoids additional valence adjustment steps often required during actinide oxide conversion.

A systematic multiparametric study was first conducted under inactive conditions using cerium oxides as actinide surrogates [6,7]. The influence of key synthesis parameters — including initiator-to-monomer ratio, organic phase proportion, and cross-linking agent content — was investigated in order to optimize gel formation and precursor homogeneity. The most promising conditions were subsequently transferred to active systems, enabling the synthesis of four controlled compositions of $U_{1-x}Pu_xO_2$ via the ADOA route.

Comprehensive characterization of the obtained powders is currently underway, focusing on crystallinity, phase purity, and nanoscale cation distribution. Preliminary sintering trials performed on non-optimized ADOA-derived powders already yielded pellets with relative densities reaching 94.5% TD. These early results highlight the promising sinterability of the powders produced by this route. Further optimization of both synthesis parameters and sintering conditions is expected to significantly improve densification and microstructural control.

Overall, this work demonstrates the strong potential of the ADOA process for the production of stable and ultra-homogeneous mixed actinide oxides compatible with the stringent requirements of advanced MOX fuel fabrication and future plutonium multi-recycling strategies.

References:

[1] R. Parrish et al., A review of microstructural features in fast reactor mixed oxide fuels, J. Nucl. Mater. 509 (2018) 1–18.

[2] K.V.V. Devi et al., Plutonium heterogeneity in MOX fuel: A quantitative analysis, J. Nucl. Mater. 516 (2019) 1–10.

[3] IAEA, Experiences in MOX fuel fabrication at the PFPF for the fast reactor (ou similaire revue IAEA sur fabrication MOX), ou Courtin et al., Pu multi-recycling scenarios..., EPJ N 7 (2021) 27

[4] M. Leblanc et al., Actinide mixed oxide conversion by advanced thermal denitration route, J. Nucl. Mater. 519 (2019) 157–165.

[5] H. Colledge et al., A review of alternative finishing options for uranium/plutonium mixed oxide fuels, Prog. Nucl. Energy (2023) or similaire revue récente citant ADOA.

[6] J.-F. Vigier et al., Structural Investigation of (U0.7Pu0.3)O2-x Mixed Oxides (ou une ref sur Ce surrogate dans sol-gel/denitration), Inorg. Chem. 54 (2015) 5691–5700.

[7] R.W. Harrison, J. Morgan, J. Buckley, T. Abram, D.T. Goddard, N.J. Barron (2021). Spark plasma sintering of (U,Ce)O_2 as a MOx nuclear fuel surrogate. Journal of Nuclear Materials, 557, 153302.

Pu(IV) silicate, synthesis and advanced characterization of a key compound for plutonium environmental behavior

P. Estevenon[1*], M. Rousselle[1], T. Barral[1], M. Autillo[2], P. G. Yot[3], L. Amidani[4,5], C. Hennig[4,5], K. O. Kvashnina[4,5], N. Dacheux[6]

[1] CEA, DES, ISEC, DMRC, Univ Montpellier, Marcoule, France;
[2] CEA, DES, ISEC, DPME, Univ Montpellier, Marcoule, France;
[3] ICGM, Univ. Montpellier, CNRS, ENSCM, Montpellier, France;
[4] Institute of Resource Ecology, Helmholtz Zentrum Dresden-Rossendorf (HZDR), PO Box 510119, 01314 Dresden, Germany;
[5] The Rossendorf Beamline at ESRF, The European Synchrotron, CS40220, 38043 Grenoble Cedex 9, France;
[6] ICSM, Univ Montpellier, CNRS, CEA, ENSCM, Bagnols-sur-Cèze, France;
paul.estevenon@cea.fr

Actinides, and mainly plutonium, are the main contributors to the long-term radiotoxicity of spent nuclear fuel [1]. In representative geological conditions, the interactions between these radioelements and silicate species could influence the mobility of the actinides in the environment and thus, could affect the safety of the storage facilities. Specifically, the formation of actinide silicate, $AnSiO_4$, has to be taken into account, since thorium and uranium silicate are ubiquitous in environmental silicate rich media and under reductive conditions. Moreover, the formation of actinide oxy-hydroxy-silicate colloids has been observed for thorium, uranium, neptunium and plutonium [2,3] and are suspected to play a huge role on actinide mobility in environmental conditions. Additionally, the formation of silicate-type compounds is also a significant concern in the field of severe nuclear accident. Indeed, during the Chernobyl nuclear power plant accident, interactions between the corium and surrounding materials led to the formation of $(Zr,U)SiO_4$ silicate phases [4], raising questions about the behavior of plutonium under such conditions and the chemical stability of these phases. The formation of $(Zr,Pu)SiO_4$ phases, was also achieved for plutonium contents below 10 wt.% [5]. In this context, the study of pure $PuSiO_4$ is also a key parameter for understanding the $(Zr,U,Pu)SiO_4$ system which may be formed in accidental conditions.

However, although the existence of the $PuSiO_4$ phase was first reported as early as the 1960s [6], the chemical conditions required for its formation remained poorly understood for a long time, and most of its properties—particularly its thermodynamic properties—could only be estimated through calculation [7]. More recently, the conditions developed for the synthesis of $CeSiO_4$ [8] were drawn to develop a new synthesis protocol for $PuSiO_4$ [9]. This synthesis relies primarily on the preparation of a plutonium (III) silicate, followed by its oxidation under hydrothermal conditions to form a plutonium (IV) silicate.

Further optimization of this synthesis protocol has enabled us to form plutonium (IV) silicate while minimizing impurities (Fig. 1) and to implement a washing protocol involving alternating treatments in alkaline and oxidizing acid media to obtain $PuSiO_4$. This treatment was inspired by previous studies on $USiO_4$ and $(Zr,U)SiO_4$. In this way, $PuSiO_4$ was obtained with a purity level sufficient to perform a series of advanced characterizations, including new structural characterizations using synchrotron radiation (HR-XRD, HERFD-XANES and EXAFS).

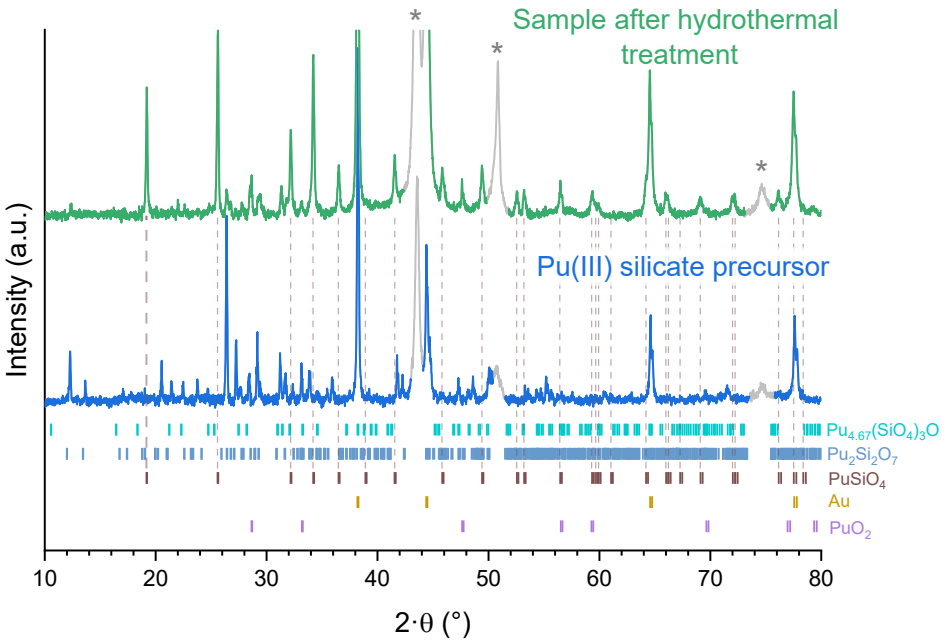


Fig. 1. PXRD pattern for the plutonium (III) silicate precursors used for the synthesis (mixture of $Pu_2Si_2O_7$ and $Pu_{4.67}(SiO_4)_3O$) and the product of hydrothermal synthesis. Gold was used as an internal standard to calibrate the positions of the XRD peaks. The positions marked with an asterisk correspond to diffraction reflections on the sample holder used.

The characterization results obtained for this compound, when considered in light of the results reported for plutonium oxo-hydroxo-silicate colloids [3], provide a better understanding of the properties of plutonium silicate phases and thus pave the way for their potential identification under accident conditions. More broadly, comparing the data for $PuSiO_4$ with all systems in the actinide silicate family—and more generally with the zircon group—also provides a better understanding of these compounds.

[1] OECD Nuclear Energy Agency, Physics and Safety of Transmutation Systems: A Status Report, No. 6090, OECD/ NEA, Paris, 2006.

[2] H. Zänker, *et al.*, *Chemistry Open Reviews*, 2016, **5**, 174–182.

[3] P. Estevenon, *et al.*, *Dalton Transactions*, 2021, **50**, 12528–12536.

[4] B. E. Burakov, *et al.*, *Radiochimica Acta*, 1994, **65**, 199–202.

[5] B. E. Burakov, *et al.*, *MRS Proceedings*, 2000, **663**, 307–313.

[6] C. Keller, *Nukleonik*, 1963, **5**, 41-48.

[7] E. D. A. Ferriss, *et al.*, *American Mineralogist*, 2010, **95**, 229–241.

[8] P. Estevenon, *et al.*, *Dalton Transactions*, 2019, **48**, 10455–10463.

[9] P. Estevenon, *et al.*, *Dalton Transactions*, 2020, **49**, 6434–6445.

Experimental Actinide Chemistry in support of UK Civil Plutonium Inventory Technical Challenges

J. V. Ferrier [1], E. M. B. MacCormick [1], C. R. T. Smylie[1], E. K. Gibson[1], M. L. Baker[2], Z. Qi [2], H. M. Steele[3], R. Bernard[3], R. M. Orr[4], J. H. Farnaby[1*]

[1]School of Chemistry, University of Glasgow, Glasgow, UK; [2]Department of Chemistry, University of Manchester, Manchester, UK; [3]Sellafield Ltd, Sellafield, Cumbria, UK; [4] Central Laboratory, United Kingdom National Nuclear Laboratory, Sellafield, UK; *joy.farnaby@glasgow.ac.uk

The management of the UK's civil plutonium (Pu) inventory by Sellafield Ltd on behalf of the Nuclear Decommissioning Authority is one the most important challenges of UK nuclear decommissioning. The Pu inventory is stored under inert atmosphere in the form of PuO_2 or mixed-actinide oxide (MOX) powders in gas-tight packages on the Sellafield site.[1,2,3] Our work to understand the chemistry of actinide oxides under industrial interim storage conditions will be presented. We have used inert atmosphere synthetic inorganic chemistry, followed by thermal decomposition of precursor complexes to AnO_2 (An = U, Th) nanoparticles (Figure 1 a) to synthesise chemically accurate surrogate materials for PuO_2 and MOX with critical properties tailored to specific technical challenges.[4] We have tested and begun to quantify reactivity with hydrogen and water at the solid-gas interface of AnO_2 under industrial conditions. We have achieved this by application of technology and spectroscopy from heterogeneous catalysis,[5] including X-ray Absorption Spectroscopy (L3 and M4 edges) and Inelastic Neutron Scattering at UK central facilities (Figure 1 b and c). Progress in establishing structure-property relationships will be critically examined. Our plans to develop *in operando* capability using Diffuse Reflectance Infrared Fourier Transform Spectroscopy (DRIFTS, Figure 1 d) and alpha irradiation experiments at the University of Manchester Dalton Cumbrian Facility will be outlined.

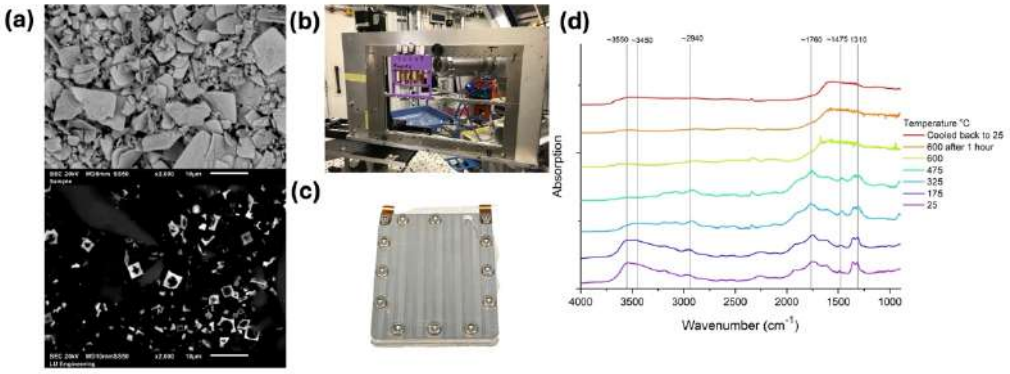


Figure 1. (a) SEM of UO_2 samples, (b) XAS set-up, (c) INS can, (d) example of DRIFTS data

We acknowledge UK Research and Innovation for the award of a Future Leaders Fellowship, the Nuclear Decommissioning Authority, Sellafield Ltd, the UK National Nuclear Laboratory, the Royal Society of Edinburgh, the Engineering and Physical Sciences Research Council, the Carnegie Trust for the Universities of Scotland, and the University of Glasgow for funding and support of this work.

References: (1) Nuclear Decommissioning Authority, Mission Progress Report, **2022**, https://assets.publishing.service.gov.uk/government/uploads/system/uploads/attachment_data/file/1121267/MPR_4_-_2022.pdf. (2) Nuclear Decommissioning Authority, Progress on Plutonium, **2019**, https://assets.publishing.service.gov.uk/government/uploads/system/uploads/attachment_data/file/791046/Progress_on_Plutonium.pdf.(3) Hyatt, N. C. *NPJ Mater. Degrad.* **2020**, *4*, 1. (4) Orr, R. M.; Sims, H. E.; Taylor, R. J. *J. Nucl. Mater.* **2015**, *465*, 756. (5) Leduc, J.; Frank, M.; Jürgensen, L.; Graf, D.; Raauf, A.; Mathur, S. *ACS Catal.* **2019**, *9*, 4719.

Pu(VI) hydrolysis in aqueous alkali and alkaline earth metal solutions: reaction pathways and thermodynamics

D. Fellhauer[1*], O. Walter[2], J. Rothe[1], D. Schild[1], K. Dardenne[1], T. Neill[3], Y. Jo[4], T. Schramm[1], A. Kuzenkova[1], M. Schorer[1], P. Müller[1], R. Meier[1], N. A. DiBlasi[1], X. Gaona[1], M. Altmaier[1], H. Geckeis[1]

[1]Institute for Nuclear Waste Disposal (KIT-INE), Karlsruhe, Germany; [2]Joint Research Centre, Karlsruhe, Germany; [3]University of Manchester, Manchester, United Kingdom; [4]Hanyang University, Seoul, Republic of Korea; *david.fellhauer@kit.edu

Hydrolysis reactions of Pu(VI) in aqueous solutions exhibit unique features among the An(VI) series. While U(VI) and Np(VI) readily form sparingly soluble An(VI)-(hydr)oxide solid phases in neutral to alkaline solutions, the hydrolytic behavior of Pu(VI) is dominated by the formation of dissolved polynuclear hydrolysis species $(PuO_2)_y(OH)_x^{2y-x}(aq)$. These species are metastable at room temperature (RT) with respect to the formation of Pu(VI)-O(H) solids. Most experimental studies on Pu(VI)-OH speciation cover acidic to near-neutral pH_c conditions [1], with few exemption [2,3]. A relatively clear picture of the polynuclear Pu(VI) speciation exists for acidic to neutral conditions, leaving significant gaps in the chemical understanding and thermodynamic description at higher alkalinity. Moreover, the kinetically slow solid phase formation at RT has made it challenging to analyze the solubility behavior of Pu(VI)-(hydr)oxide solids and to obtain a comprehensive understanding of Pu(VI)-O(H) thermodynamics.

To address these gaps, we have investigated the hydrolysis behavior of aqueous and solid Pu(VI) species in various alkali and alkaline earth metal solutions in recent years. One part of the work dealt with the formation and characterization of several new ternary M-Pu(VI)-O(H)(cr) solid phases (M = Na-Cs and Ca-Ba). They were obtained by hydrothermal synthesis and exhibit structures closely resembling those of U(VI) minerals with sheet anion topology based on pentagonal An(VI) polyhedra, while displaying Pu-specific features. Following detailed characterization (e.g., PXRD, SCXRD, Pu L_3-edge XANES and EXAFS, SEM-EDX), solubility experiments at RT yielded the corresponding solubility products. In an independent Vis/NIR study performed in NaCl-NaOH solution at RT, the aqueous Pu(VI)-OH species were systematically investigated in 1 M NaCl-NaOH as a function of pH_c and [Pu(VI)]. Thermodynamic slope analysis, model-tool application and Pu L_3-edge XAFS experiments showed that, in addition to mononuclear PuO_2^{2+} and $PuO_2(OH)_4^{2-}$ (1,4), and dimeric $(PuO_2)_2(OH)_2^{2+}$ (2,2), four trimeric species of the type $(PuO_2)_3(O)(OH)_x^{4-x}$ with x = 3-6 (i.e., (3,5), (3,6), (3,7), (3,8)) dominate the aqueous Pu(VI) speciation over wide pH_c ranges (≈6-13) and Pu(VI) concentrations. A comprehensive set of the corresponding hydrolysis constants was derived. In samples with the highest pH_c and [Pu(VI)], novel Na-Pu(VI)-O(H)(cr) compounds formed even at RT. SC-XRD revealed that these solids consist of discrete $\{Pu_{60}\}$ cage cluster units that form by a self-assembly from the predominant (3,8) solution complex [4]. Finally, long-term equilibration of Pu(VI) under strongly alkaline conditions at RT in the presence of trace divalent metal ions (M = Ca, Sr, Ba) yielded crystalline M-Pu(V)-O(H) compounds. The crystal structure and solubility behavior were successfully analyzed for the Ca phase; work on the Sr and Ba phases is ongoing.

These studies have provided access to several novel and fascinating species and compounds and help to understand the various reaction pathways of Pu(VI) in aqueous solution. Most importantly, however, the results obtained allow us to approach our principal goal, namely a more comprehensive description of the Pu thermodynamics in aqueous solutions. By combining the newly derived

chemical models, hydrolysis constants and solubility products for Pu(VI) (and Pu(V)) with the available database for Pu(III), Pu(IV) and Pu(V) (including data from Pu(III) and Pu(V) analogs), we obtained an updated Pourbaix diagram for Pu. The latter defines the stability of Pu(VI) relative to the water stability field and also clarifies the thermodynamic stability of pentavalent Pu(V). In the presentation, a brief summary of the experimental results is provided and the thermodynamic implications are discussed.

References

[1] Grenthe, I., Gaona, X., Plyasunov, A. V., Rao, L., Runde, W. H., Grambow, B., Konings, R. J. M., Smith, A. L. and Moore E. E. (2008) Chemical Thermodynamics Volume 14 – Second Update on the Chemical Thermodynamics of U, Np, Pu, Am and Tc. OECD Publishing, Paris.

[2] Reilly, S. D. and Neu, M. P. (2006). Pu(VI) hydrolysis: further evidence for a dimeric plutonyl hydroxide and contrasts with U(VI) chemistry. Inorg. Chem. 45: 1839-1846

[3] Rao, L., Tian, G., Di Bernado, P. and Zanonato, P. (2011). Hydrolysis of plutonium(VI) at variable temperatures (283–343 K). Chem. Eur. J. 17: 10985-10993

[4] Fellhauer, D., Walter, O., Rothe, J., Dardenne, K., Schild, D., Meier, R., Müller, P., Jo, Y., Gaona, X., Altmaier, M., Geckeis, H. (2026). Unexpected {Pu_{60}} cage cluster units in new plutonium(VI) oxido-hydroxides. Angew. Chem. Novit 2:e70018.

Ceramic Wasteform and Process Development for Pu Disposition

A. A. Friskney [1], M. C. Stennett [1], L. R. Blackburn*[1]

[1] *Immobilisation Science Laboratory, School of Chemical, Materials and Biological Engineering, University of Sheffield*

a.a.friskney@sheffield.ac.uk, *lewis.blackburn@sheffield.ac.uk

The United Kingdom holds around 140 tonnes of separated civil plutonium in safe and secure storage, arising from the aqueous reprocessing of spent nuclear fuel. Following a UK government policy update in January 2025 [1], all Pu will be readied for immobilisation prior to permanent disposition in a geological disposal facility (GDF). This will thereby require Pu to be converted into a passively safe ceramic wasteform, for which zirconolite-structured materials ($CaZrTi_2O_7$) are considered to be a feasible candidate system. Studies of related wasteform systems have demonstrated that Pu can be readily be incorporated within the zirconolite crystal structure alongside neutron absorbing additives and charge balancing additives up to a reasonable waste loading (e.g. ~ 20 wt. %) [2]. Potential zirconolite formulations have been refined to yield a broad understanding of its fundamental material properties through synthesis at laboratory scale and have produced a generally accepted 'baseline' composition from which performance properties can be benchmarked and further modification can be rationalised. To facilitate the translation of this product to an industrial scale, strategies must be developed to understand how the product could vary from the expected baseline when considering the constraints of a Pu-active product.

Uranium has been previously utilised as a Pu surrogate to evaluate the viability of wasteform compositions and act as a basis from which to inform future Pu validation trials. Present study has successfully reproduced the current accepted UK baseline composition using radiological hot isostatic pressing (HIP); a preferred thermal treatment route to allow batch-wise production at larger scales. A CuO process additive has been investigated, previously demonstrated to reduce the zirconolite formation temperature *via* liquid phase sintering [3]. In the context of a zirconolite ceramic contained within a stainless steel HIP canister, the more facile formation of the target actinide host phase induced by the CuO additive may reduce the requirement for high energy planetary milling and carrier fluid in the process flowsheet. The production of secondary waste streams would therefore be decreased, ensuring a more suitable powder process for manufacturing Pu wasteforms at the scales required to immobilise the UK inventory. A suite of samples has been synthesised, using a low energy dry milling approach for the radioactive fraction. Following HIP processing, CuO addition significantly reduces the fraction of undigested UO_2 observed, as well as equilibrating the U content across the bulk zirconolite phase (**Figure 1**). U L_3 edge X Ray Absorption Spectroscopy has then been applied to understand the impact of HIP and process additives on the local coordination and oxidation states of U in the zirconolite phase. This work contributes to the development and understanding of zirconolite ceramics to be produced at scale for safe Pu management.

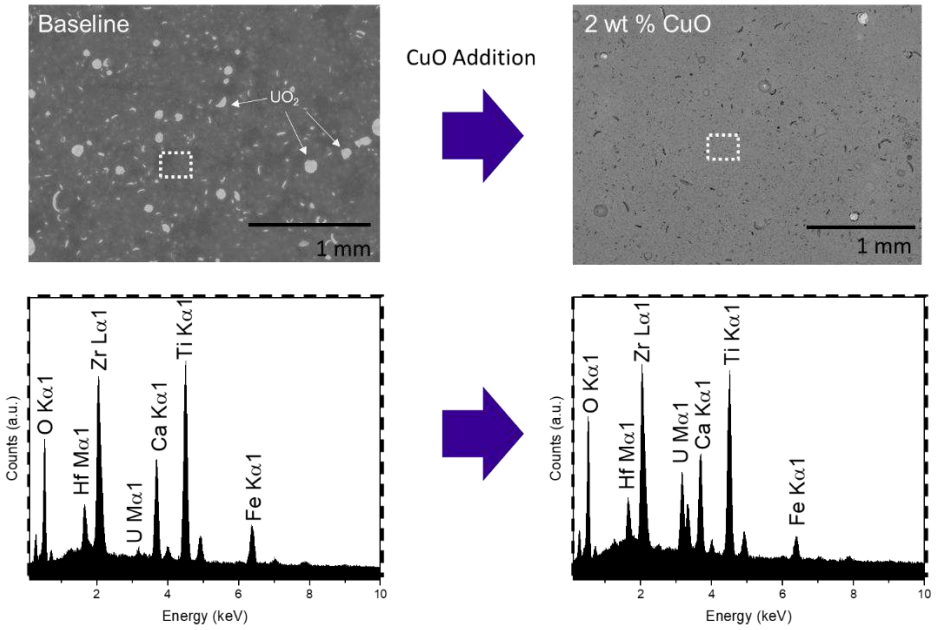


Figure 1: Direct comparison of the HIPed baseline composition $((Ca_{0.785}U_{0.2}Gd_{0.015})(Zr_{0.785}U_{0.1}Hf_{0.1}Gd_{0.015}))(Ti_{1.6}Fe_{0.4})O_7$ (left) with the 2 wt % CuO additive composition (right) after 8 hours of dry roller milling. Representative EDS spectra, over 100 μm from undigested UO_2 are given for both.

[1] Michael Shanks; Statement from Department for Energy Security and Net Zero; (24 Jan 2025)
[2] Blackburn L.R. *et al*; Adv. Appl. Ceramics; (2021); **120**; pp 69-83
[3] Friskney A.A. *et al*; Ceramics; (2023); **6**; pp678-685

Influence of Cooling Speed and Aluminum Content on the Microstructure of As-Cast δ-PuAl Alloys

Renaud Génin[1,*], Clément Ciszak[1], Benoît Oudot[1]

[1]CEA VALDUC, DAM, F-21120 Is-sur-Tille, France; *renaud.genin@cea.fr

Plutonium is one of the most complex elements in the periodic table. The existence of six phase transitions between room temperature and its low melting point, coupled with the fact that these structures have vastly different volumes, densities, and mechanical properties, limits the use of the pure metal. High ductility and good corrosion resistance are the main reasons why δ-phase is usually preferred. Aluminum is frequently used as a δ-stabilizing alloying element.

When cooling down from the liquid domain, PuAl alloys typically go through the L+ε and the ε+δ phase regions, during which the microstructure is prone to elemental segregation that will be retained down to room temperature in as-cast alloys. This coring phenomenon has been shown to be influenced by the alloying content [1], as well as the cooling rate through the ε+δ region [2].

The objective of this study is to investigate the influence of the processing parameters on the grain size, as well as the size and shape of the segregation domains. Image analyses of microstructural data obtained from the literature, completed with new experimental measurements were performed. An empirical relationship that describes the distribution of size and shape of the segregation domains that appear in as-cast PuAl alloys, as a function of both cooling speed and Al content is proposed based on these measurements.

References

[1] A. Fourmont, C. Ciszak, B. Oudot, Modeling the Microstructural Evolution of δ-PuAl Alloys as a Function of Temperature, Pu Futures 2024, Charleston, NC, USA.

[2] B. Spriet, Étude des transformations allotropiques du plutonium, PhD Thesis of the Paris-Orsay University, 1966.

Advancing Actinide Quantum Materials at INL's Glenn T. Seaborg Institute: The Case of PuB_6

K. Gofryk

Glenn T Seaborg Institute, Idaho National Laboratory, Idaho Falls, Idaho, USA
Krzysztof.gofryk@inl.gov

Actinide materials occupy a unique and pivotal position in condensed matter physics due to the dual localized–itinerant nature of their 5f electrons. Among them, plutonium stands out as one of the most complex and fascinating elements in the periodic table. Its rich phase diagram, strong electronic correlations, and delicate balance between competing ground states make it a compelling platform for discovering new quantum phenomena. However, progress in this field has historically been hindered by the limited availability of high-quality materials and the intrinsic challenges associated with handling radioactive elements. In particular, the intermediate character of 5f electrons, more extended than 4f yet more strongly correlated than d electrons, creates significant theoretical and experimental challenges, leading to a relative scarcity of comprehensive low-temperature data. Recognizing the strategic importance of advancing actinide science, Idaho National Laboratory established the Glenn T. Seaborg Institute to integrate expertise in synthesis, characterization, theory, and modeling of actinide materials. Within this framework, the Solid-State Actinide Chemistry and Physics focus area aims to uncover emergent quantum states driven by strong correlations and spin–orbit coupling.

In this talk, I will present an overview of the Solid-State Actinide Chemistry and Physics focus area within the Institute and conclude with recent advances in our studies of plutonium hexaboride (PuB_6), a promising candidate for a correlated topological insulator. By combining high-quality single-crystal synthesis, micromachining-based device fabrication, magnetotransport measurements, and detailed electronic-structure calculations, we investigate its low-temperature electronic properties. Electrical resistivity measurements reveal a narrow energy gap at the Fermi level, consistent with a two-channel conduction model comprising semiconducting bulk and metallic surface contributions. A low-temperature resistivity plateau and its dependence on surface-to-volume ratio further support the presence of surface states. Magnetoresistivity data indicate transport arising from an interplay between Dirac-like surface carriers and conventional bulk carriers, rather than a single pristine topological channel. Together, these results establish PuB_6 as a promising platform for studying the interplay between strong electronic correlations and nontrivial topology. Finally, I will discuss how the distinct energy scales of 5f systems influence topological behavior relative to 4f materials, revealing new opportunities in actinide-based quantum materials.

Plutonium Futures Conference 2026 Abstract

Title: Electrochemical behavior of Actinides (An) in molten alkali halide salts

Author: Riddhi R. Golwankar

Coauthors: Travis Marshall-Roth, Brittany L. Huffman, Thomas E. Shaw IV, Nickolas H. Anderson, Stosh A. Kozimor

For decades, researchers have advanced our understanding of 5*f*-element electronic structures and actinide bonding, largely by studying how actinide 5*f*- and 6*d*-valence orbitals interact with directly coordinated anions and ligands. However, many of these studies either neglected or insufficiently modeled the influence of molecules and ions in the outer coordination sphere. As a result, our current bonding descriptions remain incomplete, a gap that can be significant given the impact of intermolecular forces such as hydrogen bonding, ion-dipole and ion-induced-dipole interactions, and van der Waals forces. Incorporating these interactions into electronic-structure models could refine our understanding of actinide bonding and help reconcile discrepancies between theoretical predictions and experimental measurements. Motivated by ongoing community efforts to elucidate how outer-sphere ions and molecules (M) affect 5*f*- and 6*d*-bonding between actinide centers (An) and inner-sphere anions or ligands (X) across the An–X···M motif, we have developed an alternative method to quantitatively compare the effects of direct chemical bonding with those arising from the outer coordination sphere on actinide electron-transfer chemistry. Our approach uses molten salts as tunable chemical media, enabling systematic variation of both direct bonding interactions and outer-sphere influences by altering the salt composition. In this poster, we summarize our findings to date and provide new insight into how outer-sphere interactions shape electron-transfer behavior across the actinide series (Th, Np, Pu, U).

Computational Insights into Plutonium Chemistry: From Density Functional Theory to Kinetic Modeling

Ivana Gonzales[1,*], Travis Jones[1], Alex Mũnoz[1]

[1]Los Alamos National Laboratory, Los Alamos, USA; *ivana@lanl.gov

Computational approaches have become an indispensable tool for elucidating complex chemistry of actinides, where strong electron correlation and relativistic effects play a decisive role, alongside challenges such as multiple accessible oxidation states, complex bonding behavior, and limited experimental data. These methods complement experimental studies by providing mechanistic insights, supporting interpretation of experimental measurements, and allowing exploration of conditions that may be impractical to reproduce in the laboratory. By offering a balance between computational efficiency and predictive accuracy, density functional theory (DFT) in particular enables characterization of electronic structure, bonding, and reactivity, while kinetic modeling extends this capability to predict system-level behavior and time-dependent evolution.

In this work, we first explore DFT-based approaches to obtain an accurate description of the electronic structure of plutonium metal and understand defect formation as well as the interactions of these defects with hydrogen and oxygen atoms. We then examine the capability of DFT-driven methodologies to model X-ray photoelectron spectroscopy line shapes for plutonium and its oxides, providing insight into phase identification, surface structure, and the ability of computational methods to reproduce characteristic 4f spectral features. By directly linking calculated densities of electronic states to experimentally observed spectral profiles, these approaches can support interpretations and assignments beyond traditional empirical fitting techniques.

Finally, we discuss a kinetic modeling framework, implemented using Cantera software suite, to describe gas-phase radiolysis by tracking the time-dependent evolution of species generated through radiation-induced reactions. Radiation effects are represented as source terms that produce reactive intermediates, which are then propagated through a detailed reaction mechanism using Cantera's reactor network approach. We further demonstrate that coupling gas-phase and surface chemistry through heterogeneous reaction capability implementation can affect system behavior. By linking gas reactions with surface processes on plutonium, including adsorption of oxygen and oxide growth, the model captures feedback between different phases. This coupled framework provides a more complete understanding and prediction of radiolytically driven multiphase chemistry.

Solubility of Np_2O_5(cr) and Hydrolysis of Np(V) in Neutral to Alkaline NaCl-NaOH Solutions

F. Greb[1*], D. Fellhauer[1], D. Schild[1], M. Altmaier[1], X. Gaona[1], H. Geckeis[1]

[1]KIT-INE, Karlsruhe, Germany; *fabian.greb@kit.edu

Disposal of nuclear waste in deep geological repositories is considered the safest option to minimise radionuclide migration into the biosphere. Contact with aqueous solutions upon corrosion of waste containers may release radionuclides from the solid waste matrices, posing a risk for long-term safety. Relevant (geo-)chemical processes controlling mobilisation and retention (e.g. solubility and complexation, colloid and solid phase formation, interaction with mineral phases or redox processes) require comprehensive analysis. Neptunium (Np) is a component in spent nuclear fuel and redox-active in aqueous solutions. Under the reducing conditions expected in deep geological repositories, Np mainly occurs as sparingly soluble, strongly sorbing Np(IV) species. Under redox-neutral to oxidizing conditions (i.e. in the biosphere or during the early phase after repository closure), Np(V) can form, exhibiting higher solubility and lower sorption tendency. Even in the absence of additional complexing ligands, the possible formation of several hydrolysis species ($NpO_2(OH)_n^{n-1}$) and solid phases (NpO_2OH(am), Np_2O_5(cr), Na-Np(V)-OH(cr)) complicates the speciation of Np(V). This study investigates the solubility and hydrolysis of binary Np_2O_5(cr) and provides a comparative assessment of its thermodynamic stability relative to other Np(V) compounds formed in the Np(V)-Na-H-Cl-OH-H_2O(l) system.

Experiments were performed under argon atmosphere at T = 23 ± 2 °C using ^{237}Np ($t_{1/2}$ = 2.14·10^6 a). Np_2O_5(cr) was synthesized by hydrothermal equilibration (130 °C) of binary NpO_2OH(am) – the initial Np(V) reaction product obtained by precipitation of the aquo ion NpO_2^+ with NaOH – and characterised by powder X-ray diffraction (XRD) and scanning electron microscopy equipped with energy-dispersive X-ray spectrometry (SEM-EDX). Batch solubility experiments with Np_2O_5(cr) were conducted starting from undersaturation conditions in 0.1 m NaCl-NaOH solutions with pH_m = 8-13. The equilibration of the samples was monitored by repeated measurement of pH_m (glass combination electrode) and Np(V) concentrations (liquid scintillation counting, solvent extraction) as a function of time. Post-mortem analyses (XRD, SEM-EDX) confirmed that Np_2O_5(cr) was the solubility controlling solid phase throughout this study. The observed solubility curve follows a similar trend in comparison to NpO_2OH(am), while Np_2O_5(cr) is significantly less soluble. A linear decrease in the solubility with a slope of ≈ −1 from pH_m 8 to ≈ 10 is in line with the solubility equilibrium 0.5 Np_2O_5(cr) + H^+ ⇔ NpO_2^+ + 0.5 H_2O(l). A flattening decrease (slope > −1), followed by a solubility minimum at pH_m ≈ 11.5 with log $m_{Np(V)}$ = −6.7 (Δlog $m_{Np(V)}$ ≈ 1.4 compared to NpO_2OH(am)), visualises the gradual formation of NpO_2^+ hydrolysis species according to 0.5 Np_2O_5(cr) + (n−0.5) H_2O(l) ⇔ $NpO_2(OH)_n^{(1-n)}$ + n−1 H^+. An increasing solubility at greater alkalinity (slope > 0) further indicates the presence of anionic hydrolysis complexes with n ≥ 2. A thermodynamic SIT (specific ion interaction theory) model was derived based on the observed solubility level, in combination with hydrolysis constants derived from solubility measurements for the ternary Na-Np(V) hydroxide phases $Na_{0.5}[NpO_2(OH)_{1.5}]\cdot 0.5H_2O$(cr) and $Na[NpO_2(OH)_2]$(cr), respectively, as reported in the literature. The present study provides a solubility constant log K° for Np_2O_5(cr), indicating a solubility level partially in line with expectations based on literature data, but also, for the first time, data consistent with current findings on the hydrolysis behaviour of Np(V) ($NpO_2(OH)_n^{n-1}$ with n = 0-3), i.e. across a wider pH_m range. The available data allow a comparative assessment of the Np_2O_5(cr) stability in relation to other solid Np(V) phases in the studied system. The binary oxide is thermodynamically stable up to pH_m ≈ 11, and metastable in more alkaline solutions, as the stability of sodium-containing phases increases at higher ionic strengths.

Metallophilic Actinide-Platinum Interactions in Bimetallic Pyridyloxy Complexes

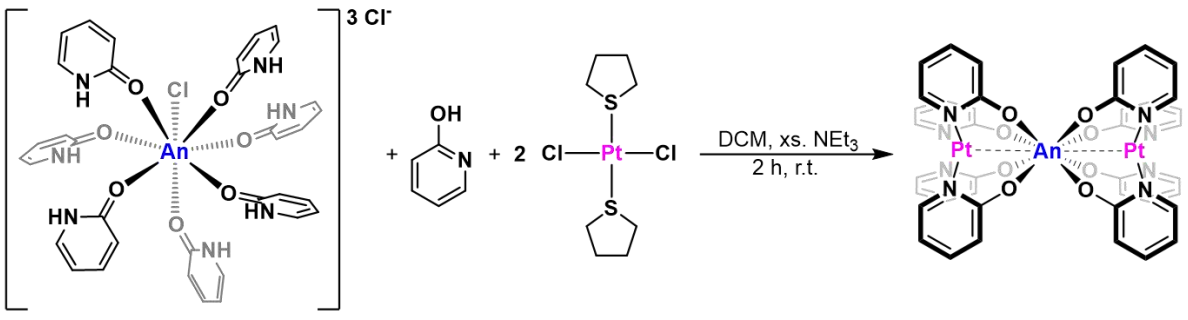
Dennis Grödler[1*], Peter Kaden[1], Moritz Schmidt[1,2] and Robert Gericke[1]

[1]Helmholtz Zentrum Dresden-Rossendorf, Institute of Resource Ecology, Dresden, Germany;
[2]Institute of Materials Chemistry, Brandenburg Technical University, Senftenberg, Germany
*d.groedler@hzdr.de

Pyridin-2-olate (PyO^-) is an established chelating ligand for the construction of heterobimetallic architectures featuring bonds between transition metals and/or main-group elements.[1,2] Well-defined metal–metal interactions remain uncommon in actinide coordination chemistry, especially beyond uranium, despite the rich redox chemistry and typically high coordination numbers of these elements.

Owing to their typically high coordination numbers and accessible oxidation states, actinide 2-hydroxypyridinolate complexes offer the structural flexibility needed to accommodate a range of transition metals. By strategic preorganization of the ligand environment and deliberate consideration of the preferred coordination geometries of the individual metal centers, we synthesized a homologous series of complexes with the general formula $[Pt(\mu\text{-}PyO)_4An(\mu\text{-}PyO)_4Pt]$ (An = Th, U, Np, Pu). These compounds represent the first structurally characterized heterotrimetallic transuranium complexes featuring Pt(II).

Structural elucidation by single-crystal X-ray diffraction confirms the formation of discrete heterotrimetallic assemblies with An–Pt distances near the sum of their corresponding covalent radii. Their electronic and magnetic properties were examined by SQUID magnetometry and multinuclear NMR spectroscopy, corroborated by quantum-chemical calculations. Notably, ^{195}Pt NMR spectroscopy proved to be a sensitive probe for assessing and quantifying intermetallic interactions. We report, to the best of our knowledge, the first observation of ^{195}Pt chemical shifts significantly perturbed by close proximity to a paramagnetic actinide center.



An = Th, U, Np, Pu

[1] J. Wagler, R. Gericke, Molecules 2023, 28, 5442.
[2] R. Gericke, J. Wagler, Inorg. Chem. 2020, 59, 9, 6359-6375.

This research is funded by the German Federal Ministry for the Environment, Climate Action, Nature Conservation and Nuclear Safety under project number 1501667 (Am-BALL).

Actinide (VI), and Nitric Acid Speciation Studies in Separation Processes using N,N-Dialkylamide Extractants

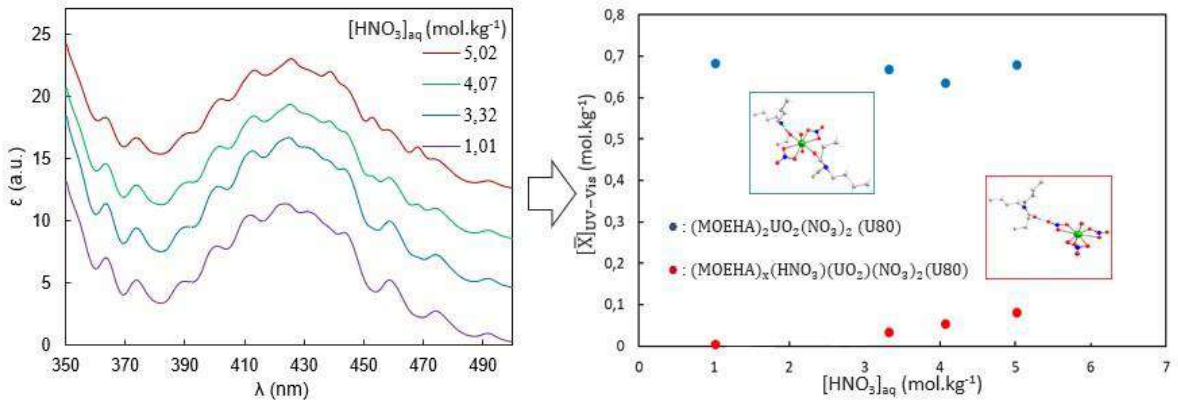
Thibau Blanc[1], Younes Nourine[1], Pauline Moeyaert[1], Christelle Tamain[1], Donatien Gomes Rodrigues[1], Thomas Dumas[1], Philippe Guilbaud[1*]

[1]CEA, DES, ISEC, DMRC, Univ Montpellier, Marcoule, France
*philippe.guilbaud[at]cea.fr

N,N-dialkylamides demonstrated their potentiality in the recovery and recycling of plutonium and uranium, for the reprocessing of MOX spent nuclear fuels using solvent extraction processes. First, they exhibit a good stability towards radiolysis and hydrolysis. Secondly, distribution ratios of plutonium (IV) and uranium (VI) with N,N-dialkylamide are such that their extraction and separation is possible, without using any reducing agent for the uranium – plutonium partitioning.

The extraction process model used by CEA is currently based on thermodynamic equilibrium calculations solving mass action law that uses activity coefficient for both aqueous and organic phases. For this model, hypothesis have to be made regarding the speciation of the species, which include N,N-dialkylamides, metallic cation, nitric acid and/or water, formed in the organic phase. Therefore, a thorough understanding of this speciation is essential for developing a robust model.

In order to obtain speciation diagrams of the complexes formed during the extraction of nitric acid and uranium (VI) with a N,N-dialkylamide, batch experiments were performed to determine extraction isotherms, and to study concomitantly the behavior of water, nitric acid and U(VI) in N,N-dialkylamide organic phases: UV-Vis and IR spectroscopies analyses have been performed and principal component analyses have been used in combination with molecular dynamic simulations to obtain new speciation diagrams. These speciation diagrams were then incorporated into the model.



This new approach has enabled us to identify a group of species with N,N-dialkylamide, U(VI), HNO_3 and water for which experimental and calculated data are in good agreement, both in terms of distribution and speciation. More recently, the same approach has been used for the speciation of neptunium (VI) in similar organic phases. Using these speciation diagrams, derived from complementary experimental techniques and molecular models, this approach enhances the robustness of the model, particularly for chemical conditions outside the range in which the experimental data were originally obtained.

The Effect of Diluent on Uranium(VI) and Plutonium(IV) Solvent Extraction with Monoamide Extractants

D. Guillaumont*[1], C. Poulin-Ponnelle[1], A. Masmoudi[1], A. Garine-Wichatitsky, C. Marie [1], T. Dumas[1] L. Berthon[1]

[1]*CEA, DES, ISEC, DMRC, Univ. Montpellier, Marcoule, Bagnols sur Cèze 30207, France*
*dominique.guillaumont@cea.fr

Irradiated nuclear fuels can be reprocessed to recover uranium(VI) and plutonium(IV) and to reduce the volume of high-level radioactive wastes. Selective separation of actinides can be achieved by solvent extraction, in which spent fuel is dissolved in a nitric acid solution and suitable organic ligands are diluted in a hydrocarbon diluent to extract actinide cations into an organic phase. The diluent, being the major constituent of the organic phase, can strongly influence the degree of metal extraction, the selectivity, and the nature of extractant-metal complexes and the radiolytic degradation.

We have investigated the solvent extraction of U(VI) and Pu(IV) in the absence of diluent, using an organic phase composed of pure extractant molecule and have compared the results with those obtained in the presence of a hydrocarbon diluent. The extractant molecules studied are N,N-dialkyl amides (monoamides). These molecules are promising candidates for U(VI) and Pu(IV) extraction from irradiated nuclear fuels through solvent extraction due to their high selectivity toward fission product, strong resistance to irradiation and their ability to be incinerated, thereby minimizing secondary waste.[1,2] Moreover, N,N-dialkyl amides present tunable extraction properties depending on the branching and length of their alkyl chains. In the present work, N-méthyl-N-octyl-(2-éthyl)-hexanamide (MOEHA) and N,N-(2-ethylhexyl)isobutyramide (DEHiBA) were investigated.[3]

The composition of the organic solution was analyzed after nitric acid and metal extraction using both pure and diluted monoamide solutions. The physical and chemical properties, including viscosity and density, were also measured. The metal-extractant complexes of Pu(IV) and U(VI) with these monoamides were characterized using UV-Vis, X-ray absorption spectroscopy (EXAFS) and electrospray ionization mass spectrometry (ESI-MS).[4–6] The effect of the diluent on the radiolytic degradation of the organic solution was also evaluated using gamma radiolysis. The result show that the diluent has a considerable influence on the composition of the organic solution, the degree of extraction and the underlying extraction mechanisms. In particular, the absence of diluent increases significantly uranium and plutonium extraction and alter the coordination structures of the actinide complexes in the organic phase.

(1) Miguirditchian, M.; Baron, P.; Lopes Moreira, S.; Milanole, G.; Marie, C. Novel Dissymmetric N,N-Dialkylamides, the Synthesis Thereof and Uses of Same. WO2017017193, 2017.
(2) Berger, C.; Marie, C.; Guillaumont, D.; Zekri, E.; Berthon, L. Extraction of Uranium(VI) and Plutonium(IV) with Tetra-Alkylcarbamides. *Solvent Extr. Ion Exch*. **2019**, *37* (2), 111–125.
(3) Blanc, T.; Golfier, L.; Moreno Martinez, D.; Guillaumont, D.; Dumas, T.; Moeyaert, P.; Guilbaud, P. Extraction of Nitric Acid with a Monoamide: Understanding Study and Thermodynamic Modeling. *Ind. Eng. Chem. Res.* **2025**, *64* (26), 13376–13387.
(4) Berger, C.; Marie, C.; Guillaumont, D.; Tamain, C.; Dumas, T.; Dirks, T.; Boubals, N.; Acher, E.;

Laszczyk, M.; Berthon, L. Coordination Structures of Uranium(VI) and Plutonium(IV) in Organic Solutions with Amide Derivatives. *Inorg. Chem.* **2020**, *59* (3), 1823–1834.
(5) Acher, E.; Dumas, T.; Tamain, C.; Boubals, N.; Solari, P. L.; Guillaumont, D. Inner to Outer-Sphere Coordination of Plutonium(IV) with N,N-Dialkyl Amide: Influence of Nitric Acid. *Dalton Trans.* **2017**, *46* (12), 3812–3815.
(6) Acher, E.; Hacene Cherkaski, Y.; Dumas, T.; Tamain, C.; Guillaumont, D.; Boubals, N.; Javierre, G.; Hennig, C.; Solari, P. L.; Charbonnel, M.-C. Structures of Plutonium(IV) and Uranium(VI) with N,N-Dialkyl Amides from Crystallography, X-Ray Absorption Spectra, and Theoretical Calculations. *Inorg. Chem.* **2016**, *55* (11), 5558–5569.

Title

Bridging Scales: Comparative Elastic-Modulus Measurements by Resonant Ultrasound Spectroscopy, Nano-Indentation, and Bulk Mechanical Tests

-Mathew Hayne, Zachary Levin, Roger Jaramillo, Michael Kopriva, Isaac Hernandez, Todd Martinez, Veronica Anghel

Abstract

The reliable determination of elastic moduli for engineering alloys is essential for component design, yet the values obtained from resonant ultrasound spectroscopy (RUS), continuous-stiffness-measurement (CSM) nano-indentation, and conventional bulk mechanical testing often diverge. In this work we systematically compare these three techniques on a series of single-phase metallic alloys (e.g., δ-phase plutonium and 1100 aluminum). The findings help delineate the capabilities and limitations of each method for characterizing elastic properties of single-phase alloys. By establishing quantitative correction factors and uncertainty bounds, the study provides a practical framework for interchanging measurement techniques—enabling rapid screening via CSM or non-destructive evaluation by RUS while retaining confidence in the bulk-level material response. The methodology is directly applicable to rapid alloy development and designed for manufacturing programs where accurate elastic-modulus data are a prerequisite for reliable finite-element modelling and structural certification.

Keywords: elastic modulus, resonant ultrasound spectroscopy, continuous stiffness measurement, nano-indentation, bulk mechanical testing, δ-phase plutonium, multiscale characterization.

LA-UR-26-21925

Approved for public release; distribution is unlimited.

Title:	Oxygen Vacancies Drive f-orbital Density into the Band Gap of Np/Pu Oxides
Author(s):	Heiner, Benjamin Ray Beaux, Miles Frank II
Intended for:	Plutonium Futures, 2026-09-13/2026-09-17 (Edinburgh, UNITED KINGDOM)
Issued:	2026-03-13

Los Alamos
NATIONAL LABORATORY







Los Alamos National Laboratory, an affirmative action/equal opportunity employer, is operated by Triad National Security, LLC for the National Nuclear Security Administration of U.S. Department of Energy under contract 89233218CNA000001. By approving this article, the publisher recognizes that the U.S. Government retains nonexclusive, royalty-free license to publish or reproduce the published form of this contribution, or to allow others to do so, for U.S. Government purposes. Los Alamos National Laboratory requests that the publisher identify this article as work performed under the auspices of the U.S. Department of Energy. Los Alamos National Laboratory strongly supports academic freedom and a researcher's right to publish; as an institution, however, the Laboratory does not endorse the viewpoint of a publication or guarantee its technical correctness.

Oxygen Vacancies Drive *f*-orbital Density into the Band Gap of Np/Pu Oxides

Benjamin R. Heiner, Miles F. Beaux

Los Alamos National Laboratory, P.O. Box 1663, Los Alamos, New Mexico 87545 USA
benheiner@lanl.gov

With the recent availability of single crystals, we have characterized the surface of Np_2O_5 using scanning tunneling spectroscopy (STS) at cryogenic temperatures. In addition to the band gap, two electronic features were observed on the surface: finite electron density in the previously observed band gap and a semimetallic suppression of the density of states at the Fermi Energy. These were unexpected and unpredicted, but using a proven theoretical model, we attribute these behaviors to areas of the crystal surface with variable oxygen vacancies. The model predicts that as oxygen vacancies are added to the calculation, the neptunium 5*f* orbital density fills in the band gap of pure Np_2O_5 until the crystal eventually becomes semimetallic. This work contextualizes the characterization of plutonium substoichiometric sesquioxide by STS, which contradicts calculation of plutonium oxides to be semiconductors. That the band gap of Np_2O_5 collapses into semimetallic behavior leads us to hypothesize that stoichiometric plutonium oxides would also have band gaps, but the electronic structure of actinide oxides are sensitive to even slight deviations to atomic ratios.

ToF-SIMS Analysis of Heat-Treated Aged 2 at.% Ga-Stabilized δ-Pu

Sarah C. Hernandez[1], James Mudd[1], Aaron Martinez[1], Alberto Gomez[1], Michael Kopriva[1], Kristen Pace[1], Najeb Abdul-Jabbar[1]

[1]Los Alamos National Laboratory, Los Alamos, New Mexico, United States Country
*hernansc@lanl.gov

Time-of-Flight Secondary Ion Mass Spectroscopy (ToF-SIMS) is a unique surface science technique that is highly sensitive to the first 1-2 monolayers of the surface (<1nm) and can detect all isotopes (including hydrogen) at parts-per-million levels, which gives a comprehensive survey of surface constituents. This technique also provides a structural and reactivity, chemisorption versus physisorption, information and complements other surface science techniques, such as X-ray photoelectron spectroscopy (XPS). In general, ToF-SIMS may provide a more in-depth analysis of surface constituents that otherwise might not be detected or deconvolved from a complex XPS spectra. A newly installed ToF-SIMS nanoToF 3 at Los Alamos National Laboratory uses a 30 kV Bi_3^{++} liquid metal ion gun as the primary ion source and has a mass resolution of 12,000 (Δm/m), thus providing a new level of mass resolution and sensitivity on Pu surfaces that was not previously achieved.

We recently applied ToF-SIMS analysis to a heat-treated aged 2 atomic % (at.%) Ga stabilized δ-Pu. This sample was heated to 525°C for 5 hours in the ε-phase in a dilatometry instrument, which resulted in a volume expansion. Upon cooling, the resulting surface showed a series of nodules protruding and pitting from the surface (Figure 1). Upon further inspection using the SEM, there are pitted "bubblelike" morphology similar that was observed by Wheeler and Roussel [1]. Chemical analysis of these regions showed a concentration of transition metal impurities at the "bubblelike" features (Figure 2a), where there is an overlap with $^{24}Mg^+$, $^{52}Cr^+$, and $^{56}Fe^+$. Using Ar^+ ion sputtering to ~19.2nm in depth, a 3-dimensional depth profile mapped showed columnar features, which is an artifact-induced by the ion sputtering thus indicating that these chemical impurities are most likely an inclusion that cannot be eroded away (Figure 2c). Segregation of impurities to He bubbles is known as radiation-induced segregation (RIS) and has been observed in other materials such as ferritic-martensitic steels [2] and FeNiCoCr high-entropy alloy [3]. This observed chemical heterogeneity will be discussed in more detail.

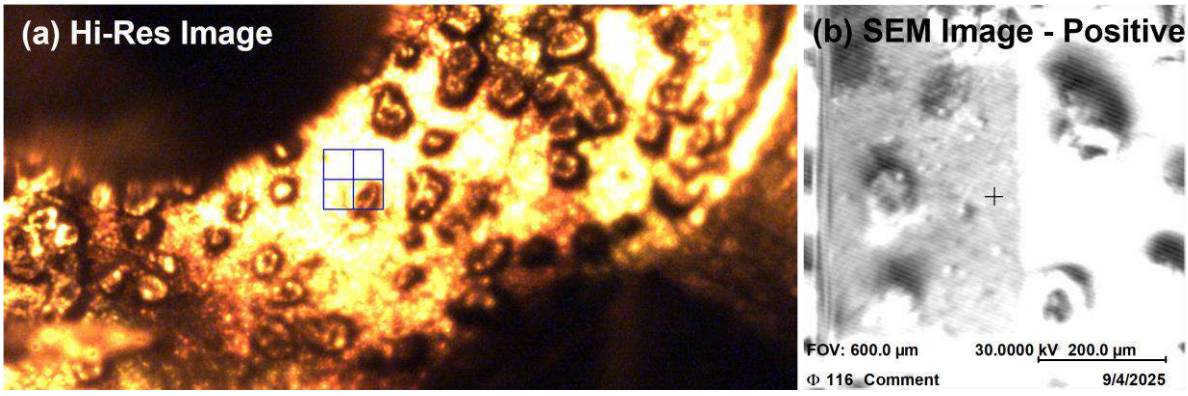


Figure 1: ToF-SIM (a) high-resolution (Hi-Res) image and (b) SEM image taken in the positive ions for the heat-treated 2 at.% Ga stabilized δ-Pu.

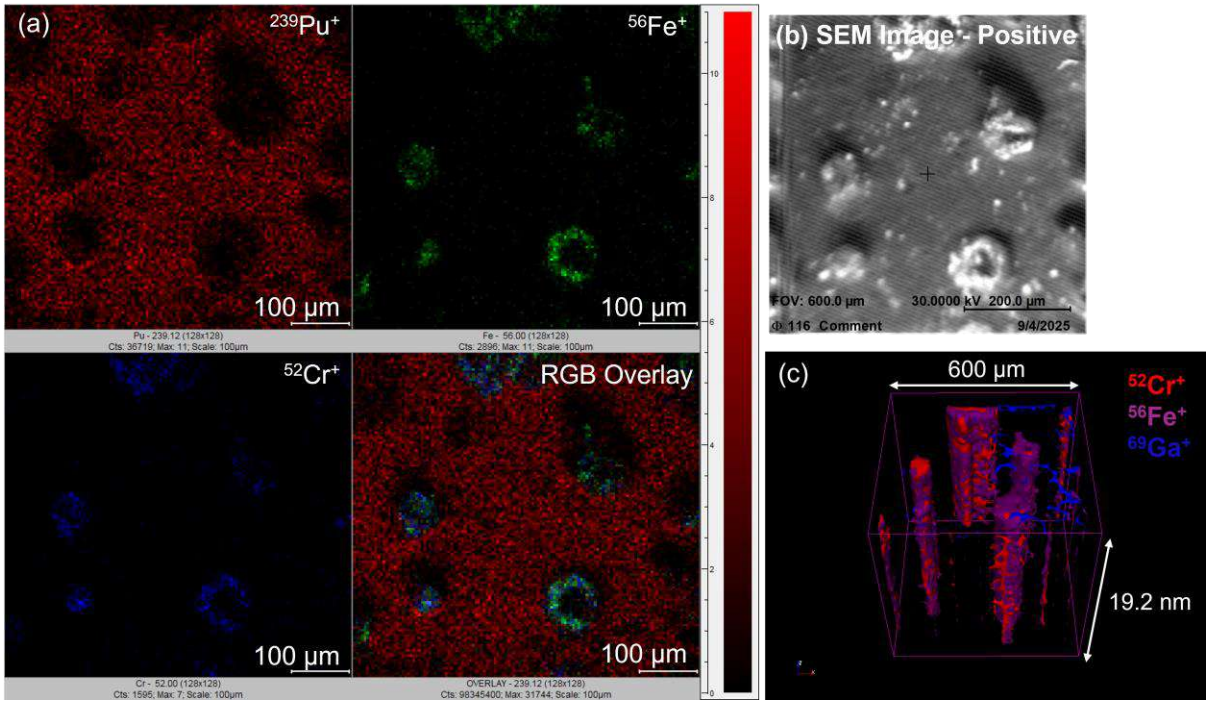


Figure 2: ToF-SIMS (a) red-green-blue overlay chemical mapping of $^{239}Pu^{+}$, $^{52}Cr^{+}$, and $^{56}Fe^{+}$ before Ar^{+} ion sputtering, (b) SEM image taken in positive ions after sputtering at a depth of ~19.2nm, and (c) 3D image chemical mapping of $^{52}Cr^{+}$, $^{56}Fe^{+}$, and $^{69}Ga^{+}$.

Acknowledgements to the Office of Experimental Science and Aging and Lifetimes programs for supporting this work.

1. Wheeler, D.W. and P. Roussel, *Review of the behavior of helium bubbles in aged plutonium and their influence on material properties.* Journal of Vacuum Science & Technology A, 2025. **43**(2).
2. Liu, X., et al., *Understanding the effect of minor alloying elements on helium bubble formation in ferritic-martensitic steels.* Journal of Nuclear Materials, 2025: p. 156045.
3. Lin, W., et al., *He-enhanced heterogeneity of radiation-induced segregation in FeNiCoCr high-entropy alloy.* Journal of Materials Science & Technology, 2022. **101**: p. 226-233.

Developments in plutonium analysis at the AWE

Matthew Higginson[1], Philip Kaye[1], Thomas Shaw[1], Stuart Dunn[1], Louise Ingman[1], Alice Shilling[1], Christopher Puxley[1], Susan Dare[1], Karlie Woods[1],

[1]AWE Nuclear Security Technologies, Aldermaston, Reading, Berkshire, RG7 4PR,
*matthew.higginson@awe.co.uk

The precise and accurate analysis of plutonium materials is essential to ensure the safe and secure application of nuclear technology for societal benefit. The analysis requirement is enduring in the context of international safeguards, material processing, certification, nuclear security, and environmental compliance.

With six allotropic crystal phases at ambient pressure, pure plutonium is the most complex elemental solid in the periodic table. As chemical composition is intimately linked to materials properties and performance, plutonium is also fascinating to study as it is extremely sensitive to the addition of alloying elements and tramp impurities. Therefore, the quality assured analysis of plutonium materials is needed to enhance our understanding of electronic structure, bonding, ageing, corrosion and maintain nuclear facility operations. Challenges remain for practitioners to maintain the current skills, tools and techniques as well as developing safer and more efficient processes to enable the wider application of analytical tools to the actinides, reducing complexity, waste and cost.

This presentation will give an overview of recent work to accelerate and improve the characterization of actinide materials at the AWE. We will present innovations to conventional approaches and current research from the laboratory. Examples developing trace transuranics in actinides will be discussed as well as efforts to consolidate extant analytical techniques. [1-7]

References

1. Higginson, M. et al. J Radioanal Nucl Chem 330, 901–911 (2021). https://doi.org/10.1007/s10967-021-08043-w
2. Higginson, M. et al. J Radioanal Nucl Chem (2023). https://doi.org/10.1007/s10967-023-09253
3. Higginson, M. et al. Env. Radiochem. Analysis VII, Royal Society of Chemistry, 2023, vol. 357, ch. 4, pp. 43-49.
4. Higginson, M.et al., J Radioanal Nucl Chem 331, 4829–4835 (2022). https://doi.org/10.1007/s10967-022-08411-0
5. Higginson, M.et al. J Radioanal Nucl Chem 331, 3591–3600 (2022). https://doi.org/10.1007/s10967-022-08410-1
6. Higginson, M., et al. J Radioanal Nucl Chem 320, 689–698 (2019). https://doi.org/10.1007/s10967-019-06542-5
7. Wood, A.D., et al. J Radioanal Nucl Chem. https://doi.org/10.1007/s10967-025-10667-1 (2025).

The Influence of Transuranic Actinyl Complexation on Ligand Radiolysis

G. P. Holmbeck[1*], C. D. Pilgrim[1], T. S. Grimes[1], J. R. McLachlan,[2] A. R. Cook[3], and S.P. Mezyk[4]

[1]Center for Radiation Chemistry Research, Idaho National Laboratory, Idaho Falls, ID United States; [2]Department of Chemistry and Biochemistry, Lawrence Berkeley National Laboratory, Berkeley, CA United States; [3]Chemistry Division, Brookhaven National Laboratory, Upton, NY United States; [4]Department of Chemistry and Biochemistry California State University Long Beach, Long Beach, CA, United States; *gregory.holmbeck@inl.gov.

As efforts toward more sustainable used nuclear fuel (UNF) management intensify, direct dissolution reprocessing approaches employing monoamide extractants such as *N*,*N*-di-(2-ethylhexyl)butyramide (DEHBA) and *N*,*N*-di-(2-ethylhexyl)isobutyramide (DEH*i*BA) have emerged as promising alternatives to tributyl phosphate (TBP), offering reduced secondary waste generation and improved solvent longevity.[1,2] Building on prior observations that uranyl (UO_2^{2+}) complexation can paradoxically reduce steady-state ligand loss despite accelerating initial radical reaction rates,[3,4] we present our findings on the influence of neptunyl (NpO_2^{2+}) and plutonyl (PuO_2^{2+}) complexation on the radiation-induced oxidation of TBP, DEHBA, and DEH*i*BA by the *n*-dodecane radical cation ($C_{12}H_{26}^{\bullet+}$).

Time-resolved electron pulse radiolysis was used to determine rate coefficients for the reactions of $C_{12}H_{26}^{\bullet+}$ with $[NpO_2(Ligand)_2(NO_3)_2]$ and $[PuO_2(Ligand)_2(NO_3)_2]$ complexes, where Ligand = TBP, DEHBA, or DEH*i*BA. Consistent with observations for UO_2^{2+}, the chemical reactivity of TBP towards $C_{12}H_{26}^{\bullet+}$ was unaffected by complexation.[3] However, transuranic actinyl complexation significantly increased the reaction rates of the monoamide ligands compared to both their free-ligand and UO_2^{2+}-bound counterparts, revealing a strong actinyl-dependent enhancement in oxidative susceptibility. These results suggest active participation of NpO_2^{2+} and PuO_2^{2+} in electron-hole transfer pathways and provide new insight into how redox flexibility and ligand architecture influence early-time radiolytic chemistry.

Together, these kinetic measurements deliver the first systematic comparison of U, Np, and Pu actinyl effects on ligand oxidation, offering a mechanistic foundation for rational extractant design. By tailoring electronic structure, counterion environments, and actinide–ligand covalency, it may be possible to engineer solvent systems that suppress detrimental radical-driven pathways while favoring self-repair mechanisms essential for long-term stability in advanced fuel-cycle technologies.

Acknowledgements: Data collection was funded by the U.S. Department of Energy Assistant Secretary for Nuclear Energy, under the Material Recovery and Waste Form Development Campaign, DOE-Idaho Operations Office Contract DE-AC07-05ID14517. Data analysis was supported by the U.S. Department of Energy, Office of Science, Basic Energy Sciences, Division of Chemical Sciences, Geosciences, and Biosciences through an Early Career Research Program project under contract DE-AC07-05ID14517 at Idaho National Laboratory.

References: (1) Arm, *Nucl. Technol.* **2022**, *208(7)*, 1124; (2) Hall, Bessen, Zalupski, Campbell, Grimes, Peterman, Lumetta, *Solvent Extr. Ion Exch.* **2023**, *41 5)*, 545; (3) Celis-Barros, Pilgrim, Cook, Grimes, Mezyk, and Horne, *Physical Chemistry Chemical Physics* **2021**, *23*, 24589; (4) Kynman, Dang, Grimes, Mezyk, Wilbanks, Zarzana, Deokar, Cook, Boglaienko, Hall, and Horne, *ACS Omega* **2025**, *10(8)*, 7822.

Study of elements distribution in the δ-Pu oxide scale

Lionel Jolly[1*], Brice Ravat[1], Elodie Aubert[1], Ingrid Roure[2], Philippe Bienvenu[2], Denis Menut[3], Isabelle Zacharie-Aubrun[2], Thierry Blay[2], Catherine Sabathier[2], Doris Drouan[2], Benoît Oudot[1]

[1]CEA, DAM, Valduc, 21120 Is-sur-Tille, France
[2]CEA, DES, IRESNE, Cadarache 13108 Saint-Paul-Lez-Durance, France
[3]Synchrotron SOLEIL, L'Orme des Merisiers, Départementale 128, 91190 Saint-Aubin, France
Corresponding author*: lionel.jolly@cea.fr

Plutonium, due to its unique physico-chemical properties, is one of the most complex elements to study. Among its distinctive characteristics, its high sensitivity to corrosion is being studied with growing interest.
In an oxidizing environment, the formation of two oxide forms occurs: the sesquioxide (Pu_2O_3), which is located just above the metal substrate, and the dioxide (PuO_2), which is located above the former.

Pu Metal is typically stabilized in the δ-phase through the addition of a solute element such as gallium. For several years, the oxidation of the δ-$PuGa_{1at.\%}$ alloy has been investigated. The examined characteristics include the nature and the complex microstructure of the oxides that form on the metallic alloy surface, the oxidation kinetics and the diffusion of the solute element gallium within the oxide scale.

In this study, we aim to investigate the diffusion of oxygen and the behaviour of the solute element, gallium, through the complex oxide scale formed by O_2 exposure. To this end, the proportion between PuO_2 and Pu_2O_3 was controlled in the oxide scale by tuning the O_2 exposure parameters. Secondary Ion Mass Spectrometry (dynamic SIMS) was performed on samples exposed to ^{18}O in order to determine the oxygen diffusion coefficient and the gallium concentration profile in the oxide scale. Complementary X-ray absorption characterizations using synchrotron radiation (Extended X-ray Absorption Fine Structure technic, EXAFS at SOLEIL synchrotron) coupled with reverse Monte-Carlo modelling allowed us to describe the location of gallium in the atomic structure of PuO_2 and Pu_2O_3.

Speciation of Plutonium in Molten Salt Environments

S. N. Kelly[1,2*], B. C. Childs[1], M. G. Kerlin[1], M. J. Monreal[2], K. A. Erickson[2], L. E. Banks[1]

[1]Lawrence Livermore National Laboratory, Livermore, USA; [2]Los Alamos National Laboratory, Los Alamos, USA; *sheridon@llnl.gov

Understanding of actinide and fission product chemistry and properties in molten salt environments is in ever-growing demand, with applications in pyroprocessing of spent nuclear fuel, allowing for closure of the nuclear fuel cycle, and in the development of molten salt reactors (MSRs). One major gap in this area of research is the understanding of chemical speciation of relevant actinides in molten salts. Attempts to characterize analytes at molten temperatures have been hindered by the complexity of developing in-line spectroscopy tools that are compatible with high temperature and air- and water-free environments necessary for such research. Post-mortem samples (i.e.: analyzed after heating and cooling) can give some idea of changes created by the heating process, but do not give insight into the intermediate species that would be present at high temperatures.

Despite these challenges, a complete picture of chemical speciation in molten salts would allow for better-informed decisions on the steps to pyroprocessing: what species need to be oxidized or reduced to isolate the desired actinide? How much reductant or what voltage needs to be applied given this information? What other species are present that need to be mitigated? Additionally, assessing chemical speciation will aid in understanding upcoming molten salt reactors, as properties such as melting point, thermal stability, etc., can be assessed in relation to the species present in the fuel.

In this work, we focus on the chemical speciation of plutonium (Pu), supported by studies of cerium (Ce) as a surrogate, in calcium chloride. Studies of Ce offer meaningful insight into actinide speciation as we develop analytical techniques to assess both in-situ and post-mortem samples. Speciation as a function of temperature and as a function of analyte concentration were studied. Analysis of powder X-ray diffraction data from post-mortem samples indicates conversion of dioxide starting material to oxychloride at higher temperatures when calcium metal is absent as a potential reductant. Meanwhile, scanning electron microscopy images reveal morphological evolution from small, round particles to larger sheets as temperature increases. Infrared and Raman spectroscopy studies further support the speciation of oxide in the salt environment and provide insight into the Pu or Ce-O and Pu or Ce-Cl bonding. Post-mortem samples have been studied, and in-situ techniques are being developed in order to determine what intermediate species might be present when the salts are at molten temperatures.

Prepared by LLNL under Contract DE-AC52-07NA27344.

Plutonium Bearing Metallic Transmutation Fuels – Phase Relations and Thermal Properties

J. Rory Kennedy[1*]

[1]Glenn T. Seaborg Institute, Idaho National Laboratory, Idaho Falls, Idaho, U. S. A.;
rory.kennedy@inl.gov

Understanding the properties and thermal behavior of the actinide elements and their compounds is important for not only the applied aspects of, for example, nuclear fuel development but also in deciphering the role of 5f electrons in actinide properties. Research performed at Idaho National Laboratory (INL) under the United States Advanced Fuels Campaign's development of metallic transmutation fuels in conjunction with the Glenn T. Seaborg Institute will be presented with the goal of demonstrating example research opportunities in actinide science at INL. Additions of the so-called minor actinides (e.g., Np, Am, Cm) to plutonium bearing fuels in order to transmute long-lived fission products as part of a burner reactor program may influence the behavior of the fuel in-reactor with respect to such phenomena as elemental migration, microstructure development, and fuel-cladding interactions. Understanding the phase relations, microstructural development, and thermal properties of the fresh fuels is thus critical to interpreting the final fuel performance. In this presentation, we will look at the phase relationships and thermal properties of uranium, neptunium, plutonium, and americium as they alloy with each other and with Zr. Specifically, we will compare the binary 60Pu-40Zr alloy with the ternary 48Pu-12Am-40Zr alloy to the pentary 35U-29Pu-4Am-2Np-30Zr alloy. Phase identification, transition temperature analyses, microstructural analyses, heat capacity measurements, thermal expansion measurements, and thermal conductivity determinations will be presented.

Aqueous Recovery of Plutonium at Lawrence Livermore National Laboratory

T. A. Kohlgruber[1*], S. A. Di Pietro[1], M. G. Ferrier[1], C. A. Santoyo[1], D. Ashley[1], J. K. Puthenpurayil[1], S. L. Harris[1], M. C. P. Fischer[1], E. R. Tardiff[1], T. L. Steiner-Leach[1], B. C. Childs[1], L. S. Ripplinger[1]

[1]Lawrence Livermore National Laboratory, Livermore, CA, United States of America
*kohlgruber2@llnl.gov

The recovery and purification of plutonium (Pu) at Lawrence Livermore National Laboratory's (LLNL) Pu Facility is performed in the aqueous recovery laboratory. The main processing line utilizes a nitric acid-based aqueous flowsheet for the recovery of high value plutonium (**Figure 1**). Since the establishment of this laboratory, several processing campaigns have been performed since 2021 with changes in feed materials, redox reagents, and experimental conditions, with each process run providing valuable insight for subsequent runs. During the most recent campaign that took place earlier this year, Pu metal feed material was successfully reprocessed and purified to Pu oxide for future use. Unique to this run, UV-vis-NIR spectroscopy was heavily relied upon to understand the chemical conditions throughout processing. Key measurement points included estimating the Pu dissolved after nonideal lower heating temperatures; adjusting Pu solutions for acid concentrations between 7-8M to ensure reliable anion exchange performance coordinated with long residence times and large wash volumes; measuring ion exchange effluent streams to prevent Pu from diverting into waste streams; and measuring Pu(III) oxalate precipitation efficiencies before and after filtration of material. These grab sample spectra are not only useful data points for this run, but they will be helpful in building and testing chemometric and machine learning models to calculate Pu and acid concentrations. As more becomes understood, multivariate analysis on UV-vis-NIR spectra will be correlated to radioanalytical techniques currently being developed to provide full comprehensive understanding of Pu from dissolution to final oxide production. These topics of process conditions, spectroscopic data, and infrastructure additions will be discussed in greater detail.

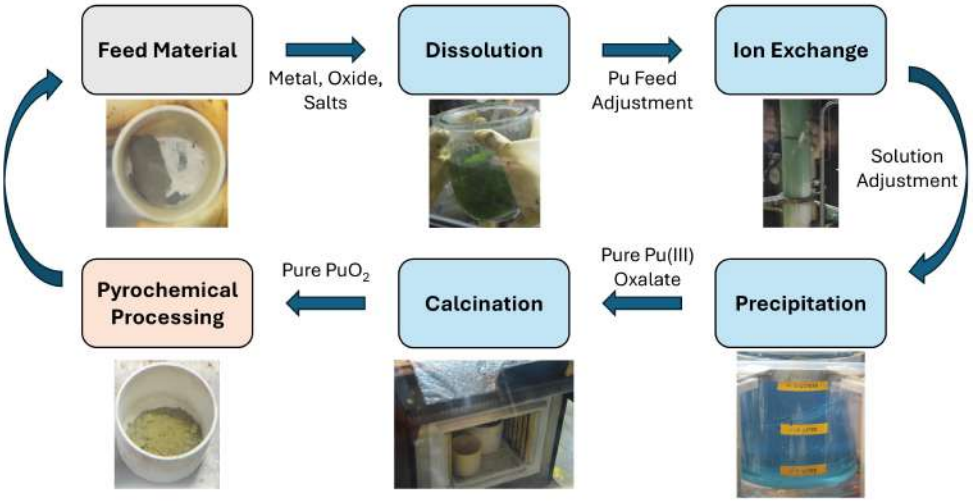


Figure 1. The aqueous flowsheet utilized at LLNL with images from our most recent process run.

This work was performed under the auspices of the U.S. Department of Energy by Lawrence Livermore National Laboratory under Contract DE-AC52-07NA27344. (LLNL-ABS-2016810).

Reactions of Pu(VI) and Pu(V) in Alkali Hydroxide Solutions: New Pu Solid Phases and Insights into Pu Speciation at High pH

Dmytro V. Kravchuk[1], Richard E. Wilson[1]

[1]Chemical Sciences and Engineering Division, Argonne National Laboratory, Lemont IL USA; *dkravchuk@anl.gov

Actinide oxide and hydroxide phases play a crucial role in thermodynamic models used for predicting and assessing risks in nuclear waste management, geological disposal, reactor accidents, and environmental remediation. The accuracy of these models depends on a thorough understanding of both the solid and solution phases they encompass, as well as their reactivity within these systems. Plutonium exhibits particularly complex aqueous chemistry due to its ability to exist in four different oxidation states in solution.[1] The most detailed thermodynamic models of plutonium speciation indicate that its aqueous behavior is governed by the solubility of PuO_2, its hydrates, and nanoparticulate or colloidal forms, along with a dynamic redox equilibrium involving Pu^{3+}, Pu^{4+}, $Pu^{V}O_2^{+}$, and $Pu^{VI}O_2^{2+}$, with $Pu^{V}O_2^{+}$ being one of the predominant dissolved species.[2]

Despite its significance in plutonium speciation, $Pu^{V}O_2^{+}$ remains poorly studied, particularly in terms of its solid-phase chemistry. This knowledge gap is largely due to challenges in preparing $Pu^{V}O_2^{+}$ in a pure oxidation state and controlling its redox behavior, as it tends to disproportionate in acidic solutions. Currently, only ten $Pu^{V}O_2^{+}$ complexes have been structurally characterized via single-crystal X-ray diffraction, none of which are hydroxides or oxides. As a result, the hydrolysis and solubility constants of $Pu^{V}O_2^{+}$ are available only as upper limit estimates, primarily extrapolated from $Np^{V}O_2^{+}$ data. A recent capillary electrophoresis mass spectrometry study by Aupais has confirmed the accuracy of these extrapolations.[3]

Our laboratory focuses on investigating the reactivity of transuranium elements in alkali metal hydroxide solutions and melts. Previous studies on actinide speciation in alkaline environments have aimed to determine the solid-phase speciation and solubility of uranium compounds, with applications in environmental systems, high-level waste storage at sites such as Hanford and Savannah River, and reactor accident scenarios. However, uranium is relatively stable in its hexavalent state, and most of the characterized phases involve $U^{VI}O_2^{2+}$ oxides, hydroxides, and alteration products containing peroxide or superoxide species. Our research extends to transuranium elements such as neptunium and plutonium in these alkaline systems, leading to the discovery of novel neptunium compounds, including single-crystal materials previously observed only as powders.

Investigations into neptunium reactivity under alkaline conditions revealed a clear dependence of the isolated solid phase on hydroxide concentration. For instance, varying the LiOH concentration in hydrothermal reactions with $Np^{VI}O_2(NO_3)_2$ produced distinct ternary oxides of hexavalent neptunium: Li_2NpO_4 formed at [LiOH] < 5M, while Li_4NpO_5 was obtained at [LiOH] > 5M.[4] In reactions involving pentavalent neptunium, the choice of alkali metal significantly influenced crystalline packing. With K^+ cations, $Np^{V}O_2(OH)_5^{4-}$ units were restricted to one-dimensional chains in $K_4[(Np^{V}O_2)_2(OH)_6] \cdot 4H_2O$. In contrast, Na^+ cations facilitated actinyl-actinyl interactions (CCIs) between neighboring Np^{V} metal centers, forming a 2D network in $Na[Np^{V}O_2(OH)_2]$. Further, the introduction of Rb^+ cations led to the transformation of this 2D network into a 3D framework in $Rb_4[(Np^{V}O_2)_4(OH)_8] \cdot 2H_2O$.[5, 6]

Building on this work, we explored the reactivity of $Pu^{VI}O_2^{2+}$ in hydroxide solutions under mild hydrothermal conditions (150–200 °C). In the presence of RbOH, hexavalent plutonium readily formed a hydrated diplutonate phase, $Rb_2Pu^{VI}_2O_7 \cdot 0.5H_2O$, while reactions with CsOH yielded

$Cs_6[(Pu^{VI}O_2)_3O_4(OH)_2](NO_3)_2$. Both structures are newly identified and isostructural with Np^{VI} analogues synthesized under similar conditions. Notably, the addition of solid alkali peroxides as synthetic reagents enabled redox reactions of $Pu^{VI}O_2^{2+}$ in concentrated alkali hydroxide solutions. This led to the isolation of previously unreported $PuVO_2^+$ hydroxide compounds as single crystals[7]: $Na[Pu^VO_2(OH)_2(H_2O)] \cdot 2.5H_2O$, $Na_2[Pu^VO_2(OH)_3] \cdot 2H_2O$, and $K_4[(Pu^VO_2)_2(OH)_6] \cdot 4H_2O$, as shown in **Figure 1**. These findings provide new insights into plutonium's redox behavior in alkaline environments and solid-phase chemistry, which can be used to benchmark plutonium solution speciation.

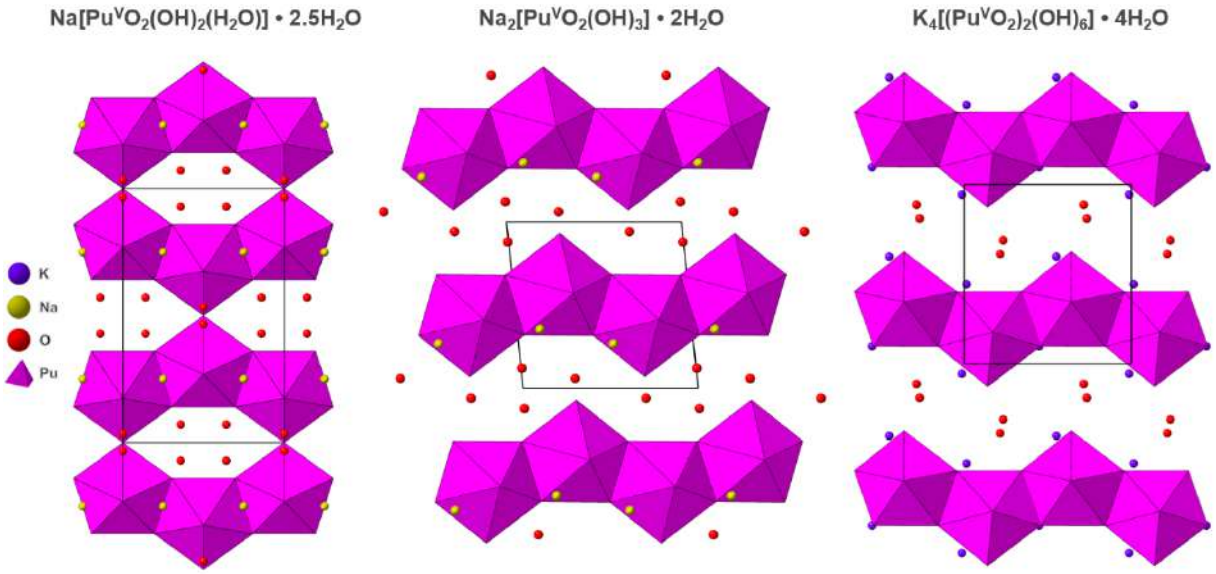


Figure 1. Unit cell packing of $Na[Pu^VO_2(OH)_2(H_2O)] \cdot 2.5H_2O$, $Na_2[Pu^VO_2(OH)_3] \cdot 2H_2O$, and $K_4[(Pu^VO_2)_2(OH)_6] \cdot 4H_2O$.

Acknowledgements

This work was conducted at the Argonne National Laboratory, operated by UChicago Argonne LLC for the United States Department of Energy (U.S. DOE) and supported by the U.S. DOE Office of Science, Office of Basic Energy Sciences, Chemical Sciences, and Geological and Biosciences Division, Heavy Element Chemistry under Contract DE-AC02-06CH11357.

References

1. Clark, D. L.; Hecker, S. S.; Jarvinen, G. D.; Neu, M. P., Plutonium. In *The Chemistry of the Actinide and Transactinide Elements*, Morss, L. R.; Edelstein, N. M.; Fuger, J., Eds. Springer Netherlands: Dordrecht, 2011; pp 813-1264.

2. Lemire, R. J., Chemical thermodynamics of neptunium and plutonium. **2001**.

3. Aupiais, J.; Christin, C.; Levier, M., Aquatic Chemistry of Pentavalent Plutonium: Determination of the First Hydrolysis Constant. *Inorg. Chem.* **2023,** *62* (11), 4533-4539.

4. Hutchison, D. C.; Kravchuk, D. V.; Rajapaksha, H.; Stegman, S.; Forbes, T. Z.; Wilson, R. E., Synthesis of Single Crystal Li2NpO4 and Li4NpO5 from Aqueous Lithium Hydroxide Solutions under Mild Hydrothermal Conditions. *Inorg. Chem.* **2023,** *62* (40), 16564-16573.

5. Wilson, R. E.; Stegman, S.; Tarlton, M. L., Reactions of Neptunium(V) in Alkali-Metal Hydroxides. *Inorg. Chem.* **2021,** *60* (23), 17480-17486.

6. Almond, P. M.; Skanthakumar, S.; Soderholm, L.; Burns, P. C., Cation−Cation Interactions and Antiferromagnetism in Na[Np(V)O2(OH)2]: Synthesis, Structure, and Magnetic Properties. *Chem. Mater.* **2007,** *19* (2), 280-285.

7. Kravchuk, D. V., Mikeska, E. R., Wilson, R. E., Accessibility and Reactivity of Pentavalent Plutonium under Alkaline Conditions. *J. Am. Chem. Soc.* **2026**, 148(7), 6926-6938.

Improved Characterization of Helium Bubble in Naturally Aged Plutonium with Scanning Transmission Electron Microscopy (STEM)

Theresa M. Kucinski[1]*, Douglas S. Smith[1], Magdalen Grismer[1], Gordon M. Moore[1]

[1]Los Alamos National Laboratory, Los Alamos, NM, United States; *theresakucinski@lanl.gov

We report improved characterization of helium bubble size and number density in naturally aged plutonium with the use of aberration-corrected (Cs) scanning transmission electron microscopy (STEM). Previously, helium bubbles in aged plutonium were measured using Fresnel contrast TEM which is an inherently subjective measurement that is dependent on many variables including bubble size and sample thickness. STEM allows for the direct imaging of in-focus bubbles that resolves previous measurement complications. Previously, the average radius of aged plutonium was assumed to stagnate at a radius of approximately 0.7 nm, which had agreed with the modeling of bubble growth in body-centered cubic (BCC) metals at the time. More recently, modeling of FCC metals has shown that the critical pressure for growth is lower than predicted for BCC metals due to the presence of stacking faults indicating that bubbles in FCC metals may be able to exceed the previously held bubble size assertion. Our results indicate average bubble radius is larger than previous reports with an average radius above 2 nm for aged material. The high resolution and contrast of our technique enabled the unprecedented observation of bubbles in samples as young as 2 years old, which were considerably smaller than the more mature material.

Ab initio modeling of He bubbles in δ-Pu

Kyoung E. Kweon* **and Babak Sadigh**
Lawrence Livermore National Laboratory, Livermore, California, United States
*kweon1@llnl.gov

Helium bubble formation in plutonium has generally been understood as a vacancy-mediated process, since vacancies serve as nucleation and growth sites for He in most metals. However, our recent work using state-of-the-art spin/orbital-polarized density functional theory (SOP-DFT) indicate that self-interstitials are the dominant intrinsic defect in δ-Pu, leading to a negligible equilibrium vacancy concentration. In this talk, we study the self-trapping mechanism via spontaneous Frenkel pair formation that can explain He bubble nucleation and early-stage growth in δ-Pu in the absence of free vacancies. Using SOP-DFT calculations, we search for the lowest energy configurations of He clusters containing up to 18 He atoms and compute their formation energies. We identify the critical bubbles that can reduce their energy by kicking out a self-interstitial and thereby increasing in volume due to the vacancy left behind. We thus find that the He-to-vacancy ratios in the bubbles tend to approximately 2.5, in good agreement with the positron annihilation experiments.

This work was performed under the auspices of the U.S. Department of Energy by Lawrence Livermore National Laboratory under Contract DE-AC52-07NA27344.

The Role of Transient Plutonium Oxidation States in the Radiation-Induced Redox Cycling of Pu(VI) in Aqueous Nitric Acid Solutions

A. E. Kynman[1,2*], G. P. Horne[1], A. R. Cook[3], and T. S. Grimes[1,2*]

[1]Radiochemical Separations and Radiation Science Department, Idaho National Laboratory, Idaho Falls, ID United States; [2]Glenn T. Seaborg Institute, Idaho National Laboratory, Idaho Falls, ID United States; [3]Chemistry Division, Brookhaven National Laboratory, Upton, NY United States; *amy.kynman@inl.gov, travis.grimes@inl.gov.

The redox behavior of plutonium in aqueous nitric acid solutions plays a critical role in nuclear fuel reprocessing and waste management, where multicomponent radiation fields are present. Concurrently, multiscale computer modeling offers a valuable method to understand and predict radiation-induced redox behavior of actinide elements.

Previously, we developed an experimentally evaluated multi-scale computer model for the prediction of gamma radiation-induced Pu(IV) redox chemistry in concentrated nitric acid solutions (1.0, 3.0, and 6.0 M). Under these conditions, cobalt-60 gamma irradiation afforded negligible net change in the steady-state oxidation state distribution of Pu(IV). Multi-scale calculations, in excellent agreement with experimental data, indicated that this observation was due to radiation-induced redox cycling between Pu(IV) and Pu(III), as achieved by the reduction of Pu(IV) by radiolytic nitrous acid and hydrogen peroxide, and the oxidation of Pu(III) by nitrate and hydroxyl radicals, alongside plutonium's inherent disproportionation reactions.

Building on these results, here we leverage electron pulse radiolysis and dose accumulation (in-situ alpha and ex-situ gamma) irradiation techniques to develop a further iteration of our plutonium model which describes the radiation-induced redox chemistry of Pu(VI) in 1.0, 3.0, and 6.0 M nitric acid. Our calculations demonstrate that Pu(VI) reduction can be facilitated by nitrous acid, while the disproportionation of Pu(V) in acidic media creates a dynamic redox cycle that maintains a constant Pu redox distribution. The findings highlight the significance of transient plutonium species in influencing the overall longevity of Pu(VI) in acidic environments and provide critical insights into the mechanisms governing plutonium chemistry under radiation.

Redox Chemistry and Reactivity of Homo-and Heteroleptic Neptunium and Plutonium Complexes

Henry S. La Pierre[1,2,3*], Matilda I. Duffy,[1] Kaitlyn S. Engle[1], Julie E. Niklas,[1] Haruko Tateyama,[1] Andrew C. Boggiano,[1] Chad M. Studvick,[4] Sabyasachi Roy Chowdhury,[5] Bess Vlaisavljevich,[5] Ivan A. Popov[4]

[1]School of Chemistry and Biochemistry, Georgia Institute of Technology, Atlanta, Georgia; [2]Nuclear and Radiological Engineering and Medical Physics Program, School of Mechanical Engineering, Georgia Institute of Technology, Atlanta, Georgia; [3]Physical Sciences Division, Pacific Northwest National Laboratory, Richland, Washington; [4]Department of Chemistry, The University of Akron, Akron, Ohio; [5]Department of Chemistry, University of South Dakota, Vermillion, South Dakota.*hsl@gatech.edu

This presentation will describe our group's comparative kinetic and thermodynamic studies of proton-coupled electron transfer across the mid-actinides (U^{5+}, Np^{5+}, Pu^{5+}) and consider the changes in chemical bonding driving the observed changes chemical reactivity. The implications for the electronic structure for high-oxidation state plutonium will be presented in the light of this group's recent characterization of the first molecular praseodymium 5+ complex. Furthermore, ligand and complex design criteria developed for high-oxidation state cerium complexes will be demonstrated to support lanthanide and actinide 4+ (Ce^{4+}, U^{4+}, and Np^{4+}) hydride and σ-bonded hydrocarbyl complexes. The reactivity and spectroscopic features of these molecular complexes will be presented in the context of dihydrogen corrosion of plutonium metal.

An *ab initio* Molecular Dynamics Study of Key Thermodynamical Input Parameters for Computer Simulation of U-6Nb Solidification

A. Landa[1*], L. Burakovsky[2], P. Söderlind[1], L.H. Yang[1], B. Sadigh[1], J.D. Roehling[1], J.T. McKeown[1]

[1]Lawrence Livermore National Laboratory, Livermore, California 94551, USA;
[2]Los Alamos National Laboratory, Los Alamos, New Mexico 87545, USA; *landa1@llnl.gov

The key to metallic fuel development is the fabrication of uranium metal and alloys into fuel forms. U-Nb alloys are one of the best candidates for a metallic fuel alloy with high-temperature strength sufficient to support the core, acceptable nuclear properties, good fabricability, and compatibility with usable coolant media. Melt processing has been a key component of the metallic fuel cycle, and process models require thermophysical parameters at elevated temperatures, particularly above the melting temperatures, regarding which experimental data are scarce, for accurate simulations and process development. By means of *ab initio* density-functional theory (DFT) quantum molecular dynamics (QMD), we have calculated the main thermophysical parameters—the density, thermal expansion coefficient, specific heat, thermal conductivity, melting temperature, latent heat of fusion, and viscosity—used in the modeling of the U-6 wt.% Nb alloy casting. The melting temperature of the U-6 wt.% Nb alloy at ambient pressure is obtained by means of QMD simulations using the Z-method. The ambient volume change and latent heat of melting of U-6 wt.% Nb are also derived from QMD simulations in conjunction with analytical fitting for the energy and pressure. The thermal conductivity for the solid U-Nb alloy is calculated from the semi-classical Boltzmann transport equation combined with an estimate of the electron relaxation time obtained from DFT simulations.

Micromechanical Characterization of α- and δ-Phase Plutonium via Advanced Nanoindentation Techniques

-Zachary Levin, Clarissa Yablinsky, Roger Jaramillo, Veronica Anghel, Todd Martinez, Isaac Hernandez

Nanoindentation provides a powerful approach for probing the small-scale mechanical behavior of radioactive materials, where conventional mechanical testing is often impractical. We present a comprehensive nanoindentation study of actinide materials, including plutonium (Pu) and uranium (U), performed using a newly customized glovebox-integrated nanoindenter. The system is based on the FemtoTools FT-I04 platform and was modified to enable safe installation and reliable operation within an inert-atmosphere glovebox while maintaining high measurement sensitivity and stability.

Multiple nanoindentation methodologies were employed to characterize elastic, plastic, time-dependent, and fracture behavior. Continuous stiffness measurement (CSM) was used to determine hardness and elastic modulus as a function of indentation depth, enabling evaluation of indentation size effects. Time-dependent deformation was investigated through creep and stress relaxation experiments. Fracture toughness was assessed using indentation-induced cracking methods. Dynamic mechanical analysis (nanoDMA) provided insight into frequency-dependent mechanical response. Additionally, spherical indentation was used to extract flow stress–flow strain behavior, allowing comparison to bulk constitutive response.

The results reveal distinct mechanical differences between α- and δ-phase Pu, including variations in hardness, modulus, deformation behavior, and time-dependent response. Comparisons with uranium further contextualize trends across actinide systems.

This work demonstrates the capability of advanced nanoindentation techniques within a glovebox environment and establishes a framework for comprehensive micromechanical characterization of actinide materials.

Oxygen K-edge Scanning Transmission X-ray Microscopy (STXM) of Plutonium Oxide

Rachel Lim[1*], Alexander Baker[1], Alexander Ditter[2], S. Olivia Gunther[2], Hendrik Ohldag[3], David Shuh[2], Scott Donald[1], Brandon Chung[1]

[1]Lawrence Livermore National Laboratory, Livermore, USA; [2]Lawrence Berkeley National Laboratory, Berkeley, USA; [3]Advanced Light Source, Berkeley, USA *lim37@llnl.gov

Scanning transmission X-ray microscopy (STXM) was used to examine plutonium oxide particles formed by the corrosion of δ-phase plutonium alloy under high-humidity conditions. O K-edge spectra collected from eight distinct particles displayed significant spectral differences, revealing heterogeneity in oxidation states within a single sample batch (Fig. 1). Comparative evaluation against literature reference spectra indicates that two particles exhibit the principal features associated with stoichiometric PuO_2. In contrast, at least one particle displays an O K-edge signature consistent with iron oxides (Fe_2O_3 and Fe_3O_4-like) and is confirmed to be iron-bearing by Fe L_3-edge mapping (Fig. 2), while additional particles exhibit intermediate spectral character suggestive of mixed Fe–Pu oxide environments. This variation suggests complex chemical environments and formation histories, which are important considerations for nuclear forensic investigations. Several particle spectra do not correspond cleanly to previously reported plutonium oxide references, highlighting the complexity of environmentally formed corrosion products and the need for expanded reference datasets to improve the interpretation and forensic utility of such measurements. These findings emphasize the potential of synchrotron-based X-ray microscopy for non-destructive, high-resolution analysis of nuclear materials.

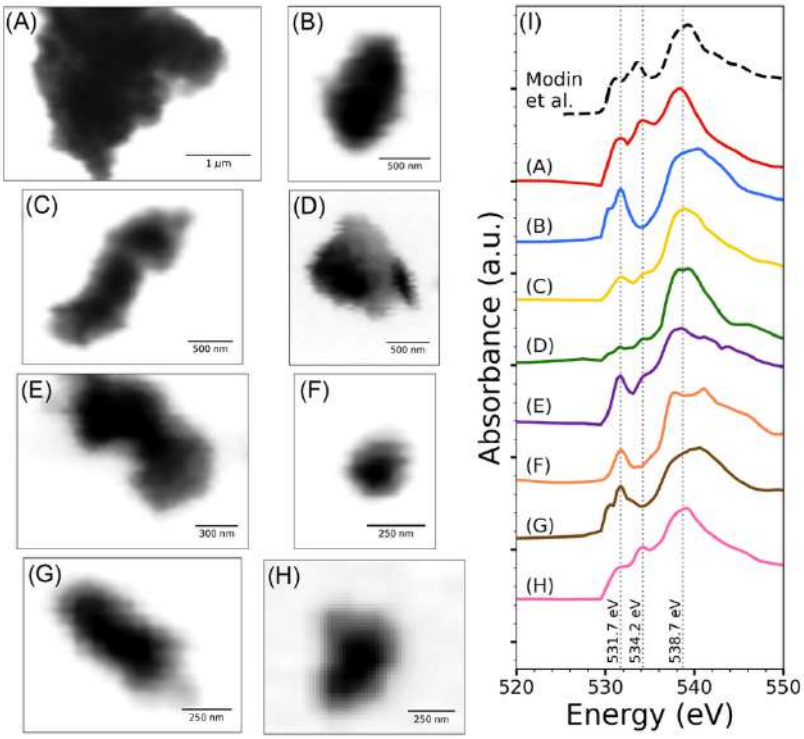


Figure 1. (A-H) Images of eight different plutonium oxide particles taken at 530 eV. (I) O K-edge spectra corresponding to each of the eight particles shows heterogeneity in the oxidation state. Vertical lines are marked on the oxygen spectra to aid in comparison of the feature locations.

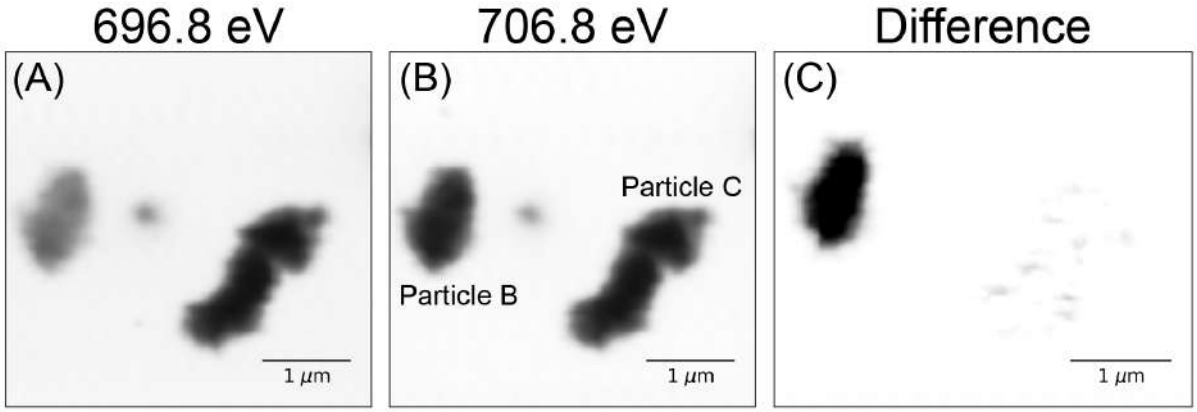


Figure 2. Image of particles B and C taken (A) below and (B) above the Fe L_3-edge with (C) the difference showing particle B contains Fe while particle C does not.

This work was prepared under the auspices of the U.S. Department of Energy by Lawrence Livermore National Laboratory under Contract DE-AC52-07NA27344. Document LLNL-ABS-863270.

Experimental and Quantum Chemical Insights into the coordination chemistry of Protactinium(V) in solution

Maloubier M[1*], Shaaban T[2], Le Naour C[1], Réal F[2], Vallet V[2]

[1]Université Paris-Saclay, CNRS/IN2P3, IJCLab, 91405 Orsay, France; [2]Université de Lille, CNRS, UMR 8523 – PhLAM- Pysique des Lasers, Atomes et Molécules, 59000 Lille, France;
*melody.maloubier@ijclab.in2p3.fr

Protactinium(V), Pa(V), occupies a unique position among actinides due to its distinctive chemical properties, notably the absence of the actinyl moiety ($AnO2^{+}$) in its condensed-phase compounds. Instead, Pa(V) forms a short mono-oxo bond, whose stability and electronic structure remain subjects of intensive debate. While previous studies in oxalate and sulfate media have reported a Pa-O bond distance of 1.75 Å, quantum chemical calculations predict a longer bond (1.85 Å), highlighting unresolved discrepancies in its coordination chemistry [1,2]. The instability of this bond, particularly in the presence of strongly coordinating ligands like fluoride, further complicates experimental and theoretical investigations. The strong tendency of protactinium to hydrolyze and polymerize even under very acidic conditions complicates experimental efforts. The difficulty of isolating significant amounts of this actinide, coupled with its radioactivity, further limits the feasibility of large-scale experimental studies.

In this study, we combine X-ray Absorption Spectroscopy (XAS) and quantum chemical calculations, to provide unprecedented insights into the stability of the mono-oxo bond and the nature of Pa(V)-chloride interactions (a weakly coordinating ligand) [2,3]. This approach is complemented by High-Energy Resolution Fluorescence Detection X-ray Absorption Near Edge Structure (HERFD-XANES) and Resonant Inelastic X-ray Scattering (RIXS) at the Pa M_4 edge, applied for the first time to Pa(V) complexes, to probe the electronic structure of Pa(V) in different coordination environment.

Our EXAFS measurements, reveal two distinct Pa(V)-chloride complex structures in 3M and 12 M HCl, with a Pa-O bond distance of ~ 1.83 Å, aligning more closely with theoretical predictions than previous experimental findings [5]. Unlike fluoride ligand, the Pa-O bond is maintained even in highly concentrated solutions (12 M). The XANES spectra exhibit a unique shoulder above the edge, never before observed in Pa(V) complexes, suggesting a stable mono-oxo bond with a ligand in trans position in chloride media.

These results reconcile experimental observations with theoretical predictions and provide a robust foundation for future studies on Pa(V) behavior in aqueous environments.

[1] Mendes, M., S. Hamadi, C. Le Naour, J. Roques, A. Jeanson, C. Den Auwer, P. Moisy, S. Topin, J. Aupiais, C. Hennig, and M.V. Di Giandomenico (2010). Inorg. Chem. 49: 9962-9971

[2] Shaaban, T., H. Oher, J. Aupiais, J. Champion, A. S. Peirera Gomes, C. Le Naour, M. Maloubier, F. Réal, E. Renault, X. Rocquefelte, B. Siberchicot, V. Vallet and R. Maurice (2024). Chemical Communications 60: 14376-14379

[3] Shaaban, T., F. Réal, R. Maurice and V. Vallet (2024). Chem. Eur. J. 30: e202304068

[4] Muxart, R., R. Guillaumont, A. Pacault, and Pannetier, G. (1974) Compléments au nouveau traité de chimie minérale. Masson.

[5] Maloubier, M., Shaaban, T., Réal, F., Le Naour, C., Oher, H., Aubert, T., Solari, P. L., Siberchicot, B., Maurice, R., Vallet, V. (2025). Angewandte Chemie International Edition, e18403.

Vibrational identification of uranyl peroxo-carbonate complexes in solution: insights from ^{18}O labeling and DFT

J. Margate[1,2], L. Floarea[2], C. Coubronne[1], E. Berrier[2], G. Milanole[3], F. Réal[1], M. Rivenet[2] and V. Vallet[1]

[1]Univ. Lille, CNRS, UMR 8523 - PhLAM - Physique des Lasers Atomes et Molécules, F-59000 Lille, France

[2]Univ. Lille, CNRS, Centrale Lille, Univ. Artois, UMR 8181 - UCCS - Unité de Catalyse et Chimie du Solide, F-59000 Lille, France

[3]ORANO Chimie Enrichissement, Hall de Recherche de Pierrelatte, BP 16, France

In carbonate-rich aqueous environments relevant to spent nuclear fuel storage and alkaline reprocessing routes, the coexistence of carbonate species and radiolytically generated hydrogen peroxide promotes the formation of uranyl peroxo-carbonate complexes. However, their identification in solution remains challenging due to the lack of robust spectroscopic markers and persistent ambiguities in vibrational assignments [1–3].

In this study [4], we investigate the uranyl peroxo-dicarbonate complex $[UO_2(O_2)(CO_3)_2]^{4-}$ under alkaline carbonate-peroxide conditions using Raman and FTIR spectroscopy combined with ^{18}O labeling ($H_2{}^{18}O_2$) and density functional theory (DFT). Distinct vibrational fingerprints are identified and clearly differentiated from those of the uranyl triscarbonate species $[UO_2(CO_3)_3]^{4-}$. Raman spectra exhibit characteristic bands at 765–769 cm^{-1} ($\nu_s(U\text{-}O_{yl})$), 845–850 cm^{-1} ($\nu(O\text{-}O)$) and 400–440 cm^{-1} ($\nu(U\text{-}O_{pero})$). The $\nu(O–O)$ mode shows a pronounced isotopic shift (≈40 cm^{-1}) upon ^{18}O substitution, in excellent agreement with DFT calculations (**Figure 1**). FTIR provides complementary evidence, while DFT reproduces the observed frequencies and isotope shifts, enabling the first unambiguous vibrational assignment in solution and clarifying solvation and counter-cation effects.

Our combined approach confirms a side-on η^2 coordination of the peroxide ligand and excludes alternative species such as diperoxo complexes. This work establishes a robust spectroscopic framework for uranyl peroxo-carbonate complexes in solution, directly relevant to uranium dissolution mechanisms and actinide speciation in carbonate–peroxide systems.

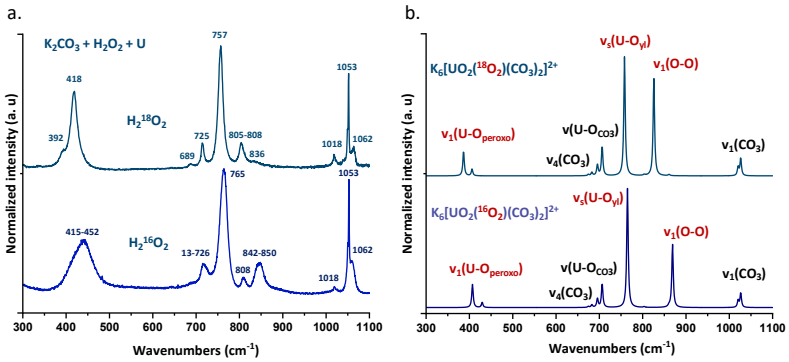


***Figure 1**: (a) Raman spectra of uranyl nitrate solutions ([U] = 50 mM, H_2O_2 = 1M) in K_2CO_3 medium with $H_2{}^{16}O_2$ and $H_2{}^{18}O_2$. (b) Simulated Raman spectra of $K_6[UO_2(O_2)(CO_3)_2]^{2+}$, using the fixed structure.*

[1] P.C. Burns et al. , Science, 2012, 335, 1184–1188. DOI : 10.1126/science.1211285.
[2] G.S. Goff et al., Inorg. Chem., 2008, 47, 1984–1990. DOI : 10.1021/ic701775g.
[3] K.-W. Kim et al., J. Phys. Chem. A, 2012, 116, 12024–12031.DOI : 10.1021/jp307062u..
[4] J. Margate et al. *ChemRxiv*. 16 February 2026. DOI: 10.26434/chemrxiv.15000099/v1

Mass Fractionation Corrections in TIMS Isotope Ratio Measurements: Comparison of Correction Factors in Total Evaporation Analysis of Actinides

Kattathu Mathew[1*], Kyle Krajewski[1], Brian Ticknor[1], Cole Hexel[1]

[1]Nuclear Analytical Chemistry, Oak Ridge National Laboratory, Oak Ridge, TN, USA.
*mathewkj@ornl.gov

Isotope ratio measurements by thermal ionization mass spectrometers (TIMS), especially using state-of-the-art analytical methodologies such as total evaporation (TE) and modified total evaporation (MTE), are expected to provide precise values for the major isotope ratios that are also free from systematic biases [1-3]. The TE and MTE analytical methodologies have been utilized the most in characterization analysis of uranium materials [4,5]. Results from these investigations show that small but statistically significant systematic biases (compared to the certified/true values) are still present in the measured TE/MTE $^{235}U/^{238}U$ major isotope ratio data. For uranium and plutonium, the residual systematic biases due to mass fractionation effects can be included into the analytical scheme through the analysis of certified reference materials (CRMs) available for these analytes. However, certified isotopic standards are not available for all actinide analytes of interest in the nuclear fuel cycle, for e.g. americium, neptunium, and thorium. In the absence of standards, assumptions are often made that the isotopic mass fractionations at these analytes are similar to that of uranium and the isotopic ratios are corrected for mass fractionation using measurements of uranium standards that are included together with the Am or Np or Th samples. Alternatively, facilities have also explored the option of making gravimetric mixtures using individual isotopic endmembers and using these working standards for calibration and quality control [6]. Two thorium isotopic CRMs (IRMM-035 and IRMM-036) from IRMM are available. The $^{230}Th/^{232}Th$ ratios in these CRMs are ~$1.1x10^{-5}$ and ~$3.0x10^{-6}$. Analytical results obtained for these CRMs in several international inter-comparison studies (see [7] for a summary discussion) indicate biases w.r.t the certified values and IRMM is currently pursuing a recertification of these standards. Considering the low ratios involved, tailing corrections at ^{230}Th from the dominant ^{232}Th is expected to be significant when ^{230}Th and ^{232}Th isotopic signals are measured on the Faraday detectors. Tailing contribution can be minimized or completely eliminated through the measurement of ^{230}Th on the secondary electron multiplier (SEM). Thus, the preferred measurement techniques for extreme isotope ratios like those in IRMM-035 and IRMM-036, include utilization of different types of detectors. A total evaporation method for measurement of the $^{230}Th/^{232}Th$ ratios in IRMM-035 and IRMM-036 standards, using an SEM equipped with an RPQ to minimize the tailing contributions from the ^{232}Th isotopic signal was developed. Manufacturer' specified abundance sensitivity of $<2.0\ x10^{-8}$ for the Triton TIMS instrument assures that peak tail corrections at ^{230}Th from ^{232}Th are insignificant for IRMM-035 and IRMM-036 (with $^{230}Th/^{232}Th$ ratios of ~$1.1x10^{-5}$ and ~$3.0x10^{-6}$, respectively). Only the ^{230}Th isotope was measured on the SEM and the ^{232}Th isotope was measured on a Faraday detector equipped with a 10^{11} Ω amplifier. We also performed $^{235}U/^{238}U$ isotope ratio measurements on a well characterized uranium CRM C129A using the same methodology (^{235}U was measured on the SEM and ^{238}U was measured on a Faraday connected to a 10^{11} Ω amplifier) to evaluate if the mass fractionation observed at Th and U are similar. Mass fractionation observed at the $^{235}U/^{238}U$ ratio, with ^{235}U measured on the SEM, are compared with literature data for mass fractionation of U (where Faraday detectors are used for both ^{235}U and ^{238}U). The validity of the assumption that mass fractionation at actinide elements is similar is evaluated, in view of the new data.

References: [1] Callis and Abernathy, IJMS 1991, 103, 93 [2] Richter and Goldberg, IJMS 2003, 229, 181 [3] Richter et al., JAAS 2011, 26, 550 [4] Mathew et al. JAAS 2013, 28, 866 [5] Mathew et al., JRNC 2015, 305(1), 277 [6] Mathew et al., IJMS 2020, 458, 116430 [7] Varga, Wallenius, and Mayer, Talanta 2025, 292, 127896.

X-ray Photoemission Studies of Pu_6Fe

Alessandro R. Mazza[1,*], Alexandra L. Nagelski[1], William S. Ponder[1], Derek Prada[1], David Arellano[1], Alexander Boehm[1], Daniel T. Olive[1]

[1]Materials Science and Technology, Los Alamos National Laboratory, Los Alamos, USA;
*armazza@lanl.gov

The Pu-Fe eutectic is of great interest, where small changes in concentration can have a dramatic effect on the melting temperature of the solid, the crystallographic phase, and physical properties of the system. To better understand these effects, Pu_6Fe was successfully synthesized by arc melting. The phase was confirmed by x-ray diffraction. In this presentation, photoemission studies of the intermetallic compound will be discussed. The Pu4f line shape is compared to spectra from α-Pu and δ-Pu metal, where a screening peak akin to δ-Pu is observed. In addition to characterization of the metal surface, oxidation studies were completed at various pressures for exposures up to 200 L. These results and the oxidation kinetics will be presented in the context of published oxidation results on Pu alloys and intermetallic compounds.

The Launch of the Plutonium Science Laboratory (PluS Lab) at Los Alamos National Laboratory

Marisa Monreal[1]* and Karla Erickson[1]
[1]Los Alamos National Laboratory, Los Alamos, NM, USA
*mmonreal@lanl.gov

The Plutonium Science Laboratory (PluS Lab) at Los Alamos National Laboratory advances fundamental plutonium science to address current and emerging nonproliferation challenges while developing and sustaining the specialized workforce required for this mission. The PluS Lab integrates three complementary capability pillars: Aqueous Systems, Molecular Chemistry and Materials Science, and Molten Salt Science, each focused on advancing understanding of plutonium behavior across a range of chemical environments. This presentation traces the progression from concept development and facility renovation to the initiation of first plutonium research activities.

Following commissioning and receipt of its first plutonium material, the laboratory initiated its first plutonium experiment in January 2026 and has since continued phased scientific investigations. The PluS Lab is thus in its first year of technical ramp-up, with approved experiments underway while subsequent studies of increasing complexity and novelty are being prepared. A suite of analytical capabilities, including Raman and scanning electron microscopy, FT-IR and UV-vis spectroscopy, electrochemical instrumentation, differential scanning calorimetry, mass spectrometry, and X-ray diffractometry, enables comprehensive characterization of plutonium compounds and materials.

Within the Molecular Chemistry and Materials Science pillar, initial efforts focus on solid-state characterization to establish analytical capability and validate experimental methodologies; halide synthesis via new synthetic routes will follow. Within Aqueous Systems, first work focuses on ion-exchange separations, electroanalytical characterization, and implementation of a laboratory-scale ultrasonic separations method. In Molten Salt Science, initial studies focus on plutonium speciation, redox chemistry, and materials interactions in high-temperature molten salt environments.

A defining feature of the PluS Lab is the deliberate coupling of research with workforce development. Postdoctoral researchers, under the guidance of plutonium subject matter experts, develop procedures and perform experiments; graduate student engagement in research activities will expand as the PluS Lab matures. Engagement with student consortia and cross-institutional collaborations strengthens knowledge transfer pathways and supports stewardship of the plutonium and nonproliferation science workforce.

Having progressed from concept to an established plutonium research capability, the PluS Lab is now positioned to advance fundamental plutonium science while strengthening the next generation of the plutonium and nonproliferation science workforce.

LA-UR-26-21915

Stability and Aging Pathways of Pu(IV) Hexanuclear Clusters in aqueous solution: Influence of Ligand Environment and Alpha Radiolysis

Maëva Munoz[1*], Christelle Tamain[1], Matthieu Virot[2], Valérie Vallet[3] and Dominique Guillaumont[1]

1CEA, DES, ISEC, DMRC, Univ Montpellier, Marcoule, France.

2ICSM, Univ Montpellier, CEA, CNRS, ENSCM, Marcoule, France.

3Univ. Lille, CNRS, UMR 8523 – PhLAM -- Physique des Lasers Atomes et Molécules, Lille, France

*maeva.munoz@cea.fr

Understanding the aqueous chemistry of Pu(IV) remains a central challenge in actinide science. Plutonium speciation governs solubility, transport, and reactivity, directly influencing nuclear fuel reprocessing, long-term waste management and environmental behavior. Due to its strong propensity toward hydrolysis, Pu(IV) readily undergoes olation and oxolation reactions, leading to the formation of well-defined oxo-hydroxo polynuclear clusters.[1, 2] These species occupy a key position at the interface between discrete molecular complexes and extended PuO_2-like structures [3, 4] and are therefore critical to describing the early stages of actinide polymerization.

Among the structures identified for tetravalent plutonium, the hexanuclear $[Pu_6O_4(OH)_4]^{12+}$ cluster is one of the most recurrent. [1, 2, 4–6] Although extensively characterized, its thermodynamic stability and long-term persistence in solution remains uncertain. [2, 5, 6] A fundamental question is whether such clusters represent stable molecular species under given chemical conditions or transient intermediates whose evolution depends on ligand environment and self-radiolytic effects.

In this work, we investigated the aging behavior of the hexanuclear Pu(IV) cluster in solution in the presence of two different ligands: acetate and DOTA (1,4,7,10-tetraazacyclododecane-1,4,7,10-tetraacetic acid). Acetate[7], a weakly coordinating carboxylate ligand, allows hydrolytic processes to develop and leads to a coordination number of 9 around Pu(IV), whereas DOTA, a strong macrocyclic chelator, imposes a more constrained coordination sphere with a coordination number of 8. A multi-technique approach combining UV–Vis–NIR spectroscopy, EXAFS and SAXS was employed to investigate the structure of the cluster in solution during aging. Comparisons were performed using Pu isotopes exhibiting different α-dose rates (8, 13, and 213 $Gy \cdot h^{-1}$) in order to evaluate the role of α-radiolysis in the structural transformations.

Comparison of the results obtained with the two ligands and with Pu isotopes exhibiting different α-dose rates demonstrated that ligand coordination strength and radiolytic conditions play a decisive role in governing the stability and aging pathways of Pu(IV) clusters. In acetate medium, the hexanuclear cluster progressively evolved toward PuO_2 nanoparticles, most probably accompanied by aggregation at larger length scales. In contrast, DOTA significantly stabilized the Pu(IV) coordination environment and slowed structural evolution. Increasing α-dose rates accelerated these transformations, highlighting the combined role of coordination chemistry and α-radiolysis in controlling cluster stability. The proposed ligand- and dose-dependent aging pathways are summarized in Figure 1.

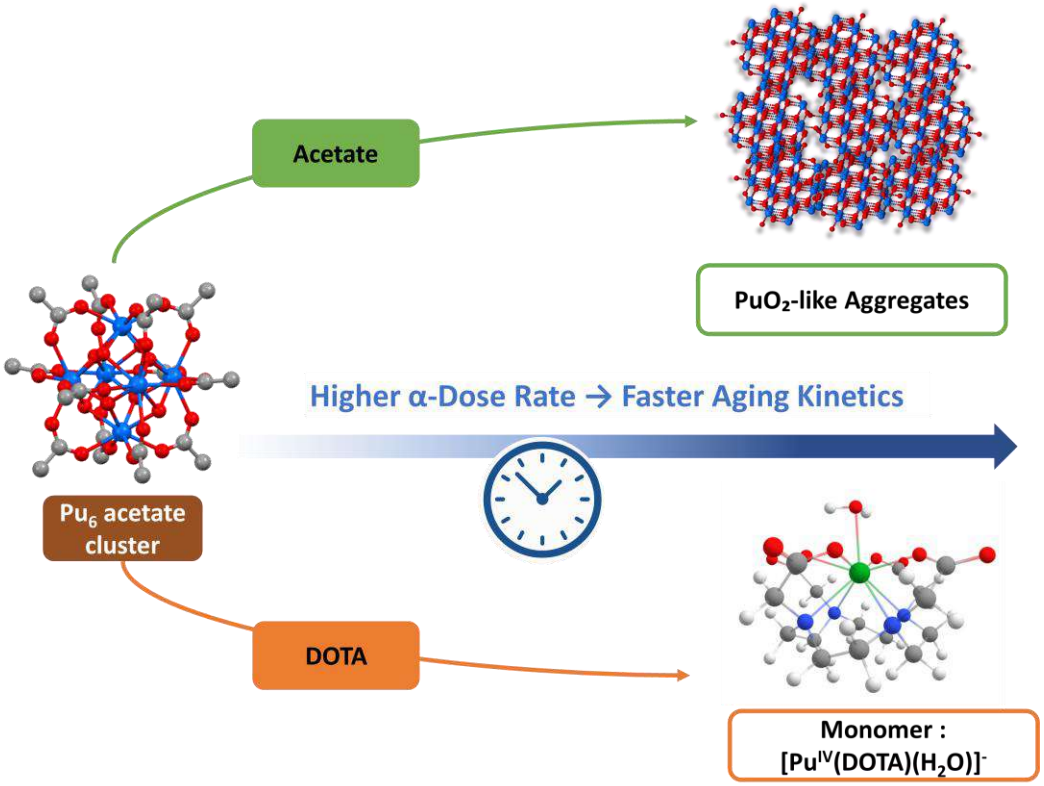


Figure 1: Schematic representation of the aging pathways of the hexanuclear Pu(IV) cluster in acetate and DOTA media. Increasing α-dose rate accelerated structural reorganization toward PuO_2 nanoparticles and aggregation processes.

[1] Knope, K. E.; Soderholm, L. *Chem. Rev.*, **2013**, *113* (2), 944–994. https://doi.org/10.1021/cr300212f.

[2] Tamain, C.; Dumas, T.; Hennig, C.; Guilbaud, P. *Chem. – Eur. J.*, **2017**, *23* (28), 6864–6875. https://doi.org/10.1002/chem.201700493.

[3] Cot-Auriol, M.; Virot, M.; Dumas, T.; Diat, O.; Menut, D.; Moisy, P.; Nikitenko, S. I. *Chem. Commun.*, **2022**, *58* (94), 13147–13150. https://doi.org/10.1039/D2CC04990B.

[4] Sigmon, G. E.; Hixon, A. E. **2019**, *25* (10), 2463–2466. https://doi.org/10.1002/chem.201805605.

[5] Chupin, G.; Tamain, C.; Dumas, T.; Solari, P. L.; Moisy, P.; Guillaumont, D. *Inorg. Chem.*, **2022**, *61* (12), 4806–4817. https://doi.org/10.1021/acs.inorgchem.1c02876.

[6] McCusker, T. L.; Vanagas, N. A.; Szymanowski, J. E. S.; Surbella, R. G.; Bertke, J. A.; Arteaga, A.; Knope, K. E. *CrystEngComm*, **2025**, *27* (4), 507–515. https://doi.org/10.1039/D4CE01042F.

[7] Maëva M, Tamain C, Virot M, Bayle S, Dourdain S, Dumas T, Solari P.L, Menut D, Vallet V , Guillaumont G. Inorg. Chem, accepted for publication, **2026**

Plutonium Oxidation Studied at Different Temperatures

D. T. Olive[1*], A. R. Mazza[1], S. Blackwell[1], A. Boehm[1], H. Milenski[1], W. S. Ponder[1]

[1]Los Alamos National Laboratory, Los Alamos, United States of America; *dolive@lanl.gov

Understanding the oxidation of plutonium metal is important for safe storage and use. Studies on the plutonium oxide surface using X-ray photoemission spectroscopy (XPS) conducted under ultra-high vacuum conditions are plagued by autoreduction of the plutonium dioxide away from it's normal oxidation state found on the surface under ambient conditions. In this study, oxygen gas dosing is performed at different temperatures to better understand the kinetics of plutonium oxidation in general, produce stable plutonium dioxide surfaces for analysis, and to try and elucidate aspects of the autoreduction phenomenon.

Probing the Effects of Iron and Uranium Impurities on the Melt Behavior of Plutonium Alloys using Differential Scanning Calorimetry

Kristen Pace[1*], Najeb Abdul-Jabbar[1], Alberto Gomez[1], Michael Kopriva[1], Shane Mann[1], Jeremy Mitchell[1]

[1]Los Alamos National Laboratory, Los Alamos, NM, USA; *kpace@lanl.gov

For decades, a topic of significant interest and controversy within the plutonium science community centered on questions related to the long-term phase stability of delta-stabilized Pu-Ga alloys. Although disagreements on the correctness of the Russian versus so-called Western versions of the Pu-Ga binary phase diagram have since been resolved, similar questions remain for analogous alloys exhibiting more complex compositions such as those containing impurity phases. For example, little is known regarding the phase stability and thermodynamic properties of Pu-Ga alloys containing iron and uranium, which are commonly present impurity constituents in aged plutonium alloys stemming from synthesis environments and natural radiogenic decay of Pu-239, respectively. The development of thermodynamic modeling tools such as CALPHAD (CALculation of PHAse Diagrams) has enabled prediction of the impacts these impurities may have on relevant thermodynamic properties and phase equilibria. Experimental data is nevertheless needed to validate the calculated phase diagrams.

In this presentation, recent differential scanning calorimetry (DSC) data obtained on a variety of Pu-Ga alloys containing known amounts of iron and uranium impurities will be discussed, and comparisons will be made to published CALPHAD predictions of the quaternary Pu-U-Fe-Ga system. Consistent with recent predictions, DSC results indicate an inversely proportional relationship between melting onset temperatures of Pu-Ga alloys and the concentrations of iron and uranium impurities.

Qualification of Plutonium and Iron Analysis Capabilities within Los Alamos National Laboratory Plutonium Facilities

T. Gannon Parker[1*], Journey R. Nolan[1], Justin N. Cross[1], Mary A. Knaak[1], Stephanie M. Andrade[1], David T. Fox[1], Lav Tandon[1]

[1]Los Alamos National Laboratory, Los Alamos, New Mexico, United States
tgparker@lanl.gov

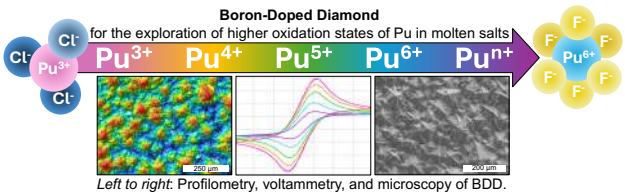
The capabilities for the assay of plutonium using a Corpel titration method at Los Alamos National Laboratory will be detailed, along with the complementary method for measuring iron in plutonium materials, and the process for qualifying these techniques for analysis of production samples will be described. The Corpel titration method is designed to determine the plutonium content in metals, oxides, alloys, and other plutonium materials. The solid Pu sample is dissolved and the solution is diluted with sulfuric and nitric acids, treated with sulfamic acid, reduced with Ti(III), over-titrated with excess Ce(IV), and finally back titrated with Fe(II). The equivalence points are determined potentiometrically using a combined platinum electrode. Since iron is an interferent in the assay measurement, a separate analysis is performed for this element (along with measurements for Np and U, not detailed here) to perform corrections for the plutonium assay value. In this method, aliquots of the dissolved plutonium material are treated with hydroxylamine hydrochloride to reduce Fe(III) to Fe(II), followed by precipitation of the plutonium in the form of its oxalate, and subsequent isolation of Fe(II). The iron is then complexed with o-phenanthroline and analyzed by UV-Vis spectrophotometry. These techniques are being developed for new facilities at the Lab to complement current methods in labs with aging infrastructure that have been in use since the era immediately following the Manhattan Project.

LA-UR-26-21254

Diamonds are an Actinide's Best Friend: Electrochemical Discrimination of U and Pu Redox Couples Using Boron-Doped Diamond

Hannah K. Patenaude[1], Dylan M. Tharp-Eralie[1], Jarom L. Chamberlain[1], Samuel R. Lee[1], Clare A.J. Hatfield[1], Nathaniel K. Rood[1], Karla A. Erickson[1], Marisa J. Monreal[1*]

[1]Los Alamos National Laboratory, Los Alamos, NM, USA; *mmonreal@lanl.gov



Left to right: Profilometry, voltammetry, and microscopy of BDD.

The resurgence of molten salt reactor (MSR) technologies and continued advancement of pyroprocessing methods demand robust analytical tools capable of operating in extreme chemical environments. Real-time monitoring of special nuclear material (SNM), particularly plutonium, remains a critical gap for safeguards, process control, and fuel cycle accountability. Electroanalytical methods offer a promising pathway; however, conventional electrode materials used in high-temperature molten salts (metals, graphite) suffer from large background currents, limited potential windows, and corrosion, restricting their analytical utility.

Plutonium detection in molten salts has traditionally focused on the Pu^{3+}/Pu^{0} couple due to its relevance to bulk electrolysis and metal production. However, this reaction presents challenges for quantification in reactor-relevant environments: 1) the Pu^{3+}/Pu^{0} reduction potential closely overlaps with the analogous U^{3+}/U^{0} reaction, complicating selective detection in mixed-actinide systems, and 2) the process involves a soluble-to-insoluble phase transition, introducing kinetic and mass-transport complexities. In contrast, the soluble-to-soluble Pu^{4+}/Pu^{3+} redox couple exhibits greater electrochemical distinction from the uranium equivalent, representing a more promising target for in situ SNM quantification. Despite this advantage, Pu^{4+}/Pu^{3+} remains largely underexplored in molten salts due to insufficient electrode resolution and high capacitive backgrounds.

Here we investigate boron-doped diamond (BDD) as a designer electrode platform for high-resolution actinide electrochemistry. BDD exhibits wide potential windows, low background currents, rapid electron-transfer kinetics, and exceptional chemical inertness owing to its predominantly sp^3-hybridized carbon lattice. Boron incorporation introduces acceptor states that enhance sensitivity toward oxidative processes, making BDD particularly well suited for probing higher oxidation states of actinides. Unlike metal electrodes suitable for bulk electrolysis for pyroprocessing, BDD enables mechanistic interrogation of soluble redox couples critical for analytical applications.

The result of this work is a systematic evaluation of uranium and plutonium redox chemistry across aqueous and molten salt environments to benchmark electrode performance and establish structure-property relationships governing actinide electron transfer. Aqueous measurements of uranium and plutonium redox couples using BDD provide foundational diffusion, kinetic, and thermodynamic characterization that can be used to benchmark and validate analytical methodologies. Molten chloride and fluoride salt studies of U^{4+}/U^{3+} are presented to demonstrate BDD electrode stability and signal resolution under extreme conditions not previously reported in the literature. Complementary aqueous plutonium data establish proof-of-concept detection of the Pu^{4+}/Pu^{3+} couple, and ongoing efforts extend this approach to plutonium in molten salts, ultimately targeting quantitative discrimination in mixed-actinide systems like that of MSR fuels.

By shifting emphasis from bulk metal deposition to soluble redox chemistry, this analytical framework advances materials science for extreme environments, supports next-generation safeguards strategies, and enables improved monitoring of actinides in advanced nuclear fuel cycles. These studies establish boron-doped diamond as a durable and sensitive platform for actinide electrochemistry, pioneering fundamental plutonium molten salt electrochemistry while providing a new capability for MSR and pyroprocessing applications.

Multi-Fidelity Gaussian Process Regression for Modeling the Thermal Properties of MOX Nuclear Fuel

D. Piccinelli[1*], J. Tranchida[1], B. Kerleguer[2], E. Bourasseau[1]

[1]CEA, DES, IRESNE, DEC, Cadarache, France; [2]CEA, DAM, DIF, Arpajon, France;
*Davide.PICCINELLI@cea.fr

Fourth-generation Fast Neutron Reactors (FNRs) are expected to exploit MOX (Mixed Oxide) fuels, optimizing uranium consumption and reducing long-lived nuclear waste. These polycrystalline ceramic fuels are composed of a mixture of uranium and plutonium dioxides.
The current state of the art in fuel modeling is represented by Fuel Performance Codes (FPCs), which base their calculations on behavioral laws to describe the thermo-mechanical behavior and evolution of MOX fuels inside the reactor. Therefore, to obtain accurate results, it is essential to obtain reliable constitutive laws that precisely estimate their physical properties.
However, on the one hand, MOX experimental data are expensive and difficult to obtain (particularly at high temperatures), with some conditions that are hard to control driving large uncertainties.
On the other hand, atomistic simulations have demonstrated their effectiveness in deepening physical insight and establishing constitutive laws, but they cannot alone capture all the relevant physical effects.

This research project aims at addressing these issues by developing a machine learning model that combines experimental data and results from atomic-scale simulations to predict key thermal material properties, such as thermal conductivity, thermal diffusivity, and specific heat.
These three properties are intrinsically related (knowing two out of three allows the third one to be readily determined), as is their evolution with temperature, mixture composition (plutonium content), and stoichiometry (oxygen content).

Where beneficial, a Multi-Fidelity (MF) approach is adopted, implementing hierarchical models that account for different levels of confidence associated with the training data in order to produce more accurate predictions. Where this is not possible, more agnostic methods are explored, guided by data analysis and noise evaluation.
The model is also able to estimate the uncertainty of its predictions, which is important for supporting the planning of future experiments (for which rigorous adaptive methodologies exist, but are not yet standardized within the MOX experimental community) and improving the reliability of fuel performance modeling.

The methods involve Gaussian Process regressions applied to the aforementioned quantities, combining different data fidelities within a MF mathematical framework, together with database selection, grouping, evaluation, and construction. In particular, the project makes use of an existing MOX experimental database and a simulation database constructed ad hoc using different tools, including Classical Molecular Dynamics and *ab initio* methods.

Keywords: MOX fuel, thermal conductivity, Gaussian process regression, multi-fidelity modeling.

Helium Bubble Evolution in Aged Plutonium

J. Plohr[1*], N. Mathew[1], I. Chesser[1], J. Startt[1], M. Nithol[1], A. Hunter[1], S. Fensin[1]

[1]Los Alamos National Laboratory, Los Alamos, New Mexico, U.S.
*jplohr@lanl.gov

Self-irradiation from α-decay drives plutonium (Pu) aging by generating both uranium (U) recoil atoms and helium (He) atoms (α particles). Helium migrates through the Pu matrix, and a fraction of these atoms agglomerates into nanometer-scale bubbles. Over time, these bubbles diffuse through the lattice and coalesce, forming progressively larger bubbles.

This work focuses on modeling the evolution of He bubbles in aged δ- and ε-phase Pu at elevated temperatures. We develop a Python code, *Bubble Merger*, to simulate He-bubble migration and coalescence at experimentally relevant densities and time scales. The model is parameterized using diffusion coefficients for δ-Pu obtained from molecular dynamics (MD) simulations. We identify several plausible mechanisms contributing to He-bubble diffusivity in δ-phase Pu alloys, with both volume diffusion and faceted-bubble diffusion showing favorable agreement with experimental observations reported by Wheeler (2007) and Jeffries (2011). This framework provides an essential predictive tool for assessing the long-term performance of Pu-alloy components and for guiding future surveillance and manufacturing efforts.

Wheeler et al., Evaluation of the nucleation and growth of helium bubbles in aged plutonium, *J. Alloy. Compd*. 2007
Jeffries et al., He bubble coarsening by migration and coalescence in annealed Pu–Ga alloys, *J. Nuc. Mat.* 410, 2011

Development of Water-Equivalent Solid Calibration Standards for Plutonium Gamma-Ray Nondestructive Assay

Bianca Ramirez[1*], David Kunsberg[1], Stephen Cope[1]

[1]Los Alamos National Laboratory, Los Alamos, NM, United States *bramirez@lanl.gov

Non-destructive assay by high-purity germanium gamma spectrometry is a mainstay technique for the quantification of plutonium in the radiochemistry community. To ensure reliable and precise measurements are gathered, periodical calibrations with standards are required. For plutonium, aqueous solutions are commonly employed as calibration standards as they best reflect the samples being analyzed. However, liquid standards of plutonium suffer from safety and integrity drawbacks that severely limit their use in routine calibration. Furthermore, the inherent instability of aqueous plutonium solutions due to radioactive decay and plutonium precipitation makes the manufacturing and storage of reliable and well-characterized solutions difficult. To circumvent these limitations, we aim to substitute aqueous standards with sturdy and multi-use water-equivalent solid standards. This work focuses on the matrix screening, method development, and validation of water-equivalent solid calibration standards for plutonium gamma-ray nondestructive assay. Preliminary results show that the constructed solid standards closely replicate the liquid calibration standards and afford reproducible measurements over a multi-month timeframe.

Utilizing 244Pu for High Resolution Plutonium Concentration Determinations Via Isotope Dilution Measurements and Thermal Ionization Mass Spectrometry

Ramos, F.C.[1a], Windorff, C.J[1]. Brewer, C.A.[1]

[1]New Mexico State University, Las Cruces, New Mexico, USA *framos@nmsu.edu

The potential for isotope dilution for measuring plutonium concentrations is becoming increasing critical considering the decreasing plutonium concentrations currently in atmospheric collected samples due to the limited number of recent detonations and testing. The potential of using 244Pu for such measurements will allow for greatly reduced measurements far exceeding those at the detention limits using quadrupole ICPMS analyses. With the potential use of 244Pu, the isotopic nature of plutonium sources may also be characterized thus fingerprinting the source of plutonium in addition to the concentrations measured. Here , we will evaluate the potential of using 244Pu for such measurements in environmental samples collected in New Mexico.

Oxidation of Pu Alloys Stabilized in δ-Phase: Characterization of the Microstructure of the Oxide Scale

Brice Ravat[1*], Lionel Jolly[1], Elodie Aubert[1], Catherine Sabathier[2], Doris Drouan[2], Isabelle Zacharie-Aubrun[2], Thierry Blay[2], Ingrid Roure[2], Philippe Bienvenu[2], Benoît Oudot[1]

CEA, DAM, Valduc, F-21120 Is-sur-Tille, France
CEA, DES, IRESNE, Cadarache, F-13108 Saint-Paul-Lez-Durance, France
Corresponding author*: brice.ravat@cea.fr

Although δ-Pu oxidizes at a lower rate than other phases, it still remains very sensitive to corrosion, which may be severe in long-term storage under an inadequately controlled atmosphere. Consequently, despite the corrosion of δ-Pu alloys has been studied for several decades, the characterization of the corrosion products and the oxide scale morphology, the determination of growth kinetics, and, more generally, understanding the oxidation process remain topics of significant interest. Therefore, numerous recent studies have focused on the influence of various exposure parameters –such as temperature, composition of the oxidizing gas, presence of moisture– on the properties of the Pu oxide scale.

It is usually accepted that high temperature oxidation under oxygen atmosphere results in the formation of an oxide scale composed of an outer layer of face-centered cubic PuO_2 and an inner layer of Pu_2O_3. The inner layer of Pu_2O_3 exhibits polymorphic characteristics as both cubic and hexagonal (so-called α-and β-phases) crystallographic structures may be present. The oxide scale growth kinetics involve an initial parabolic growth stage primarily due to the thickening of the α-Pu_2O_3 layer, followed by linear growth of PuO_2. Furthermore, oxidation leads to a surprising destabilization of the δ-phase suggesting that it also alters the structure of the alloy.

While the composition, the kinetics of formation of Pu oxide scale have been widely addressed in the literature, few studies focus on the influence of exposure conditions on its morphology and microstructure.

The purpose of this work is to enhance the knowledge of the microstructure of the oxide formed under different experimental exposure conditions. To achieve this, the subsurface structure of the oxide scale was investigated using ion milling FIB and subsequent analysis of the cross-section via SEM. In addition, thin lamellae specimens were prepared for TEM analysis. The obtained results revealed that the microstructure of the oxide scale is significantly impacted by the exposure conditions leading either to the formation of an inner mixed layer of α-Pu_2O_3 composed of thin platelets or needles propagating into a metallic zone corresponding to the stable phase of unalloyed Pu or the occurrence of single crystals of Pu oxide with sizes that can reach several hundred nanometers.

The Signature of the Mono-Oxo Bonding in Protactinium(V) in the M_4-Edge HERFD spectrum: a theoretical and experimental study

T. Shaaban[1], C. Le Naour[2], H. Oher[2], T. Aubert[2], P. L. Solari[3], T. Burrow[3], M. Hunault[3], A.S.P. Gomes[1], F. Réal[1,*], V. Vallet[1], R. Polly[4], M. Maloubier[2]

[1]Université de Lille, CNRS, UMR 8523 – PhLAM – Physique des Lasers, Atomes et Molécules, F-59000 Lille, France.

[2]Université Paris-Saclay, CNRS/IN2P3, IJCLab, 91405 Orsay, France.

[3]Synchrotron Soleil, Saint-Aubin, F-91192 Gif-sur-Yvette, France.

[4] Institut für Nukleare Entsorgung (INE), 76021 Karlsruhe, Germany.

*email:florent.real@univ-lille.fr

Protactinium (Z = 91) exhibits unique redox behavior, oscillating between Pa(IV) [1] and Pa(V). In aqueous media, Pa(V) predominates as Pa^{5+} or PaO^{3+}, while PaO_2^{+}, common in heavier actinides, has not been observed [2,3]. The presence of a potential mono-oxo bond in Pa(V) can be investigated using X-ray spectroscopies [4].

In February 2024, a series of advanced spectroscopic experiments utilizing HERFD-XANES, RIXS, and EXAFS were conducted at the MARS beamline (SOLEIL synchrotron) to explore the structural and electronic properties of actinide complexes, specifically those of protactinium (Pa). An intriguing discovery was made, as the spectra of Pa(V) in both oxalate and fluoride solutions displayed pronounced similarities (Figure 1). This observation challenges prior interpretations that proposed the formation of mono-oxo species in oxalic media [5]. To further investigate these findings, we employed sophisticated quantum chemical methods, including relativistic time-dependent density functional theory (TD-DFT) [6] and restricted active space self-consistent field (RASSCF) [7] simulations at the L_3 and M_4 absorption edges, guided by EXAFS-derived structural models. These theoretical approaches not only provided an accurate reproduction of the experimental spectra but also offered significant insights into the underlying nature of the electronic transitions, thereby enhancing our understanding of the behavior of Pa complexes in different environments.

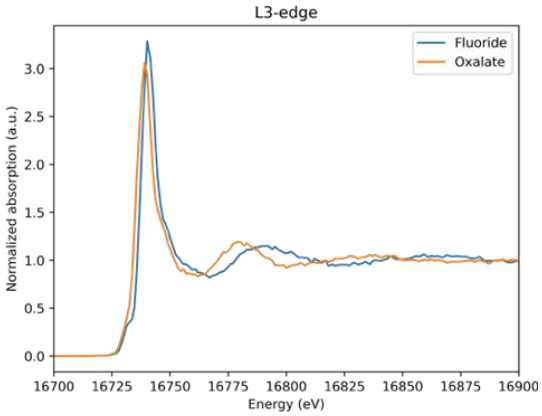


Figure 1: HERFD-XANES L_3 edge spectra of $Pa^{(V)}$ in hydrofluoric and

This work was supported by ANR (ANR-21-CE29-0027), LABEX CaPPA (ANR-11-LABX-0005-01), and I-SITE ULNE (ANR-16-IDEX-0004 ULNE).

References

[1] N. Banik et al., Dalton Trans. **2015**, 45, 453-457.
[2] C. Le Naour et al., Inorg. Chem. **2005**, 44, 9542-9546.
[3] T. Shaaban et al., Chem. Eur. J. **2024**, e202304068; Ibid, Chem. Comm **2024**, 60, 14376–79.
[4] C. Den Auwer et al., EurJIC **2003**, 21, 3843-3859.
[5] M. Mendes et al., Inorg. Chem. **2010**, 49, 9962-9971.
[6] W. Misael et al., Inorg. Chem. **2023**, 62, 11589-11601.
[7] R. Polly et al., Inorg. Chem. **2021**, 60, 18764–76.

Synthesizing Pu-U-Ga Ingots for the Advancement of the First Multiscale Alloy Prediction Model

Geronimo Robles[1*], David Arellano[1], Derek Prada[1], Sarah Hernandez[1], Najeb Abdul-Jabbar[1]
[1]Los Alamos National Laboratory, Los Alamos, United States of America; *robles_g@lanl.gov

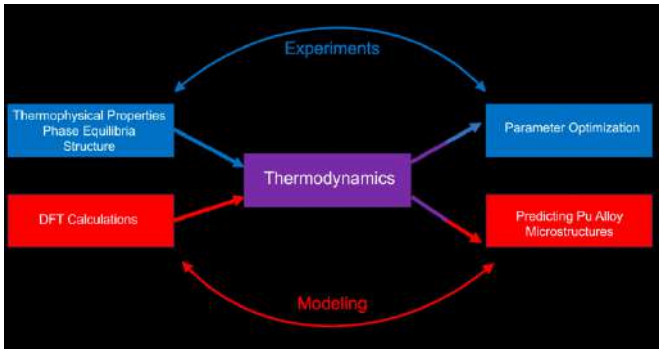


Figure 1 A flowchart depicting how the Pu-U-Ga multiscale alloy prediction model will operate. Data from the experimental effort will aid in optimization while also provide inputs for atomistic DFT calculations. Modeling will be used to predict alloy microstructures for potential subsequent syntheses.

Alloying of the binary Pu-U and Pu-Ga systems has been thoroughly investigated, historically. However, the thermodynamic understanding of the effect of Pu allotropes on the ternary alloying behavior of the Pu-U-Ga system by way of the ingrowth of Uranium remains in its infancy. Elucidation of the necessary details to garner an experimental understanding of these Pu-bearing materials is limited by extremely regulated capabilities. Figure 1 illustrates a modern effort to build upon historical data and combine them to investigate the ternary Pu-U-Ga system with an iterative cradle-to-grave method that has a thermodynamically focused aim. Pu-U-Ga is synthesized and characterized and its microstructural evolution is investigated. Then, those results are applied to the predictive models via DFT calculation. Model results can then be re-evaluated in the understanding of the overall thermodynamics. Here, the first step in the process, synthesis and microstructure analysis, is not only presented but showcased for its streamlined efficiency.

The suite of Pu-U-Ga alloys chosen for this study are shown in Figure 2 and targeted five compositions representative of δ-Pu+ η, δ-Pu+η+ ζ, δ-Pu+ζ+ $PuGa_3$, U+Pu+Ga, and U+Pu regions of a calculated isothermal section of the ternary phase space. Each Pu-U-Ga alloy was produced via arc melting due to the method's quickness and accuracy. Pure metal-basis constituents were heated until molten and combined to yield solid ingots. Consolidated ingots were then flipped and remelted a minimum of five times to encourage homogeneity of mixing. On average, a sample was arc melted in less than 10 minutes. Metallographic sample preparation focused on retaining a solid, metallic ingot that could be reused. Each ingot was bisected, cast into an epoxy-resin puck and hand polished to 9µm to be analyzed via scanning electron microscopy, X-ray diffraction, and electron microprobe to investigate their microstructure at various stages of heat treatment. Just before each measurement, the sample surface was retouched to eliminate the potential for unwanted α'-Pu phase and impurities.
In total, three sample sets were evaluated. For the first set, a phase evolution study was conducted on the composition at location "5" in Figure 2 which lies on the Pu-U binary. SEM, XRD and EPMA data was collected for as-fabricated (directly after arc melting) and annealed (24h and 48h at 400°C) conditions and compared to the results of Ellinger and Lawson for the U-Pu system. The second set of samples was annealed for 672h at 400°C and the third set for 672h at 600°C. SEM, XRD and EPMA was collected only after annealing for set 2 and 3. Resultant microstructure is reported here in terms of accuracy to historical data as well as its proximity to calculated phase diagrams. Subsequently, data acquired would then be applied to the overarching study determining thermodynamics on two fronts. For experimentation, parameter optimization could hone thermophysical properties, phase equilibria and structure of the system. Modeling efforts utilized the results in DFT calculations to predict Pu alloy behavior and system microstructures.

The development of a sophisticated and experimentally-driven study to predict Pu alloy microstructure was founded in experimental synthesis then incorporated into models to understand how U is incorporated into the Pu-Ga system. Ultimately, the narrowly understood ternary Pu-U-Ga system is broadened.

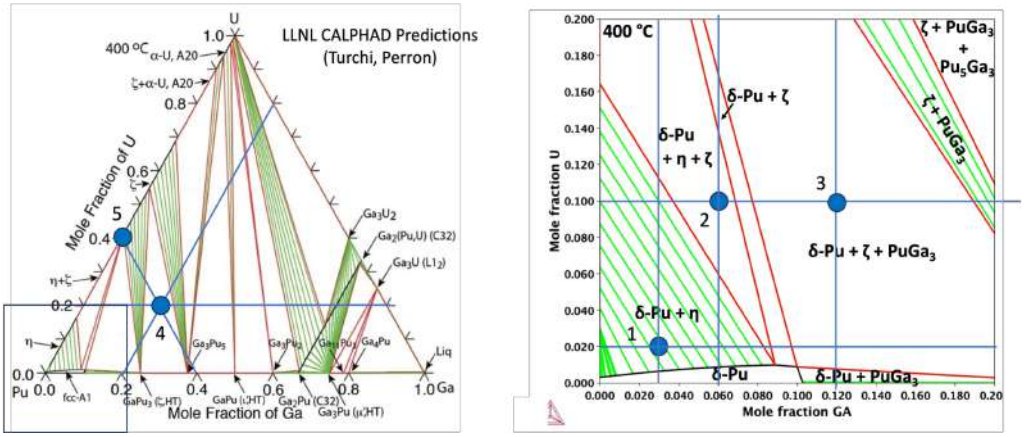


Figure 2 An isothermal section of the Pu-U-Ga system at 400°C as calculated by the work of Turchi and Perron at LLNL. Each of the five compositions are shown such that their respective predicted structures are also listed. On the right, the inset showcases the difference in predicted structures over a very narrow area of U and Ga concentrations.

Gas Dosing and Growth of Pu Oxycarbide Films: Characterization of the Surface using XPS and ToF-SIMS

Daniel J. Rodriguez[1], Timothy J. Gorey[1], Raymond Atta-Fynn[1], and Sarah C. Hernandez[1]

[1]Los Alamos National Laboratory, Los Alamos, New Mexico, USA, djrod@lanl.gov

Plutonium oxycarbides (PuO_xC_y) are interesting compound materials since they have different surface reactivities than Pu metal, Pu oxides (PuO_2, Pu_2O_3), and Pu carbides (PuC, Pu_2C_3). This experimental study will describe how to grow a thin film of Pu oxycarbide on top of the Pu metal surface in UHV using high purity H_2 gas, which yields a singular carbide phase in comparison to native oxycarbide layers and other Pu oxycarbides reported in the literature that show dual peaks. After growth, the film is analyzed by X-ray photoelectron spectroscopy (XPS) and time-of-flight secondary ion mass spectrometry (ToF-SIMS). XPS provides electronic structure and chemical state measurements with attention toward the response of the Pu 4*f*, O 1*s*, C 1*s*, and valence regions. ToF-SIMS is used to measure surface species on the topmost 1-2 monolayers which gives context to various adsorbates. Our experiments include the general stability of the Pu oxycarbide film with respect to time under UHV conditions and its response to dosing from various gases.

Fig. 1 gives visualization of the Pu oxycarbide layer after having been grown with H_2 gas. XPS region scans for Pu 4*f*, O 1*s*, and C 1*s* are depicted. In the Pu 4*f*, there is not much difference in comparison to metal Pu due to the PuO_xC_y film thickness being on the order of a couple nanometers. However, both the O 1*s* and C 1*s* regions showed the presence of oxygen and carbon. For example, the C 1*s* has a prominent peak at ~281 eV, which is indicative of Pu carbide.

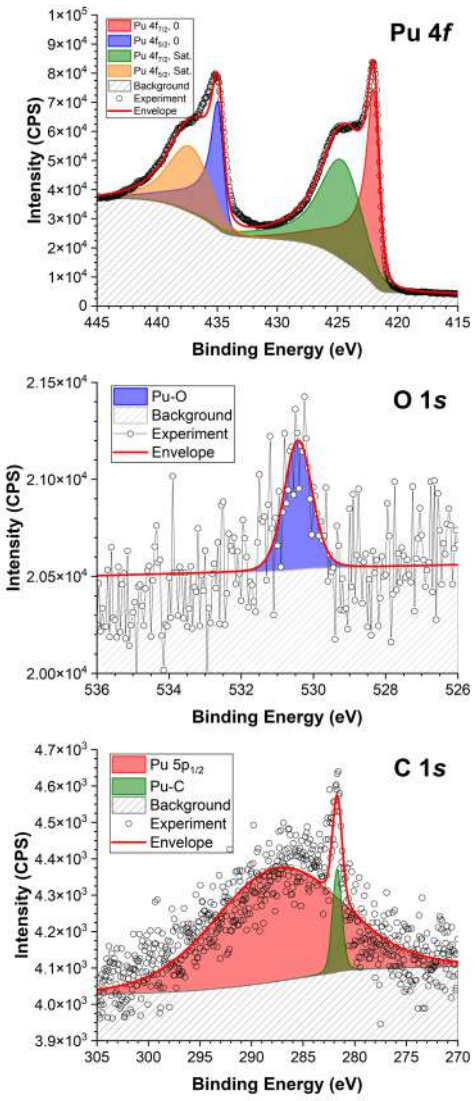


Figure 1: XPS spectra of a Pu oxycarbide film grown on Pu metal. Top: The Pu 4*f* spectrum showing the metal (red, blue) on the 7/2 and 5/2 peaks and the satellites (green and orange). Middle: The O 1*s* peak showing oxygen in the form of Pu-O (blue). Bottom: The C 1*s* peak showing the broad Pu $5p_{1/2}$ peak (red) with Pu-C (green) at ~281 eV.

In search of the σ-Pu phase

Paul Roussel[1*], Mike Matthews[1], David Wheeler[1]

[1]AWE plc, Aldermaston, Reading, Berkshire, RG74PR U.K; *email paul.roussel@awe.co.uk

Plutonium has long been regarded as the "connoisseur's element" owing to its uniquely complex metallurgy and electronic structure. Metallic plutonium exhibits phenomena rarely observed elsewhere in the periodic table, including negative thermal expansion in the low-density face-centred cubic δ-phase and an extraordinary sequence of six temperature-dependent allotropes. The sensitivity of these phases to impurities was established shortly after the Manhattan Project, when the δ' phase was identified only after sufficiently pure metal became available [1].

In 2014, a seventh allotrope—the σ phase—was reported in alloyed material derived from high-purity plutonium, based exclusively on synchrotron hard X-ray techniques (EXAFS, pair distribution function, and powder diffraction) [2]. Notably, this phase has not been independently confirmed, and its fundamental nature remains unresolved.

Here, we present synchrotron soft X-ray photoelectron spectroscopy (XPS) measurements of the same high-purity starting material to probe the electronic structure associated with the reported σ-Pu phase [3]. These results are complemented by microscopic imaging and electron probe microanalysis (EPMA), enabling correlation of chemical heterogeneity, microstructure, and electronic signatures. Together, the data provide new insight into whether the σ phase represents a distinct allotrope, a metastable impurity-stabilized structure, or a previously unrecognized compositional regime in plutonium metallurgy.

[1] E. R. Jette, Some physical properties of plutonium metal, Journal of Chemical Physics **23** (1955) 365.
[2] S. D. Conradson et al., Nanoscale heterogeneity, premartensitic nucleation, and a new plutonium structure in metastable δ fcc Pu-Ga alloys, Physical Review B **89** (2014) 224102.
[3] The authors are indebted to R. K. Schulze, J. Terry and J. Tobin for sharing the synchrotron XPS data.

UK Ministry of Defence © Crown Owned Copyright 2026/AWE

Point Defect and Impurity Incorporation in Plutonium Oxides

Andrew J. E. Rowberg[1*], Kyoung E. Kweon[1], Scott B. Donald[1]

[1]Lawrence Livermore National Laboratory, Livermore, USA
*rowberg1@llnl.gov

The incorporation of point defects and impurities in materials is vital for understanding their properties, stability, and performance. The stability of metallic plutonium is largely governed by the permeability of its heterogeneous surface oxide, which typically adopts the stoichiometry of PuO_2 or Pu_2O_3. Here, we use hybrid density functional theory calculations to compute formation energies and kinetic barriers of migration for native point defects and common environmental contaminants in PuO_2. Oxygen vacancies and small polarons form readily in PuO_2, while nitrogen-, fluorine-, and hydrogen-based impurities can also be favorable under certain conditions. Oxygen vacancies and hydrogen interstitials are highly mobile, but their prevalence depends on the chemical potential conditions. Accordingly, monitoring the prevalence of these species is key for maintaining the stability of plutonium and its native surface oxide.

This work was performed under the auspices of the U.S. DOE by Lawrence Livermore National Laboratory under Contract DE-AC52-07NA27344.

Nanoscale Effects in Plutonium Dioxide: How Size Shapes Structure and Electronic Properties

G. N. Roy[1,*], S. Bayle[2], P. Estevenon[2], L. Amidani,[3] C. E. Silva,[3] C. Hennig,[3] M. Munoz[3], M. Hunault[4], C. Tamain[3], T. Dumas,[2] K. Kvashnina,[3] M. Virot[1]

[1]ICSM, Univ Montpellier, CEA, CNRS, ENSCM, Marcoule, France; [2]CEA, DES, ISEC, DMRC, Univ Montpellier, Marcoule, France; [3]The Rossendorf Beamline at ESRF, The European Synchrotron, Grenoble, France; [4]Synchrotron SOLEIL, L'Orme des Merisiers, Saint-Aubin, France

*gabriel.roy@cea.fr

Since the early investigations conducted during the Manhattan Project, it has been well known that the hydrolysis of tetravalent Pu produces colloidal suspensions characterized by their remarkably stable nature and distinctive emerald-green color.[1,2] Operational constraints related to nuclear fuel cycle processes, typically requiring strongly acidic conditions to maintain plutonium solubility, have long hindered fundamental investigations related to plutonium hydrolysis and condensation reactions.[1-4] For decades, the product of Pu(IV) hydrolysis was described as amorphous and ill-defined polymeric aggregates. Some recent studies have significantly revised this view.[1,5-8] Synchrotron-based X-ray absorption and scattering techniques have demonstrated that hydrolytic Pu(IV) products consist of nearly spherical, crystalline nanoparticles with typical diameters of 2-3 nm and a local structure consistent with bulk PuO_2.[4-8] Studies further established size-structure correlations and identified surface contributions in X-ray absorption spectroscopy analyses.[6]

In order to pursue the systematic investigation of the relationship between size and properties, this work examines the evolution of the electronic and structural properties of PuO_2 nanoparticles as a function of their size. Three PuO_2 samples exhibiting different particle sizes were synthesized and subsequently characterized using laboratory and synchrotron-based techniques, in addition to an oxo-hydroxo hexameric cluster of plutonium (IV). The latter was recently suggested as a transient intermediate in PuO_2 colloidal nanoparticle formation and also provides Pu oxo-hydroxo bonds that are likely to be representative of the nanoparticle surface.[5,6] High-resolution X-ray diffraction (HR-XRD) was first employed to determine the coherent domain sizes of the three PuO_2 samples and confirmed the structural integrity of all four samples. The HR-XRD results indicated that all three samples exhibit the PuO_2 fluorite structure, while the hexameric cluster structure was also consistent with structural data. Subsequently, the electronic structure of the samples was probed using high-energy-resolution fluorescence-detected X-ray absorption near-edge spectroscopy (HERFD-XANES) at the plutonium M_4 edge. The HERFD-XANES spectra unequivocally demonstrated the absence of oxidation states other than Pu(IV) in the PuO_2 samples. Furthermore, the results revealed that the electronic structure depends on particle size. Comparison with numerical simulations suggested that these spectral changes originate from crystal-field effects associated with surface atoms. These results provide the first evidence of the size-dependent electronic structure in PuO_2.

References

[1] D. Clark, S. Hecker, G. Jarvinen and M. Neu, in The Chemistry of the Actinide and Transactinide Elements, eds. L. Morss, N. Edelstein and J. Fuger, Springer Netherlands, 2011, DOI: 10.1007/978-94-007-0211-0_7, ch. 7, pp. 813-1264.

[2] M. Virot et al. Synthesis and multi-scale properties of PuO2 nanoparticles: recent advances and open questions. *Nanoscale Adv.* 4 (2022) 4938-4971. DOI: 10.1039/D2NA00306F.

[3] C. Walther and M. A. Denecke, Actinide colloids and particles of environmental concern. *Chem. Rev.* 113 (2013) 995-1015. DOI: 10.1021/cr300343c.
[4] E. Gerber et al. The missing pieces of the PuO_2 nanoparticle puzzle. *Nanoscale* 12 (2020) 18039-18048. DOI: 10.1039/D0NR03767B.
[5] M. Cot-Auriol et al. First observation of $[Pu_6(OH)_4O_4]^{12+}$ cluster during the hydrolytic formation of PuO_2 nanoparticles using H/D kinetic isotope effect. *Chem. Commun.* 58 (2022) 13147-13150. DOI: 10.1039/D2CC04990B.
[6] L. Bonato et al. Probing the local structure of nanoscale actinide oxides: a comparison between PuO_2 and ThO_2 nanoparticles rules out PuO_{2+x} hypothesis. *Nanoscale Adv.* 2 (2020) 214-224. DOI: 10.1039/C9NA00662A.
[7] L. Amidani et al. Actinide Nanoparticles: Revising Early Developments and Recent Insights from High-Energy-Resolution Fluorescence-Detected X-Ray Absorption Near Edge Structure and Synchrotron Techniques. *Small Sci.* 1 (2026) e202500312. DOI: 10.1002/smsc.202500312
[8] L. Soderholm et al. The Structure of the Plutonium Oxide Nanocluster $[Pu_{38}O_{56}Cl_{54}(H_2O)_8]^{14-}$. *Angew. Chem. Int. Ed.* 2 (2007) 298-302. DOI: 10.1002/anie.200704420.

Plutonium isotopic and elemental analysis by resonance ionization mass spectrometry

Michael Savina[1*], Danielle Ziva Shulaker[1], Whitney Harmon[1]
[1]Lawrence Livermore National Laboratory, Livermore CA, USA; *savina1@llnl.gov

Debris collected in the aftermath of a nuclear detonation contains nuclides created by fission and by neutron capture on, among other things, the actinide fuel of the device. Such material can be analyzed for clues to device characteristics. Methods such as decay counting and mass spectrometry have been developed for such analyses. Both methods begin with dissolution of the solid debris followed usually, though not in all cases, by chromatographic purification of the elements of interest prior to analysis to remove interfering species. In the case of mass spectrometry this means removing isobaric (i.e. same mass) species, for example separating Am from Pu to resolve the isobar at mass 241. The separations are highly effective but involve time and labor; methods that do not require them would therefore be useful.

Resonance Ionization Mass Spectrometry (RIMS) is one such method. In brief, material is removed from a solid by a pulsed laser or ion beam and ionized in the gas phase above the surface by one or more lasers tuned to electronic resonances in the element of interest. The photo-ions created by the lasers are detected by time-of-flight mass spectrometry. Because the ionization mechanism is resonant, the element of interest is detected with far higher efficiency than other elements present in the sample. This results in a high degree of discrimination against isobars so that prior separation is usually unnecessary.

There are additional characteristics that make RIMS useful. Resonant ionization is very efficient, resulting in higher detection efficiency than other forms of mass spectrometry. For example, RIMS has a maximum U detection efficiency of 38% [1], compared to ~2-5% for other forms of mass spectrometry (SIMS, TIMS, ICPMS). The resonant nature of the process means that a slight detuning of the lasers effectively extinguishes the signal and allows for the quantitative measurement and thus subtraction of backgrounds from all sources, including non-resonant ionization of isobars. This is important when an interfering species is present in overwhelming amounts and some non-resonant ionization is unavoidable. This is often the case for ^{238}U which is present at far higher concentration than ^{238}Pu, often >20,000:1. Figure 1 plots RIMS Pu spectra on- and off-resonance and shows residual ^{238}U under the ^{238}Pu peak which would not be accounted for using baseline fitting techniques.

Lastly, the ionization process is pulsed, so that the times of birth of various ions, and thus their arrival

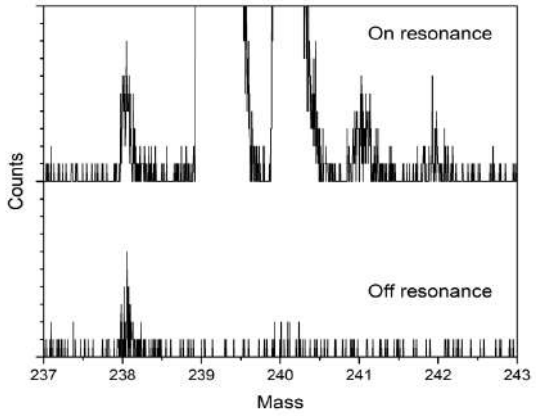


Figure 1: Plutonium RIMS spectra on- and off-resonance (upper and lower respectively).

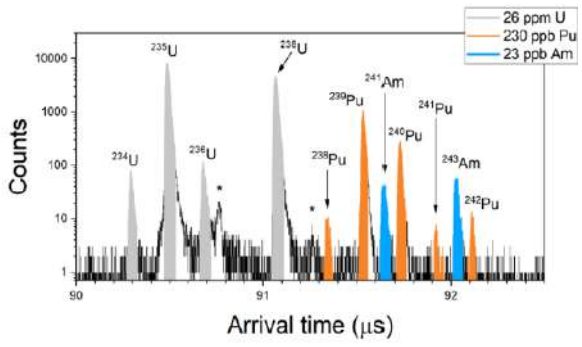


Figure 2: RIMS spectrum with Pu ionization delayed with respect to U and Am.

times at the detector, can be controlled. In this way, two elements can be analyzed simultaneously using two sets of lasers, with isobars resolved by ion arrival times. For example, Figure 2 shows that delaying the ionization of Pu with respect to U and Am enables the simultaneous analysis of isobaric pairs such as $^{238}U/^{238}Pu$ and $^{241}Pu/^{241}Am$ [2]. This lowers sample consumption since all three actinides are detected simultaneously.

We have developed RIMS methods for the analysis of irradiated uranium materials and compared the results to traditional radiochemical analysis on the sample samples. A very small amount of dissolved but unseparated material, generally a few microliters, is deposited onto a Si or Ti substrate, dried, and transferred into the instrument. Isotopic analyses are done directly on the as-received solution. For quantitative elemental analysis the solution is spiked with ^{244}Pu to determine the Pu concentration.

In this contribution we present Pu analysis of neutron- and gamma-irradiated irradiated uranium. RIMS Pu elemental and isotopic analyses compare well with traditional radiochemical analyses that require more time and material, although the uncertainties associated with RIMS measurements are larger. We describe a new laser built for rapid interleaving of on- and off-resonance spectra as in Figure 1, such that even laser shots are on resonance and odd laser shots are off resonance. This allows for real-time background correction at a repetition rate of 1500 Hz. We use this technique to demonstrate ^{238}Pu analysis trace analysis in the presence of large excesses of ^{238}U, and quantification of the minor isotope ^{242}Pu at levels below 1 ppt in unpurified material.

The combination of laser and method development has enabled us to design a user-friendly RIMS instrument that otherwise wouldn't be capable of the more advanced analyses described here. Construction is underway and will be presented.

This work was performed under the auspices of the U.S. Department of Energy by Lawrence Livermore National Laboratory under Contract DE-AC52-07NA27344. This work was supported by the U.S. Department of Energy's National Nuclear Security Administration, Office of Defense Nuclear Nonproliferation Research and Development. LLNL-ABS-2017380

References

1. Savina, M.R., et al., *New Resonance Ionization Mass Spectrometry Scheme for Improved Uranium Analysis*. Analytical Chemistry, 2018. **90**(17): p. 10551-10558.
2. Savina, M.R., et al., *Rapid isotopic analysis of uranium, plutonium, and americium in post-detonation debris simulants by RIMS*. Journal of Analytical Atomic Spectrometry, 2023. **38**: p. 1205-1212.

Increased Sensitivity of Pu M_5-edge CC-RIXS to Bond Covalency in PuO_2 in Comparison to Pu M_4-edge RIXS

Sven Schenk[1*], Bianca Schacherl[1], Harry Ramanantoanina[1], Aaron Beck[1], David Fellhauer[1], Agost Tasi[1], Tim Prüßmann[1], Olaf Walter[2], Karin Popa[2], Michelangelo Tagliavini[3], Maurits Haverkort[3], Tonya Vitova[1]

[1]Institute for Nuclear Waste Disposal (INE), Karlsruhe Institute of Technology (KIT), P.O. 3640, D-76021 Karlsruhe, Germany; [2]European Commission, Joint Research Centre (JRC), Hermann-von-Helmholtz-Platz 1, 76344 Eggenstein-Leopoldshafen, Germany; [3]Institute for Theoretical Physics (ITP), Heidelberg University, Philosophenweg 19, 69120, Heidelberg, Germany; *sven.schenk@kit.edu

In recent years, the application of high energy resolution X-ray absorption and emission spectroscopy, combined with quantum chemical calculations, has proven to provide a powerful set of tools for investigating not just the oxidation states of actinides (An), but also the involvement of 5f valence electrons in bonding, as well as the An structural and bonding properties.[1, 2, 3, 4]

In this work PuO_2 as well as $Pu^{4+}_{(aq)}$ were examined at the Pu M_4- and M_5-edges using both high energy resolution X-ray absorption near edge structure spectra (HR-XANES) and core-to-core resonant inelastic X-ray scattering (CC-RIXS) maps recorded at 90° scattering geometry. For this, a solution of 0.025 M $^{242}Pu^{4+}_{(aq)}$ in 2 M $HClO_4$ was electrochemically prepared and compared to encapsulated $^{239}PuO_2$ powder.[3] Additionally, M_4-edge CC-RIXS maps of a series of actinide oxides (ThO_2, UO_2, NpO_2) were recorded. All experiments were conducted at the ACT station of the CAT-ACT beamline at the KIT Light Source, Karlsruhe, Germany.[5, 6] By comparing the PuO_2 and $Pu^{4+}_{(aq)}$ spectra at the Pu M_4- and M_5-edges, we observe that spectra, especially at the M_5-edge, can change drastically depending on the experimental setup and the associated experimental resolution. An empirical fitting procedure was developed to account for this. It will be shown that three peaks can be fitted to the main absorption feature of the Pu M_5-edge CC-RIXS spectra of both Pu compounds. Furthermore, it will be demonstrated that our empirical approach successfully models the shape of the PuO_2 M_5-edge CC-RIXS map, which could not be accurately reproduced by calculated spectra. We will compare the differences of the CC-RIXS maps of the two Pu compounds at both edges and show that the M_5-edge spectra exhibit increased sensitivity to the distribution of valence electron density and bond covalency. In addition, we will illustrate a clear trend: the higher-energy peak of the main resonance in the actinide M_4-edge HR-XANES/CC-RIXS spectra of the series of actinide dioxides, becomes progressively more intense as the atomic number Z of the AnO_2 increases. It will be demonstrated that this experimentally observed trend agrees with the results obtained from calculations performed with the Quanty code.[7]

Overall, this systematic study in which the ligand or the actinide element was varied provides new experimental groundwork for further fingerprint analysis of the actinide M_4- and M_5-edge HR-XANES and CC-RIXS and demonstrates the potential of both edges for probing the electronic structure and, ultimately, the bonding properties of actinides.

We acknowledge financial support from the European Research Council (ERC) Consolidator Grant “The Actinide Bond” (N°101003292) under the European Union’s Horizon 2020 program.

[1] A. Bajaj, et al., Inorg. Chem. 64, 24 (2025) 12297-12312. [2] A. Schacherl, et al. Nat. Commun. 16 (2025) 1221. [3] T. Vitova, et al., Chem. Commun. 54 (2018) 12824-12827. [4] S. M. Butorin, Inorg. Chem. 59, 22 (2020) 16251-16264. [5] A. Zimina, et al., Rev. Sci. Instrum. 88 (2017) 113113. [6] B. Schacherl, et al., J. Synchrotron Rad. 29 (2022) 80-88. [7] M. W. Haverkort, et al., Phys. Rev. B 85 (2012) 165133.

Chemical bonding in actinide quinolinates from Th to Pu

Moritz Schmidt[1,2]*, Jason Ross[3], Robert Gericke[1], Bin Yeamin[3], Michael Patzschke[1], Peter Kaden[1], Juliane März[1]

[1]Institute of Resource Ecology, Helmholtz-Zentrum Dresden-Rossendorf, Dresden, Germany;
[2]Institute of Materials Chemistry, Brandenburg Technical University, Senftenberg, Germany;
[3]Technical University Dresden, Dresden, Germany; *e-mail: moritz.schmidt@hzdr.de

Coordination chemistry of the actinides still lags behind the field in other parts of the periodic table. This is despite its high relevance for separation processes, environmental remediation, nuclear waste disposal strategies, or decorporation of actinides from the human body. In all of these cases, the most important elements are the highly radiotoxic transuranium elements, e.g. Np, Pu, or Am. These are also the elements for which the lack of data is most severe. Beyond applied questions, the actinides' coordination chemistry is interesting from a fundamental point-of-view for their wide range of oxidation states and their unique electronic structures with near-degenerate 5*f*, 6*d*, and 7*s* orbitals.

Here, we will discuss a series of isostructural An^{IV} (Th, U, Np, Pu) complexes with the quinolate ligand $[An^{IV}(quin)_4]$. Quinoline-based N,O-donor systems offer a minimal yet informative structural motif capable of revealing fundamental trends in actinide coordination chemistry. Their rigid aromatic framework, simple donor set, and synthetic versatility provide an ideal platform for probing *f*-element bonding, orbital participation, and covalency across the actinide series.

The complexes were structurally characterized by single crystal X-ray diffraction (SC-XRD), while their electronic and magnetic properties were studied by ^{1}H nuclear magnetic resonance (NMR) spectroscopy and quantum chemical calculations. Single-crystal X-ray diffraction demonstrates that all compounds are isostructural, crystallizing in the triclinic space group P–1 with four ligands coordinating to the metal in an eight-coordinate biaugmented trigonal prism geometry. Each actinide is bound by four bidentate quinolinate ligands through N,O chelation, forming an N_4O_4 coordination environment. An–O and An–N bond lengths follows the expected actinide contraction trend, with significant deviations providing insight into 5*f* orbital contraction and its effect on metal–ligand covalency.

In solution, variable-temperature ^{1}H-NMR spectroscopy indicates that the $[An(quin)_4]$ species interconvert rapidly between the solid state biaugmented trigonal prism geometry and a square antiprism on the NMR timescale. For the paramagnetic actinides U, Np, and Pu, pseudocontact shifts (PCS) dominate the experimental shifts. Fitting of the PCS data suggests an S_4 symmetry axis in solution and confirms that the compounds maintain a high degree of geometric flexibility in solution.

Computational studies using quantum theory of atoms in molecules (QTAIM) and population analysis can describe chemical bonding in the compounds on the electronic level and relate it to magnetic properties. Electron density at the bond critical points and delocalization indices both increase from thorium to plutonium, confirming increasing of metal–ligand covalency across the series. Theoretical magnetic susceptibility tensors reproduce the experimental PCS patterns, validating the correlation between molecular geometry and anisotropic magnetic response.

These combined analyses provide a comprehensive insight into chemical bonding in actinide compounds with relevance to applications from the nuclear fuel cycle to the environment and the human body.

This work is funded by the Deutsche Forschungsgemeinschaft (DFG) via the ANR/DFG project ActiDecorp (530101100).

Investigation of Manufacturing and Processing Variables on the Mechanical Behavior of Tungsten During Actinide Pyroprocessing

Elise Shauf, Stephen Raiman

University of Michigan, Ann Arbor, MI, USA

Refractory metals are commonly used in actinide pyrometallurgy due to their excellent compatibility with molten chloride salt. Since the manufacturing method is typically a batch process, equipment failures during pyrometallurgical processing can be costly. Predominant failures are hypothesized to be caused by variations in the manufacturing process, and not the pyroprocessing environment.

For this work, tungsten failure mechanisms were investigated by exposing samples to cerium and molten chloride salts in an actinide pyrometallurgy environment. These exposures were conducted at 850°C for 100 hours, and the samples were strained to failure to determine if the exposures affected their mechanical properties. There was not a significant change in tungsten performance after the exposures. This result demonstrates the durability of tungsten, but exposes its sensitivity to changes in manufacturing processes. Lower rolling reductions lead to smaller grains that show a decrease in strength, but an increase in ductility.

However, there is evidence that shows increased uniformity of the as-received material after exposure to heat. This change could be due to minor grain growth or changes in dislocation density. The analytical methods utilize EBSD for changes in the grain size and texture and XRD for defect density, conducted after various heat treatments on tungsten plate.

Photochemistry of Aqueous Plutonium(VI) Oxalate

A. Kirstin Sockwell[1*], Amy E. Hixon[1]

[1]University of Notre Dame, Indiana, United States; *asockwel@nd.edu

Relatively little is understood about the aqueous-phase interactions between Pu(VI) and oxalate in comparison to the more heavily studied Pu(IV) and U(VI) oxalate systems. Most of the Pu-oxalate literature focuses on the precipitation of Pu(III) and Pu(IV) oxalates during Pu purification, including process optimization, thermal degradation, and solid characterization. However, the prevalence of oxalate throughout the nuclear fuel cycle necessitates understanding Pu interactions with oxalate in aqueous and solid-state systems across all possible Pu oxidation states.

The chemistry of aqueous U(VI)-oxalates is relatively more studied, but the system is still not fully understood. Questions surrounding the speciation and decomposition mechanisms still remain. Studies of the photochemical reduction of U(VI) to U(IV) in the presence of oxalate have not been mirrored in the Pu literature. However, the instability of Pu(VI)-oxalate complexes in aqueous and solid-state, is likely driven by a photochemical mechanism. In previous studies, we identified aqueous species of Pu(VI)-oxalate as a function of pH and metal-to-ligand ratio, and reported the structure and photochemical decomposition of crystals of $[PuO_2(C_2O_4)(H_2O)]\cdot 2(H_2O)$.[1,2] This current work furthers our understanding of the aqueous Pu(VI)-oxalate system by investigating the change in speciation after controlled exposure to light.

A spectrophotometric investigation of the aqueous speciation of Pu(VI)-oxalate was conducted on solutions directly exposed to a 254 nm UV lamp for set timepoints. Samples were monitored with UV-vis-NIR and kept out of ambient light as much as possible. Control samples were placed in dark cells between scans. The reduction of Pu(VI)-oxalate species was significantly increased with light exposure when an equimolar or excess concentration of oxalate was present. Kinetics and speciation as a function of oxalate concentration and light exposure time were determined. This study demonstrated the need to further investigate the aqueous chemistry of Pu(VI)-oxalate.

References:
[1] Sockwell, A. K.; DiBlasi, N. A.; Hixon, A. E. *Phys. Chem. Chem. Phys.* **2023**, *25*, 32904-32912.
[2] Sockwell, A. K.; Sweet, T. F. M.; Barth, B.; Burns, P. C.; Hixon, A. E. *Inorg. Chem.*, **2024**, *63*, 56-60.

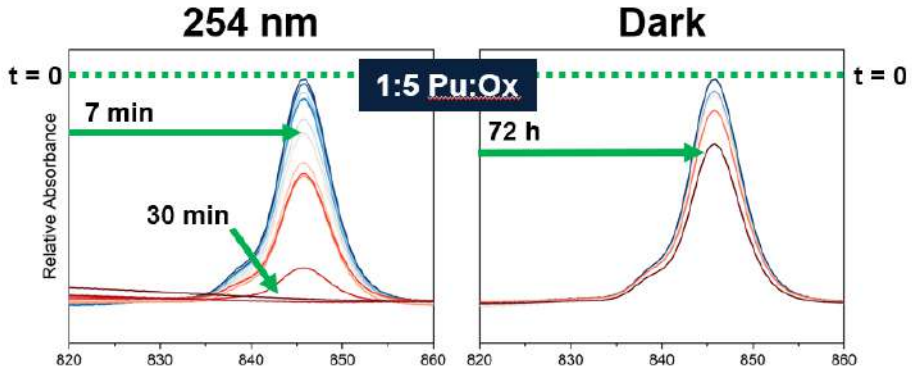


Figure 1: UV-vis-NIR spectra of 1:5 Pu(VI):oxalate at pH 3 after being exposed to 254 nm light (left) and stored in the dark (right).

Molecular Dynamics Modeling of Helium Bubbles in Delta- and Epsilon-Pu

Startt J[1*], Chesser I[1], Mathew N[1], Plohr J[1], Nitol M[2], Baskes M[2], Fensin S[2], Hunter A[1]

[1] Materials and Physical Data Group, X Computational Physics Division, Los Alamos National Laboratory, Los Alamos, NM, USA; [2] Materials Physics and Applications Division, Los Alamos National Laboratory, Los Alamos, NM, USA; *jstartt@lanl.gov

Aging in Pu metals leads to the accumulation of He gases which remain locked in the bulk of the material as nanometer sized bubbles or trapped as atomic defects in the lattice. Understanding how He interacts with other aging related defects such as point defect fluxes, nanovoids, dislocations, lattice distortion and stress-strain fields as well as other more intrinsic microstructural features such as grain boundaries is important for evaluating material lifetime and performance. Obtaining atomic level information about He bubbles is difficult, however, especially in metals as complex as Pu. With proper validation, molecular dynamics and atomistic simulations allow us to evaluate the atomic level mechanisms of He migration and coalescence.

In this work we simulate He bubbles in the Pu lattice, focusing on the FCC delta and BCC epsilon phases. We employ molecular dynamics (LAMMPS), evaluating and comparing two interatomic Pu-potentials under development at LANL (ms-meam and MTP), benchmarking against experiment where data is available. We specifically probe the atomic structure of the He bubble in the lattice, evaluating thermodynamic properties internal to the bubble, such as the relationship between bubble diameter with bubble pressure and He density and how the variance in temperature affects this relationship. We study the prevalence of faceting in small bubbles and how this might affect bubble migration and transport mechanisms, and lastly, we evaluate the mechanisms in which the Pu lattice accommodates the bubble, through stress-strain dissipation, dislocation loop punching, and the interaction with other defects. We make comparisons with other relevant FCC and BCC He-metal systems where He-containing interatomic potentials exist. Ultimately, the knowledge we gain from these studies is meant to inform larger mesoscale and continuum level Pu aging models, improving both our understanding and predictive capability in aging sciences. LA-UR-26-22593

Aging and Oxidation Mechanisms of PuO_2 and Pu-doped UO_2 based Nanomaterials under Ambient Conditions in Maintaining the Stability of Spent Nuclear Fuel

Kevin D. Stuke[1,2*], Stephan Weiß[2], Salim Shams Aldin Azzam[2], Patricia M. Große[3], Sami J. Vasala[2,4], Damien Prieur[2,4], Lucia Amidani[2,4], Christoph Hennig[2,4], Kristina Kvashnina[2,4], Gabriel L. Murphy[1], Dirk Bosbach[1] and Nina Huittinen[2,3]

[1]Institute of Fusion Energy and Nuclear Waste Management IFN-2, Forschungszentrum Jülich GmbH, Juelich, Germany; [2]Institute of Resource Ecology, Helmholtz Zentrum Dresden Rossendorf e.V., Dresden Germany; [3]Institute of Chemistry and Biochemistry, Freie Universität Berlin, Berlin Germany; [4]The Rossendorf Beamline (BM20), The European Synchrotron Radiation Facility (ESRF), Grenoble, France;
*k.stuke@fz-juelich.de

Mixed Oxide (MOX) spent nuclear fuel (SNF) is a challenging product of nuclear energy generation that has been used in many nations. The fuel is based on a mix of UO_2 and PuO_2 prepared under different ratios and mixing conditions. After a prolonged burnup of around 45-50 GWd/t_{HM} UO_2 fuel becomes significantly heterogeneous and forms the so-called "high-burnup structure" (HBS), while in MOX fuel the plutonium islands enter the HBS state almost immediately due to their high ^{239}Pu concentration.[1] The HBS is characterised by an increased porosity compared to regular grain UO_2 and MOX materials and occur as nanomaterials. Detailed investigations of these materials regarding their chemical and redox stability are pertinent to its subsequent safe interim storage and disposal in a geological repository.[1] In the present work, we performed systematic investigations of the behaviour of UO_2, PuO_2 and Pu-doped UO_2 nanomaterials under ambient aging conditions. For this propose, we have synthesized UO_2, Pu-doped UO_2 and PuO_2 based nanoparticles from a hydrothermal reducing method.[2] Investigations on the oxidation behaviour of UO_2 were examined over a period of 371 days, in which their redox and structural chemistry was examined via a combination of powder X-Ray diffraction (P-XRD), high energy resolution fluorescence detection X-Ray absorption near edge structure (HERFD-XANES), extended X-Ray absorption fine structure (EXAFS) and scanning electron microscopy (SEM). Nanoparticles were found forming single-phase cubic structure consistent with UO_2 in space group $Fm\bar{3}m$ from XRD analysis. After exposure to ambient air for 355 days, it was observed that the particles underwent gradual amorphization followed by recrystallization to the known mineral phase schoepite ($[UO_2]_4O(OH)_6](H_2O)_6$) in space group $P2_1ca$.[3] These significant microstructural changes during the ageing process are also visible in the morphology of the sample as shown by SEM-analysis of pristine and 371-days aged particles (Figure 1). This unexpected oxidation behaviour and the occurrence of schoepite structures is important since it is known to form on spent nuclear fuel under oxidising conditions and therefore can affect the release of radionuclides. To examine if Pu can follow a similar pathway, we examined PuO_2 and Pu-doped UO_2 nanoparticles, to determine whether Pu follows a schoepite oxidation type vector completely or in part via solid solution or remains stable. The redox chemistry of both, uranium and plutonium are investigated via synchrotron-based EXAFS and HERFD-XANES analysis and the structural behaviour via XRD measurements at the European Synchrotron Radiation Facility (ESRF), BM20 (ROBL). The results of this work will be presented and discussed in relation to the oxidation behaviour of MOX based HBS materials in addition to their relevance to spent nuclear fuel and, moreover, in relation to the fundamental chemistry of AnO_2 nanoparticles at Plutonium Futures Conference 2026.

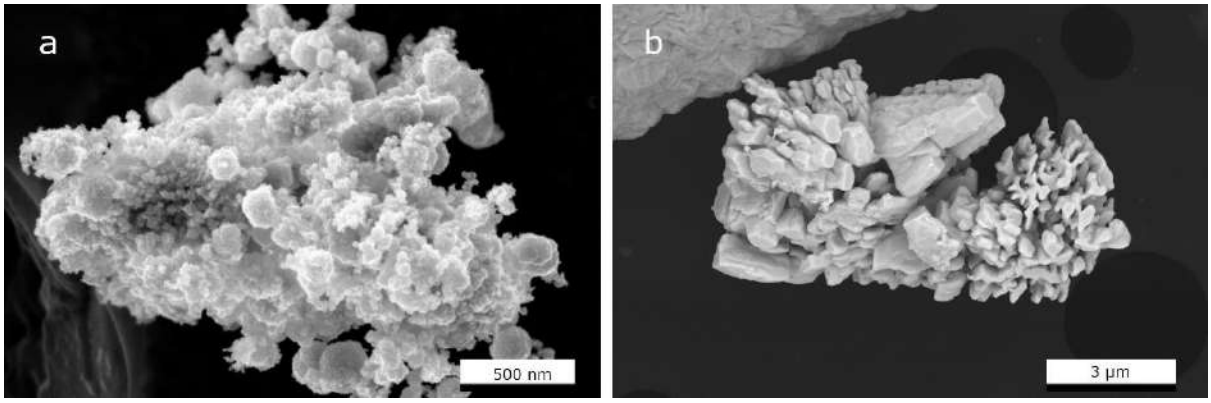


Figure 1: High magnification SEM surface micrographs of a) pristine UO_2 based nanoparticles and b) the same sample after 371 days of aging under ambient conditions. The pristine particles that are smaller than 100 nm form larger agglomerates, which seems to be symmetrical but of varying sizes. In contrast, the aged sample form significantly larger structures on a micrometre scale, which seems to be smoother and more crystalline.

References:

[1] V. V. Rondinella, T. Wiss, *Materials Today*, Volume 13, Issue 12, Pages 24-32, **2010**.
[2] R. Zhao, L. Wang, *et al*., *CrysEngComm*, Issue 13, Pages 2645-2651, **2014**.
[3] K. D. Stuke, G. L. Murphy, *et al*., *in preparation* for *Inorg. Chem. Front.*, **2026**.

Crystallization of UO_2^{2+} and Pu^{4+} Nitrato Complexes with 1,3-Adamantyl-Bridged Diamide Molecules towards Direct Co-recovery of Nuclear Fuel Materials from HNO_3(aq)

Ryoma Ono[1], Robert Gericke[2], Juliane März[2], Satoru Tsushima[1,2], Koichiro Takao[1*]

[1]Laboratory for Zero-Carbon Energy, Institute of Science Tokyo, Tokyo, Japan;
[2]Institute of Resource Ecology, Helmholtz-Zentrum Dresden-Rossendorf, Dresden, Germany;
*E-mail: ktakao@zc.iir.isct.ac.jp

Recycling U and Pu from spent nuclear fuels is one of the promising options to maintain or reinforce the long-term sustainability of nuclear energy supply, and essential to make this energy system circular-economical [1]. While the PUREX reprocessing is widely acknowledged as a standard chemical separation method for this purpose, its nuclear proliferation resistivity is not always high enough due to potential isolation of purified Pu.

In this context, we have been developing an original precipitation-based reprocessing principle named NUclear fuel MAterials selective Precipitation (NUMAP) as an alternative method for advanced nuclear fuel recycling [2], where U and Pu will be directly recovered from the feed solution dissolving spent nuclear fuels after loading nearly stoichiometric amount of an appropriately selected precipitant. Therefore, use of large excess of any extra organic solvents is no longer required. In our NUMAP method, an appropriately designed diamide precipitant (L) such as **L1** and **L2** in Fig. 1 allows simultaneous recovery of UO_2^{2+} and Pu^{4+} from HNO_3(aq), where $[UO_2(NO_3)_2(L)]_n$ coordination polymer and $(HL)_2[Pu(NO_3)_6]$ are formed as sparingly soluble phases (Fig. 2). In contrast, UO_2^{2+} can be crystallized solely in use of **L3** or **L4** (Fig. 1) to afford $[UO_2(NO_3)_2(L)]_n$, where Pu^{4+} remains dissolved in the mother liquor together with other impurities such as fission products and minor actinides. Note that there is no space for Pu isolation in this NUMAP principle, which is rather preferable to strengthen the nuclear proliferation resistivity of the nuclear fuel recycling scheme. More recently, we have employed 1,3-adamantyl bridging moiety in our molecular design of L to give **L5** (Fig. 1). As a result, it was clarified that **L5** is another promising precipitant for direct co-recovery of UO_2^{2+} and Pu^{4+} from HNO_3(aq). However, the actual chemistry there is somewhat unique, and not observed in the former systems of **L1**-**L4**. In this talk, we will focus on molecular and crystal structures of crystalline deposits of UO_2^{2+} and Pu^{4+} with **L5** as well as solubility of them in HNO_3(aq).

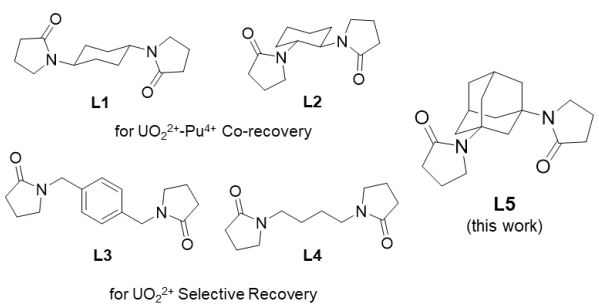


Fig. 1. Diamide precipitants developed for NUMAP Reprocessing

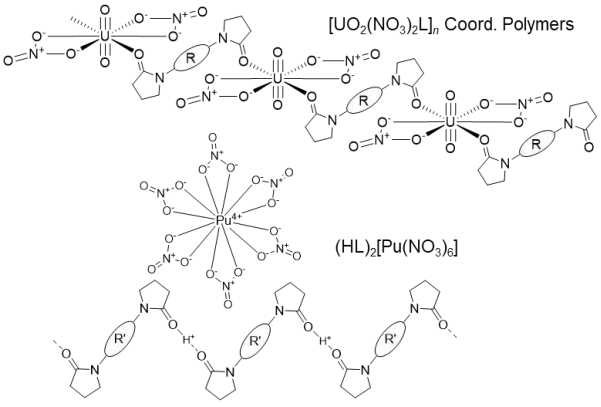


Fig. 2. UO_2^{2+}/Pu^{4+} nitrato complexes with **L** deposited from HNO_3(aq).

References. [1] K. Takao, *Dalton Trans.* **2023**, *52*, 9866-9881. [2] K. Takao, Y. Ikeda, *Eur. J. Inorg. Chem.* **2020**, 3443-3459.

Contribution of coordination chemistry studies to the speciation of neptunium and plutonium in organic phases

Tamain C[1*], Autillo A[1], Munoz M[1], Guillaumont D[1], L. Briscese[1], Berthon C[1]

[1]CEA, DES, ISEC, DMRC, Univ Montpellier, Marcoule, 30207, France
*christelle.tamain@cea.fr

Understanding the speciation of actinides and fission products is essential for predicting their behavior in organic or aqueous phases. Such information is crucial for the modelling used in the nuclear fuel cycle, or the environment. In this work, we investigate the behavior of Np(V/VI) and Pu(VI) in the presence of various organic molecules.

The chemistry of neptunium is relatively poorly understood, even in the fuel reprocessing, as its speciation in the aqueous or organic phases is not yet fully characterized. Neptunium can be stabilized in multiple oxidation states (IV, V, and VI) and be involved in numerous complexes in organic solution. In addition, neptunium can form intricate polynuclear cation–cation complexes (CCIs) [2, 3]. Although often underestimated in actinide speciation studies, these polynuclear species exert a significant influence on actinide chemistry and reactivity, which has renewed interest in their investigation in recent years. To gain a deeper understanding of neptunium speciation in organic phases, a coordination chemistry and speciation study was conducted using single-crystal X-ray diffraction (SC-XRD) analyses together with spectroscopic techniques (IR, Raman, and UV–vis) applied to the neptunium-diglycolamide system. Single-crystals of Np(V) and Np(VI) monomeric species were synthesized, along with two new CCI compounds stabilized by diglycolamide (TEDGA): one trimer and one dimer obtained through controlled and reproducible synthetic procedures. The XRD analyses provide a robust molecular model that can be correlated with spectroscopic signatures in solution. In addition, DFT calculations were performed to support the interpretation of Raman data, characterize bonding within these polynuclear species, and identify key factors governing the stability of cation–cation structures, including the nature of the counterions, the influence of alkyl chains, and the role of weak intra- or intermolecular interactions.

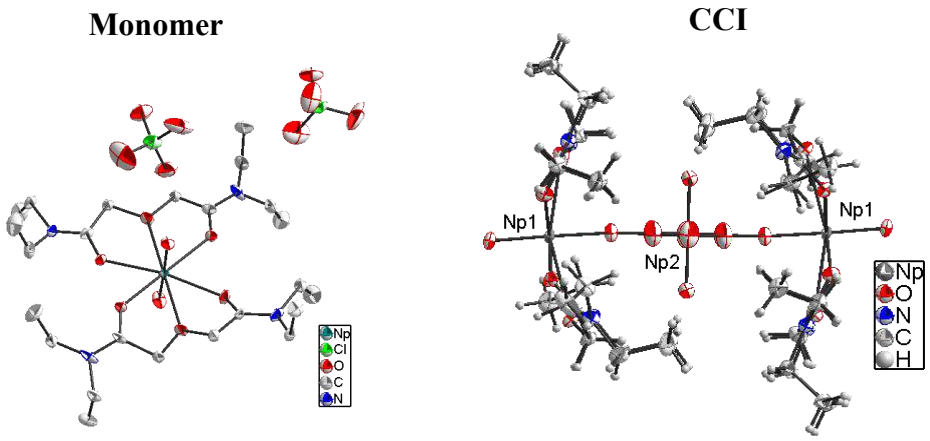


Fig. 1. Crystallographic structures of $[Np^{VI}O_2(TEDGA)_2].2ClO_4$ and $[Np^{V}O_2(TEDGA)_2]_2$ $[Np^{VI}O_2(NO_3)_2].2NO_3$

Using a similar approach, the plutonium(VI)–monoamide system was also investigated. Single crystals with various $PuO_2(monoamide)_2(NO_3)_y$ stoichiometries were synthesized and characterized and spectroscopic analyses of organic phases at various nitric acid concentration were carried out. This study showed that three distinct species may coexist in the organic phase, with relative abundances varying as a function of the initial aqueous phase acidity.

Pu 5f Population: The Case for n = 5.0

J.G. Tobin*

[1]University of Wisconsin - Oshkosh, Oshkosh, WI, USA

*tobinj@uwosh.edu

The quantitative determination of the 5f population in α-Pu and δ-Pu is reconsidered in detail. [1,2] Trends across the 5f series are discussed, including atomic sizes, 5f populations and computational modeling. A detailed spectroscopic analysis of the original Pu $N_{4,5}$ and $O_{4,5}$ x-ray absorption spectroscopy has been performed, including the correction of a fundamental flaw in the Electron Energy Loss Spectroscopy (EELS) measurements. [3] Thus, the determination of the 5f occupation (n) in elemental Pu has been re-evaluated with the result that n = 5.0 ± 0.1 for αPu and n = 4.9 ± 0.2 for δPu. These values are significantly lower than the value of ~5.5 that was propagated earlier. Additionally, an actinide $N_{4,5}$ branching ratio analysis of PuO_2 and UO_2 has been performed, including measurements with a scanning transmission electron microscope at the Advanced Light Source. It is shown that the 5f occupation of the Pu in plutonium dioxide is n ~ 5 and n = 2 in UO_2. [1,4,5]

Actinide 5f Material	BR XAS and non-derivative EELS	BR 2nd Derivative EELS	Corrected BR From 2nd Deriv. EELS	$n \pm \Delta n$ XAS/EELS and ICM[b]
αPu	**0.816 ± 0.01**[a]	0.843	0.816	**5.0 ± 0.1**[a]
δPu	**0.81 ± 0.02**[a]	0.847	0.821	**4.9 ± 0.2**[b]
PuO_2	**0.85 ± 0.05**[16]	0.874	0.851	**5.3 ± 0.6**[b]
UO_2	**0.68 ± 0.02**[42]	0.729	0.690	**2.0 ± 0.4**[b]

[a] This study.
[b] Interpolated using BR ($n = 6$) = 0.918, BR ($n = 5$) = 0.817, BR ($n = 4$) = 0.760, BR ($n = 3$) = 0.723, BR ($n = 2$) = 0.680, BR ($n = 1$) = 0.634. From [29]. Error estimates in n were based the average of the two values, rounding downwards.

Reference:

1. J G Tobin and M F Beaux II, Rep. Prog. Phys. **88**, 063101 (2025)
2. J. G. Tobin, J. Electron Spect. Rel. Phen. **276**, 147478 (2024)
3. J. G. Tobin, J. Electron Spect. Rel. Phen. **268**, 147387 (2023)
4. J. G. Tobin and S.-W. Yu, Inorganic Chemistry **62**, 6, 2592–2598 (2023)
5. J. G. Tobin, S.-W. Yu, C. H. Booth, T. Tyliszczak, D. K. Shuh, G. van der Laan, D. Sokaras, D. Nordlund, and T.-C. Weng, P. S. Bagus, Phys. Rev. B **92**,035111 (2015)

Temperature Dependent Electronic Structure and Optical Properties of δ-Pu

Roxanne M. Tutchton[1*], Jian-Xin Zhu[1,2]

[1]T-Division (T-4), Los Alamos National Laboratory, Los Alamos, NM; [2]Center for Integrated Nanotechnology, Los Alamos National Laboratory, Los Alamos, NM; *rtutchton@lanl.gov

The complex nature of *f*-electron correlations heavy fermion systems impacts material properties in diverse ways that are still being uncovered. We present an analysis of the temperature dependent optical and electronic properties of δ-Pu using dynamical mean-field theory (DMFT) combined with density functional theory (DFT). The calculations were performed for paramagnetic δ-Pu, starting with DFT as implemented in the FP-LAPW based WIEN2K [1]. The DMFT calculation implements a strong-coupling version of the continuous-time quantum Monte-Carlo method [2-5] to explicitly consider the on-site Coulomb interactions with strength U = 4.5 eV and J = 0.512 eV. The latter was derived from the Slater integrals F_2 = 6.1, F_4 = 4.1, and F_6 = 3.0 eV calculated with Cowan's atomic-structure code [6] and reduced by 30% to account for screening. Calculations were performed at a range of temperatures between T = 232 and 725 K. Our findings on electronic structure show that the *f*-electron quasiparticle coherence is enhanced with decreasing temperature. This is supported by the temperature dependent evolution of electronic spectral function and density of states. Accordingly, our optical conductivity results shows the buildup of Drude peak/weight as the temperature is lowered.

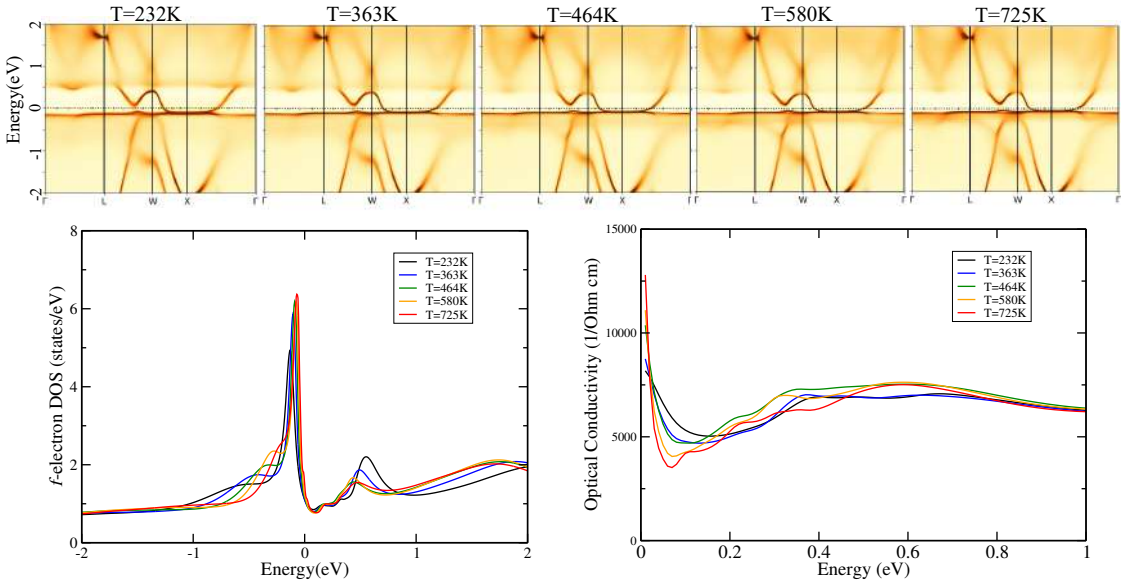


Figure 1: The effects of temperature on the electronic and optical properties are demonstrated through an analysis of the spectral energy bands, density of states, and the optical conductivity. The band dispersions (top) show the temperature dependent quasi-particle spectral energies from T=232K through T=725K. The f-electron DOS (bottom left) is shown for each temperature and is the optical conductivity as a function of frequency (bottom right).

[1] P. Blaha, K. Schwarz, G. K. H. Madsen, D. Kvasnicka, and J. Luitz, WIEN2K, An Augmented PlaneWave +Local Orbitals Program for Calculating Crystal Properties (Karlheinz Schwarz, Technical Universität Wien, Austria, 2001).
[2] J.-X. Zhu, A. K. McMahan, M. D. Jones, T. Durakiewicz, J. J. Joyce, J. M. Wills, and R. C. Albers, Phys. Rev. B 76, 245118 (2007).
[3] K. Haule, C.-H. Yee, and K. Kim, Phys. Rev. B 81, 195107 (2010).
[4] J.-X. Zhu, M. Janoschek, R. Rosenberg, F. Ronning, J. D. Thompson, M. A. Torrez, E. D. Bauer, and C. D. Batista, Phys.Rev. X 4, 021027 (2014).
[5] Roxanne M. Tutchton, Wei-ting Chiu, R. C. Albers, G. Kotliar, and Jian-Xin Zhu, "Electronic Correlation Induced Expansion of Fermi Pockets in δ-Plutonium", Phys. Rev. B 101, 245156 (2020).
[6] R. D. Cowan, Theory of Atomic Structure and Spectra (University of California Press, Oakland, CA, 1981).

Implementing the DAIL NDA Instrument for LANL TRU Waste Material Control and Accounting

R. K. Weinmann-Smith[1*], J. M. Piper[1], C.D. Rael[1], M. E. Booher[1], R. E. Lakis[1], P. A. Hypes[1], A. M. Olsen[1]

[1]Los Alamos National Laboratory, Los Alamos, NM; *rweinmann@lanl.gov

LANL's plutonium facility, PF-4, is undergoing major large construction activities to enable plutonium pit production. Many aspects of the facility are being upgraded to improve facility agility. Transuranic (TRU) waste generation will increase in parallel with the pit production mission, and waste processing is one process being redesigned for a higher throughput to support the increased activity. In FY2020 LANL produced 722 fifty-five gallon waste drums[1]. One important aspect of the redesign is incorporating an in-line nondestructive assay system into the new TRU waste glovebox, Figure 1. The objective is for the measurement to inform facility material control and accounting and to perform WIPP-qualified characterization of the material prior to packaging and shipment to the Waste Isolation Pilot Plant (WIPP). The nondestructive assay system is named the Dual Assay Instrument with List Mode (DAIL). This talk will describe the current status of DAIL implementation in PF-4. The DAIL project history, system architecture, measurement performance, novel analysis methods, optimization efforts, and qualification progress, will be detailed.

DAIL completed fabrication in February 2026, Figure 2, and characterization and calibration measurements began in March. Simulations were carried out in 2023 to optimize the instrument design prior to fabrication. The simulated detector efficiency (Cf-252) was 59% and the measured efficiency was 56%, showing close agreement. The simulations resulted in an expected total measurement uncertainty of 2%-6% at the 1σ confidence interval, depending on the waste stream and analysis methods. In comparison, the 1σ IAEA International Target Value for waste drums is 11%[4].

The waste drum measurement plus 2σ must be less than the 200g Pu fill limit per drum. Reducing the measurement uncertainty therefore allows drums to be packed more fully. Currently, waste drums are packed first and then measured. The drums are packed well below 75% full to avoid expensive remediation which is required if the mass+2σ is greater than the limit. In contrast, DAIL will measure waste first in smaller batches so the exact mass+2σ is known, and then drums will be packed, so they can be packed right up to the 200g limit while completely eliminating overfilling. This improvement will enable drums to be packed 20-40% fuller, reducing the number of drums produced and sent to WIPP.

DAIL measurements were performed with Cf-252 sources to determine the system characteristics such as stability, gain matching, efficiency, dieaway time, optimal gate width, and gate fractions. Then, various plutonium standards were measured to create calibrations. A range of Pu masses and non-nuclear waste matrices were chosen which were representative of the waste stream. The passive calibration curve technique and multiplicity analysis were evaluated for system throughput, accuracy, and precision. Novel techniques based on the list mode capabilities such as dynamic gate width optimization[2], dynamic background subtraction, and position corrected efficiency[3] were matured and calibrated. The techniques were implemented within the INCC6 software for live measurements and are enabled by the Advanced List Mode Module, a list mode capable data acquisition device. DAIL's list-mode design includes reading out individual He-3 tubes for radial position resolution, and tubes of various heights for vertical position resolution. External tube readouts enable background subtraction in real time.

The Dual Assay Instrument with List Mode is a state-of-the-art instrument which incorporates novel optimizations and technology to provide highly accurate waste measurements. It is exemplary of Safeguards by Design, where the safeguards method is designed into the facility operations from the

beginning. This project has immense potential benefits. It is expected to save the facility millions of dollars, streamline operations, reduce worker dose, and eliminate 100 or more drums produced, transported, and stored at WIPP every year.

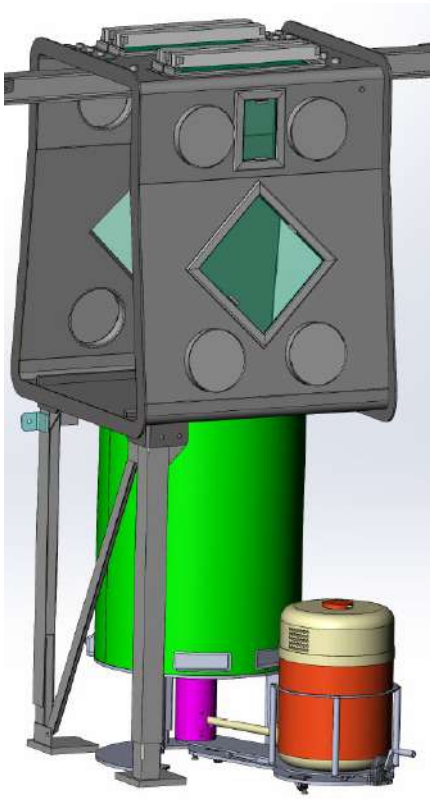


Figure 1. DAIL – glovebox integration.

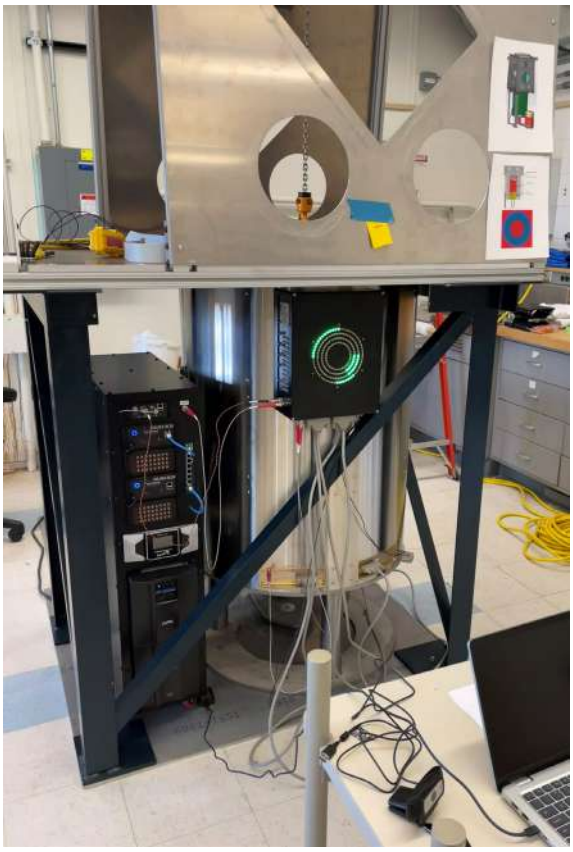


Figure 2. Fabricated DAIL neutron counter.

References

[1]LANL National Security Science Magazine "Not your average trash day" (2020)
[2]R.K. Weinmann-Smith, et al., "List-mode Enabled In-situ Analysis of Optimized Gate Widths…", 64th INMM Annual Meeting, (2023)
[3]C.J.Thompson, et al., "Enhancing Multiplicity Analysis with a Position-Corrected Efficiency Algorithm through List-Mode Data Acquisition", 64th INMM Annual Meeting, (2023)
[4]International Atomic Energy Agency "International Target Values for Measurement Uncertainties in Safeguarding Nuclear Materials" STR – 368 Revision 1.1 (2022)

The role of helium bubbles in changes to the mechanical properties of aged plutonium

D.W. Wheeler*, P. Roussel

AWE, Aldermaston, Reading, Berkshire, RG7 4PR, United Kingdom
* = David.Wheeler@awe.co.uk

The evolution of helium (He) bubbles is one product of the plutonium (Pu) ageing process along with the transmutation products americium (Am), uranium (U) and neptunium (Np) and associated damage to the Pu lattice [1-7]. The mean He bubble diameter in aged Pu stored at ambient temperature has been shown by transmission electron microscopy (TEM) to be between 1.0 and 1.5 nm [3,5], remaining largely unchanged over time, although the bubble density increases with age. Although the size and distribution of He bubbles as a function of age is well understood, their effects on the Pu mechanical properties, particularly at elevated temperatures, have been less extensively reported. Using He bubble size data from published studies in the dispersed barrier hardening (DBH) model [8], we show that it exhibits good agreement with mechanical property data reported elsewhere [9] for aged plutonium-gallium (Pu-Ga) alloys. This can be seen in Figure 1. Furthermore, the data also suggest that for aged Pu subjected to heat treatments at temperatures above 400 °C, He bubble growth may be expected to result in a marked decline in strength.

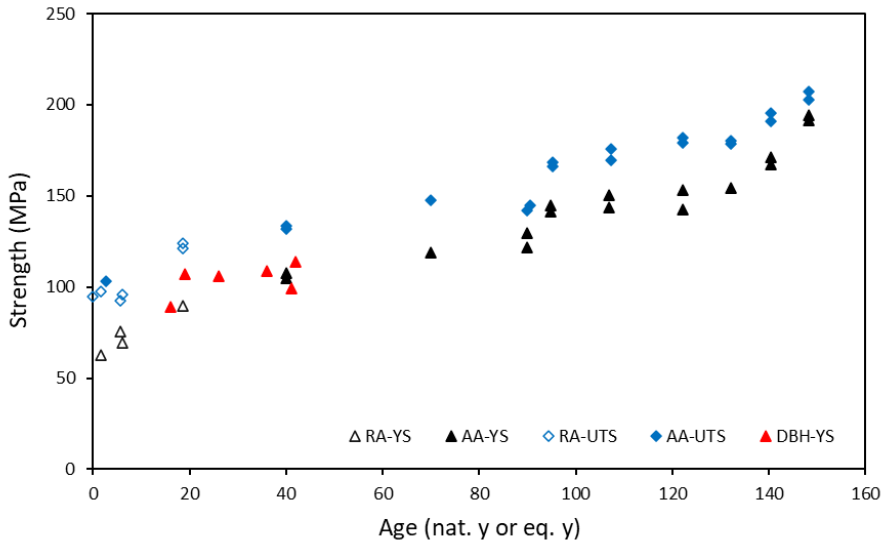


Fig. 1: Graph showing the predicted yield stress values, calculated from He bubble data using the dispersed barrier hardening (DBH) model, together with yield stress (YS) and tensile strength (UTS) data recorded by Chung et al. [9] for both naturally aged (RA) and accelerated aged (AA) Pu-Ga specimens.

References

1. S.S. Hecker, *Metall. Mater. Trans. A*, 39 (2008), 1585-1592.
2. P.G. Allen, W.G. Wolfer, M.A. Wall, *J. Vac. Sci. Technol. A*, 42 (2024), 063212.

3. A.J. Schwartz, M.A. Wall, T.G. Zocco, W.G. Wolfer, *Phil. Mag*., 85 (2005), 479-488.
4. D.W. Wheeler, P.D. Bayer, *J. Alloy. Compd*., 444-445 (2007), 212-216.
5. J.R. Jeffries, M.A. Wall, K.T. Moore, A.J. Schwartz, *J. Nucl. Mater*., 410 (2011), 84-88.
6. J.R. Jeffries, J.A. Hammons, T.M. Willey, M.A. Wall, D. Ruddle, J. Ilavsky, P.G. Allen, T. van Buuren, *J. Nucl. Mater*., 498 (2018), 505-510.
7. D.W. Wheeler, P. Roussel, *J. Vac. Sci. Technol. A*, 43 (2025), 020802.
8. S.J. Zinkle, Y. Matsukawa, *J. Nucl. Mater*., 329-333 (2004), 88-96.
9. B.W. Chung, K.E. Lema, P.G. Allen, *J. Nucl. Mater*., 471 (2016), 239-242.

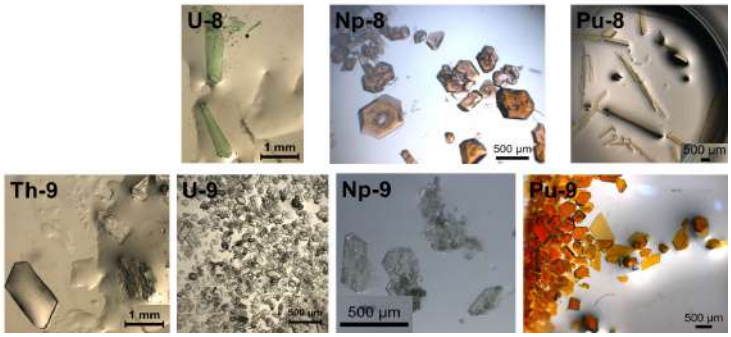
UK Ministry of Defence © Crown Owned Copyright 2026 / AWE.

Insights into the Solvation and Solvent Exchange Reactivity of Plutonium in Non-Aqueous Solutions

Emily R. Mikeska[1], Richard E. Wilson[1*]

[1]Chemical Sciences and Engineering Division, Argonne National Laboratory, Lemont, Illinois USA; *rewilson@anl.gov

The solvation and solvent exchange reactions of actinide elements impact their speciation, coordination chemistry, separations properties, and redox reactivity. While speciation and solvation concepts are established in aqueous media, little is understood about actinide speciation, solvation and its impact on redox behavior in non-aqueous media. Recently, a family of non-aqueous An(IV) dimethyl lsulfoxide (DMSO) solvento compounds have been isolated as analogs to the ubiquitous $[An^{IV}(H_2O)_x]^{4+}$ (x = 8 – 10) species in aqueous solution. The structures of the $An^{IV}(DMSO)_x(ClO_4)_4$ (An = U, Np, and Pu) compounds display similar geometries and coordination numbers to the $[An^{IV}(H_2O)_x]^{4+}$ species. Insight into the solution speciation and solvation numbers is gained through comparisons of solid-state and solution-phase spectra.[1]



Optical photographs of the actinide(IV) DMSO solvate complexes isolated in the solid state.

Optical spectra for each of nine and eight-coordinate solvent complexes in the solid state show diagnostic features indicative of the solvation environment that tracks into solution. These optical spectra allow for the determination of the solvent exchange equilibria in DMSO solvent across the series U, Np, and Pu showing good agreement with the trends calculated using quantum chemistry. Interrogation of the redox chemistry (IV)/III) of the tetravalent ions in DMSO electrolyte highlights a preference for the +IV oxidation state, presumably from the strongly coordinating DMSO solvent ligands.

In DMSO electrolyte, each actinide displays a quasi-reversible An(IV/III) couple and the ability to generate the +III oxidation state is more facile at Pu than the earlier actinides. The speciation and redox chemistry of the $An^{IV}(DMSO)_x(ClO_4)_4$ compounds are compared to the $[An^{IV}(H_2O)_x]^{4+}$ species in an effort to understand the impact of non-aqueous solvents on the fundamental properties of actinides important to controlling and manipulating their redox behavior in separations chemistry common to nuclear fuel cycles and solvent extraction systems.

This work was conducted at Argonne National Laboratory, operated by UChicago Argonne LLC for the United States Department of Energy (USDOE), and supported by the U.S. DOE Office of Science, Office of Basic Energy Sciences, Chemical Sciences Geological and Biosciences Division, under Contract DE-AC02-06CH11357.

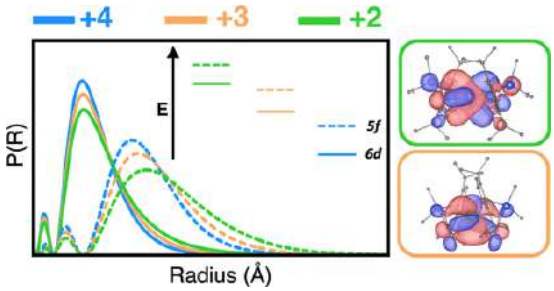
1. Mikeska, E.R., Autry, K.R., Dixon, D.A., Wilson, R.E., Homoleptic An(IV) Dimethyl Sulfoxide Complexes of Th-Pu Enable Insight into Solution Speciation and Redox. *Inorg. Chem.* 64(45), **2025**, 22451-22467.

Probing the Limits of 5f Bonding in Actinides through Oxidation State Control and Redox-Active Ligands

Maria Beltran Leiva[1], David Fiszbein[1], Enrique R Batista[1], Ping Yang[1*]

[1]Theoretical Division, Los Alamos National Laboratory, Los Alamos, United States
pyang@lanl.gov

The complex electronic structures of actinide elements—particularly plutonium—govern their diverse bonding motifs, redox chemistry, reactivity, and spectroscopic behavior. The high angular momentum and radially extended nature of 5f orbitals enable bonding interactions that are unparalleled elsewhere in the periodic table. Developing a predictive understanding of actinide–ligand (An–L) bonding is essential not only for advancing separations science, nuclear fuel cycle technologies, and environmental stewardship, but also for uncovering fundamental principles of f-element chemistry. Through the close integration of advanced density functional and multireference calculations with experiment, this work establishes oxidation state control and ligand design as strategic tools for probing the limits of 5f bonding.



Here, we demonstrate that control of the metal oxidation state, ligand symmetry, and ligand-centered redox properties serve as powerful levers for modulating 5f orbital participation, using advanced density functional and multireference calculations. On the metal side, reduction leads to increasingly diffuse and energetically destabilized 5f and 6d orbitals, enhancing covalency and enabling unconventional metal-to-ligand back-bonding. On the ligand side, symmetry dictate the accessibility of δ and ϕ bonds via back-bonding interactions, and frontier orbital alignment tune the strength of these bonds, even exceeding the strength of ϕ interactions in classical cyclooctatetraene systems. These findings motivate an extension of the Dewar–Chatt–Duncanson bonding framework to f-elements. Furthermore, redox-active ligands are found to induce pronounced and selective bonding interactions through tunable metal–ligand frontier orbital alignment, underscoring the subtle and nonintuitive nature of 5f bonding.

1. Beltran-Leiva, M.; Batista, E.; Yang, P.; Unlocking Novel δ and ϕ bonding Modes in Actinides via Oxidation State Control, *J. Am. Chem. Soc. Au,* **2025**, 5, 1746-1759
2. Fiszbein, D.; Beltran-Leiva, M.; Rao, G.; Britt, R. D.; Batista, E.; Lukens, W.; Yang, P.; Arnold, P. Amplification of Lanthanide - f-Orbital Differences by a Redox-Non-Innocent Semiquinone. August 27, **2025**. https://doi.org/10.26434/chemrxiv-2025-89g00.
3. Su, J; Gong, Y.; Batista, E; Lucena, A.; Maria L; Marçalo, J.; Van Stipdonk M.; Berden G.; Martens J.; Oomens J.; Gibson, J.; Yang, P. Unusual Actinyl Complexes with a Radical-Active N,S-Donor Ligand. *Inorg Chem,* **2023**, 62, 11016-11027.
4. Lussier, D.; Beltran-Leiva, M.; Tomecek, J.; Batista, E.; Gaunt, A.; Hanson, S.; Mason, H.; Miller, J.; Murillo, J.; Salazar, A.; Stritzinger, J.; Yang, P. Isolation of an Americium Complex Containing a Radical Ligand. *J. Am. Chem. Soc.* **2026**, https://doi.org/10.1021/jacs.5c22862